



**TRIBHUVAN UNIVERSITY
INSTITUTE OF ENGINEERING
PULCHOWK CAMPUS**

**A
FINAL YEAR PROJECT REPORT
ON
MODELING OF GRID TIED PV INVERTER TO IMPROVE ITS
PERFORMANCE DURING UNBALANCE LOAD AND
UNBALANCE FAULT**

(Submitted to the Department of Electrical Engineering as partial fulfillment of the requirement for the Bachelor in Electrical Engineering)

(EE755)

PROJECT MEMBERS

**Aashish Dahal (075BEL003)
Bibek Khanal (075BEL011)
Kulchandra Bhattarai (075BEL021)
Lenish Shrestha (075BEL022)**

PROJECT SUPERVISOR

Prof. Dr. Indraman Tamrakar

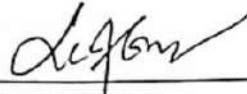
Baisakh 14, 2079 (April 27, 2023)

TRIBHUVAN UNIVERSITY
INSTITUTE OF ENGINEERING
PULCHOWK CAMPUS
DEPARTMENT OF ELECTRICAL ENGINEERING

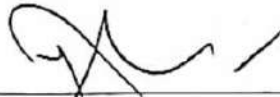
The undersigned certify that they have read, and recommend to the Institute of Engineering for acceptance, a project entitled **“MODELING OF GRID TIED PV INVERTER TO IMPROVE ITS PERFORMANCE DURING UNBALANCE LOAD AND UNBALANCE FAULT”** submitted by Aashish Dahal, Bibek Khanal, Kulchandra Bhattarai and Lenish Shrestha in partial fulfillment of the requirements for the degree of Bachelor of Electrical Engineering.



Prof. Dr. Indraman Tamrakar
Supervisor
Department of Electrical Engineering
Pulchowk Campus



Mr. Rajan Dhakal
External Examiner
Director
DCS, Bagmati Provincial Office
Nepal Electricity Authority



Mr. Yuba Raj Adhikari
Head of Department
Department of Electrical Engineering
Pulchowk Campus

Date: April 27, 2023

COPYRIGHT ©

The authors have agreed that the Library, Department of Electrical Engineering, Pulchowk Campus and Institute of Engineering may make this report freely available for inspection. Moreover, the authors have agreed that permission for extensive copying of this project report for scholarly purpose may be granted by the supervisor who supervised the project work recorded here in or, in their absence, by the Head of Department where in the project report was done. It is understood that the recognition will be given to the author of this report and to the Department of Electrical Engineering, Central Campus, Pulchowk and Institute of Engineering in any use of the material of this project report. Copying or publication or the other use of this report for financial gain without approval of the Department of Electrical Engineering, Central Campus Pulchowk and author written permission is prohibited.

Request for permission to copy and make any other use of the material in this report in whole or in part should be address to:

The Head
Department of Electrical Engineering
IOE, Pulchowk Campus
Lalitpur, Nepal

ACKNOWLEDGEMENT

First and foremost, we would like to express our sincere gratitude to our Supervisor **Prof. Dr. Indraman Tamrakar** for his patience, guidance and continuous support in our project. We are grateful for the expertise, constructive feedback, and encouragement, which has helped us achieve our goals.

We would like to express our deep respect to Head of Electrical Engineering Department for their academic and administrative support.

Our sincere thanks go to all professor and lecturers of department for their precious suggestion and kind support throughout the project duration.

Last but not the least; we extend our special thanks to all the staff of the department and our friend and families for their cooperation. We are thankful to the authors of various research articles that we referred during the course of the project.

Any sort of suggestions or criticism will be highly appreciated and acknowledged.

Aashish Dahal

Bibek Khanal

Kulchandra Bhattarai

Lenish Shrestha

ABSTRACT

With the demand of alternative source of energy, there is an increasing trend in solar power plants, as it is abundant, clean and has significantly reduced the reliance on conventional energy sources. Integrating solar through inverter brings about various challenges in the microgrids and the inverter itself.

This project aims the study of problems in the operation of inverter during unbalance load and unbalance fault condition along with the possible control measures to mitigate those problems to ensure the safe and reliable operation of the inverter.

A grid connected PV inverter is modeled using hysteresis band controller and implementing the MPPT of the PV system with the buck boost converter. During unbalance load and unbalance fault condition, the negative and zero sequence components of current exists. All the zero-sequence component of current is delivered by the grid. The negative sequence component of current also flows through the inverter resulting in high value of current and loss of stability. Also, the voltage across the dc link capacitor increases during voltage dip. The high value of current flowing through the inverter and high voltage across dc link capacitor may damages the inverter and capacitor respectively.

A modified hysteresis controller is studied to compensate the above problems, it addresses the stability issue but isn't found to be much effective as it reduces current flowing through the inverter from 950A to 330A only. Then an inverter dual current controller is introduced replacing the hysteresis band control such that the negative sequence component of current flowing through the inverter is almost mitigated from 600A to 10A and positive sequence current is also reduced relatively to a tolerable value 150A from 550A. The total current flowing through the inverter is limited to 200A from 950A and voltage across dc link capacitor is limited to 700V from 1050V during LG fault at the inverter side thus ensuring safe operation of the inverter during voltage dip condition.

A further study can be done on limiting the positive sequence component of current to a rated value and improving the performance while operating in islanded mode.

Table of Contents

PAGE OF APPROVAL	ii
COPYRIGHT ©	iii
ACKNOWLEDGEMENT	iv
ABSTRACT	v
LIST OF FIGURES.....	viii
List of Tables.....	xi
LIST OF ABBREVIATIONS	xii
CHAPTER ONE: INTRODUCTION	1
1.1 Background.....	1
1.2 Problem Statement.....	3
1.3 Objectives	4
1.4 Scope and Limitation.....	4
1.5 Project Outline.....	4
CHAPTER TWO: LITERATURE REVIEW	6
2.1 Review of paper.....	6
2.2 Related Theory	8
CHAPTER THREE: METHODOLOGY.....	18
3.1 Overview	18
3.2 Simulation Tool.....	18
3.3 Description.....	19
CHAPTER FOUR: RESULTS AND DISCUSSION	26
4.1 PV panel characteristics.....	26
4.2 MPPT verification in VSI using hysteresis band controller	27
4.3 Effects of unbalanced load condition in grid tied inverter	33
4.4 Effects of unbalanced fault condition at the grid side in grid tied inverter	37
4.5 Effects of unbalanced fault condition at the inverter side in grid tied inverter	42
4.6 Summary of the problem	48
4.7 Observations of modified hysteresis band control	48
4.8 Observations of Inverter dual current control.....	50
4.9 Comparison of the results before and after compensation	53
CHAPTER FIVE : CONCLUSION AND RECOMMENDATION.....	54

5.1 CONCLUSION	54
5.2 RECOMMENDATION	54
References	55
APPENDIX	57
Appendix: A (Simulink model)	57
Appendix: B (Script)	64

LIST OF FIGURES

Figure 1.1: Schematic diagram of grid connected PV system	2
Figure 2.1: The equivalent circuit of a PV cell	8
Figure 2.2: buck boost converter in PV system with MPPT	9
Figure 2.3: abc to $\alpha\beta$ and dq transformation	10
Figure 2.4: Flowchart for identifying MPPT	12
Figure 2.5: Three Phase VSI with L-filter.....	13
Figure 2.6: Schematic diagram and gate signals for hysteresis current controller	14
Figure 2.7: Block diagram of extraction of positive and negative sequence	15
Figure 2.8: waveforms of working of SPWM technique	17
Figure 3.1: Block Diagram of Grid Connected PV System	20
Figure 3.2: Simulation model of PV MPPT	21
Figure 3.3: Simulation model of hysteresis band controller	22
Figure 3.4: Simulation model of PV System.....	23
Figure 3.5: Inverter dual current control	25
Figure 4.1: I-V and P-V characteristics of PV system at different irradiance level.....	26
Figure 4.2: MPPT demonstration	27
Figure 4.3: Voltage before and voltage after buck-boost converter.....	28
Figure 4.5 Magnified view of inverter output line voltage before filter	29
Figure 4.4: Inverter output line voltage before filter.....	29
Figure 4.6: Magnified view of grid phase voltage	30
Figure 4.8: Magnified view of phase current delivered to grid for irradiances of 1000 W/m^2	31
Figure 4.10 Power delivered to grid for irradiances of 1000 W/m^2	33
Figure 4.11: Voltage across the capacitor for unbalanced load at the inverter side between 0.3-0.4 sec	33
Figure 4.12: Phase current flowing through the grid for unbalanced load at the inverter side between 0.3-0.5 sec	34
Figure 4.13: Phase current flowing through the grid for unbalanced load at the inverter side between 0.3-0.5 sec	34

Figure 4.14: Phase current flowing through the inverter for unbalanced load at the inverter side between 0.3-0.5 sec.....	35
Figure 4.15: +ve,-ve and zero sequence components of current flowing through the inverter for unbalanced load at the inverter side between 0.3-0.5 sec.....	36
Figure 4.16: Grid phase voltage for unbalanced fault at the grid side between 0.3-0.5 sec.....	37
Figure 4.17: Total Fault current flowing through the faulted line for unbalanced fault at the grid	38
Figure 4.18: Phase current flowing through the grid for unbalanced fault at the grid side between 0.3-0.5 sec	38
Figure 4.19: Magnified view phase current flowing through the grid for unbalanced fault at the grid side between 0.3-0.5 sec	39
Figure 4.20: Phase current flowing through the inverter for unbalanced fault at the grid side between 0.3-0.5 sec	39
Figure 4.21: +ve ,-ve and zero sequence components of current flowing through the inverter for unbalanced fault at the grid side between 0.3-0.5 sec.....	40
Figure 4.22: +ve, -ve and zero sequence components of current flowing through the grid for unbalanced fault at the grid side between 0.3-0.5 sec	41
Figure 4.23: Phase current flowing through the grid for unbalanced fault at the inverter side between 0.2-0.4 sec	42
Figure 4.24: Phase current flowing through the inverter for unbalanced fault at the inverter side between 0.2-0.4 sec.....	43
Figure 4.25:Phase current flowing through the inverter for unbalanced fault at the inverter side between 0.2-0.28 sec.....	43
Figure 4.26: +ve, -ve and zero sequence components of current flowing through the grid for unbalanced fault at the inverter side between 0.3-0.5 sec	44
Figure 4.27: +ve, -ve and zero sequence components of current flowing through the inverter for unbalanced fault at the inverter side between 0.3-0.5 sec.....	45
Figure 4.28: voltage across the capacitor for unbalanced fault at the inverter side between 0.4-0.48 sec	46
Figure 4.29: voltage across the capacitor for unbalanced fault at the inverter side between 0.3-0.5 sec	47

Figure 4.30: voltage across the capacitor for unbalanced fault at the inverter side between 0.3-0.5 sec after hysteresis controller modification	48
Figure 4.31: Phase current flowing through inverter for unbalanced fault at the inverter side between 0.3-0.5 sec after controller modification.....	49
Figure 4.32: Phase current flowing through inverter for unbalanced fault at the inverter side between 1-1.3 sec after inverter dual current control.....	50
Figure 4.33: Magnified view of Phase current flowing through inverter for unbalanced fault at the inverter side between 1-1.3 sec after inverter dual current control.....	50
Figure 4.34: +ve and -ve sequence components of current flowing through the inverter for unbalanced fault at the inverter side between 1-1.3 sec after inverter dual current control.....	51
Figure 4.35: voltage across the dc link capacitor for unbalanced fault at the inverter side between 1-1.3 sec after inverter dual current control.....	52
Figure 4.36: Active power flowing through the inverter for unbalanced fault at the inverter side between 1-1.3 sec after inverter dual current control	53
Figure A.1: Simulation model of PV system	57
FigureA.2 : Simulink model of grid connected PV along with unbalanced load of 25kw, 15kw and 1kw in respective phases at the inverter side.....	58
Figure A.3: Simulink model of grid connected PV using hysteresis band control and 3 phase fault block.....	59
Figure A.4: Simulink model of grid connected PV using hysteresis band control and 3 phase fault block at inverter side.....	60
Figure A.5 Simulink model of modified hysteresis band control	61
Figure A.6 : Overall simulation diagram for Inverter Dual current control.....	62
Figure A.7: Simulink model of Inverter dual current control	63

List of Tables

Table 3.1 : PV specifications.....	19
Table 4.1 : Current flowing through the inverter and capacitor voltage at different fault conditions	48
Table 4.2 : Comparison of result before and after compensation	53

LIST OF ABBREVIATIONS

AC	- Alternating Current
CSI	- Current Source Inverter
DC	- Direct Current
DOF	- Degree OF Freedom
DSOGI	- Dual Second Order Generalized Integrator
FOCV	- Fractional Open Circuit Voltage
FSCC	- Fractional Short Circuit Current
CF	- Curve Fitting
HC	- Hill Climbing
IC	- Incremental Conductance
DER	- Distributed Energy Resource
THD	- Total Harmonic Distortion
MATLAB	- Matrix Laboratory
MPPT	- Maximum Power Point Tracking
P&O	- Perturb and Observe
NS	- Negative Sequence
PLL	- Phase Lock Loop
PS	- Positive Sequence
SOGI	- Second Order Generalized Integrator
SPWM	- Sinusoidal Pulse Width Modulation
UPS	- Uninterruptible Power Supply

CHAPTER ONE

INTRODUCTION

1.1 Background

The global demand for electricity is growing due to the development of new technologies and higher consumption rates. Additionally, there is a growing global awareness among people and governments about environmental issues such as pollution, global warming, and their impact on human health, agriculture, and the economy. As a result, renewable energy resources like solar and wind energy are becoming more popular and are being prioritized. Renewable energy technologies, which offer a secure and environmentally friendly source of electricity, have become increasingly affordable and readily available to the general public [1]. The cost of photovoltaic panels has considerably decreased, and with new innovative technology and the use of more efficient power electronic devices, the costs associated with renewable energy power plants have also reduced.

The use of DERs such as wind, solar, and micro hydro production is increasing due to their reliability, cost-effectiveness, and ability to reduce carbon emissions. However, wind and solar DERs are dependent on environmental factors and their intermittency can be a limitation. To address this issue, DER microgrids are connected to the utility grid. This connection provides a reliable and resilient power supply, allows for effective energy management, increases efficiency, and promotes environmental benefits. The DER microgrid is connected to the utility grid through an inverter which serves as an interface.

Solar PV power plants are increasingly popular as they are the most abundant and cheapest renewable energy source, alongside wind. Ongoing research is resulting in more efficient PV cells and power electronics, and development of new control strategies.

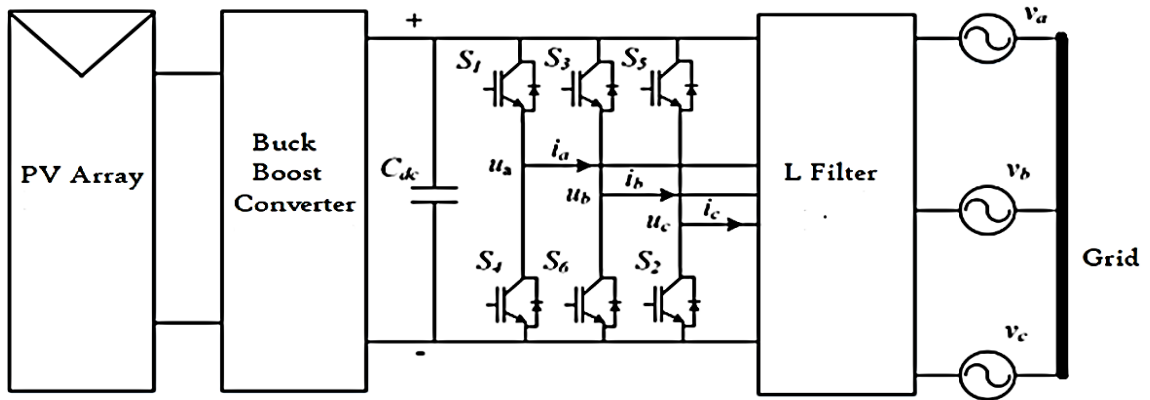


Figure 1.1: Schematic diagram of grid connected PV system

Figure 1.1 shows the schematic diagram of grid connected PV system. A PV system consists of PV arrays, a MPPT subsystem, a DC-DC converter, and an inverter, which serves as the interface with the grid. The output power of a PV cell depends on the ambient temperature and irradiance level. As these environmental factors change, the optimal voltage of the PV system also changes, which can change the overall efficiency of the operation. So, an MPPT is used to ensure maximum possible output by adapting to the changing temperature and irradiance levels. The MPPT algorithm controls the duty cycle for the operation of the buck-boost converter, which is responsible for controlling the voltage for maximum output power delivery. Additionally, the buck-boost converter helps isolate the PV side from the AC side. The inverter is acts as an interface to the grid as it can synchronize its output with the grid. It can be also be used to directly power the load [2]. The cost of these additional equipment increase the cost of the entire system but also improve the efficiency of the system making it economically feasible and with the improvement in control strategies, improving efficiency and decreasing cost of power electronic components it makes the overall system cheaper and more efficient.

Integration of renewable energy like solar and wind energy into the grid poses challenges in preserving the power quality and operational reliability of the system due to the independent operation of DERs. Different inverter control techniques and topologies is essential meet grid standards [3]. The need for grid regulation arises from both balanced and unbalanced faults, as they can have severe effects on both the grid and microgrid. Maintaining power quality is crucial, and any unbalanced event on the grid can potentially

compromise it [2]. During these unbalanced fault conditions there is flow of very high value of current which may damage the components. Also, there are active power oscillations in this situation which may cause high voltage on inverter input.

During an unbalanced fault situation, the total harmonic distortion (THD) also experiences an increase [4]. Therefore, it is of utmost importance to mitigate the harm caused to the microgrid and minimize the damage inflicted on the connected loads and the grid. For this the inverter needs to have suitable control strategies to minimize fault current and harmonics and prevent these from damaging the system components.

Conventional inverters can handle normal operations in balanced load conditions but for reliable operation of inverter in unbalanced loads and fault conditions, it is necessary to build a system for handling negative sequence currents and zero sequence current to minimize the damages caused by faults and sustain use of unbalanced load conditions [5]. This requires a control system to control the switching operation of the IGBTs effectively regulating the unbalanced sequence current components. By regulating these currents, the efficiency of three phase inverter can be effectively increased.

In order to address issues caused by unbalanced systems, it is crucial to extract both voltage and current sequence components, as the negative sequence component generated during a fault can contribute significantly to various issues [2]. This work proposes a dual current controller method, utilizing the DSOGI method for extracting sequence components of both voltage and current. The current reference generation is optimized to limit current and reduce DC-link voltage oscillations. The effectiveness of this controller a standalone PV system is demonstrated through MATLAB simulations.

1.2 Problem Statement

- Due to unbalance load and unbalance fault, the negative and zero sequence currents flows through the inverter.
- If inverter has to supply the fault current, the inverter may damage and there also occurs a stability issue.
- Voltage across the dc link capacitor increases during the unbalance load and unbalance fault.

1.3 Objectives

1.3.1 Main Objective

- To enhance the performance of grid tied inverter under unbalance load and unbalance load.

1.3.2 Specific Objective

- To control the effects of negative and zero sequence current caused due to unbalanced fault and unbalanced load.
- To regulate the current flowing through the inverter during fault.
- To maintain the dc link capacitor voltage.

1.4 Scope and Limitation

The rise in current flowing through the inverter and voltage across the dc link capacitor due to voltage dip condition at the output side of grid connected inverter is controlled to a tolerable value ensuring the safe operation of the inverter.

However, the rise in positive sequence component of current isn't mitigated completely but to a safer value. Also, the current supplied by the inverter isn't pure sinusoidal to minimize the switching loss.

1.5 Project Outline

- This project constitutes five chapters including the current chapter. This chapter explains about the grid connected PV system. Also, it covers the statement of the problem, objective of this project, and scopes and limitations.
- Chapter two provides a literature review that encompasses theoretical framework, articles and publications from IEEE conferences or transactions and books from reputable publishers. The purpose of this review is to gather existing information and examine previous findings from other researchers in the field.
- Chapter three includes the proposed layout of the project and the methods and tools that were implemented to attain the objectives of the project.

- Chapter four presents the simulation results that have been obtained during the implementation of this project. Also, the discussion on the obtained results is performed.
- Chapter five represents the conclusion and recommendation of the project.

CHAPTER TWO

LITERATURE REVIEW

2.1 Review of paper

In recent years there is a growing trend in integration of distributed energy resources (DERs) such as wind and solar into the utility grid due to the intermittency of supply of DERs. By integration to the grid the overall performance and efficiency of the DERs can be improved and also promote renewable energy resources overcoming the problem of intermittency of renewable [1]. The technology of power electronics is crucial in aligning the characteristics of distributed energy generation units with the requirements of grid connections, such as frequency, voltage, active and reactive power control, and minimizing harmonic distortion. However, the low efficiency and limited controllability of distributed power generation systems (DPGSs) based on wind and solar power are their primary drawbacks [6]. If the system of DPGSs connected to the utility network is not properly controlled it can result in grid instability or failure. Additionally, the interconnection standards for these systems are increasingly emphasizing the need for DPGSs to operate effectively during short grid disturbances. In this context, the synchronization algorithm and current controller play a critical role. Consequently, the development of effective control strategies for distributed systems is a matter of significant interest [7].

The behavior of a PV module is nonlinear and subject to variations influenced by environmental factors. Ensuring the tracking of the MPP under changing environmental conditions is crucial to achieve optimal power output and ensure reliable and efficient operation of solar-integrated power generation units [8]. While numerous algorithms have been developed, traditional methods such as P&O and incremental conductance are popular due to their simplicity [9]. The various conventional MPPT techniques such as FOCV [10], FSCC [11], CF [11], HC [12], INC [13] etc. can be also be used. These approaches differ in terms of their implementation, cost, speed, and efficiency. Among them, the commonly employed techniques include the P&O method, incremental conductance, and fuzzy logic control method. In our project, we opted for the P&O method in conjunction with a DC-DC buck/boost converter [8].

Maintaining a stable power system operation requires a constant DC-link voltage in the inverter. Fluctuations in input and output power can result in voltage variations at this specific point, potentially leading to THD in the grid current. Such distortion adversely affects the power quality of the system [14]. Traditionally, addressing this issue involves the utilization of a PI controller device, assists in regulating the power factor of the grid [15].

Most of the faults on the power system led to a short-circuit condition which results in heavy short circuit current flow through the equipment, causing heavy damage to the equipment and interruption of electricity supply to the consumers. Therefore, a robust and efficient short-circuit analysis program is essential for system planning and operation, affecting the design of various system components such as bus systems, grounding systems, circuit breakers, and substation apparatus [16]. In scenarios where the network voltages encounter imbalances caused by unbalanced loads or temporary disturbances, the regulation of current becomes more complex. This is due to the presence of a negative-sequence component in the unbalanced voltage, resulting in double fundamental frequency oscillations in both real and reactive power injections. Consequently, controlling the +ve and -ve sequence currents poses challenges that demand the implementation of straightforward PI control structures within each rotating frame of reference to effectively regulate these components [8].

Hysteresis band controller uses a nonlinear control approach to ensure that a variable within a specified range. This controller dynamically adjusts the hysteresis bandwidth based on variations in the reference compensator current to optimize the switching frequency and THD of the supply current. The hysteresis band technique offers simplicity, robust current control performance, excellent stability, rapid response, inherent peak current control, and ease of implementation [17]. Hysteresis current control method is simple to implement, has low THD and constant switching frequency. To generate reference signal for hysteresis current control while controlling positive and negative sequence component, the positive and negative sequence components are extracted. Various techniques are used to extract positive, negative and zero sequence components during unbalanced load and disturbances [18]. In PWM inverter the controlled output is obtained by adjusting ON and OFF period of the inverter components. This PWM signal is generated using gate signal from hysteresis band controller.

In the presence of system imbalance, which gives rise to a negative sequence component causing various issues during a fault, it becomes necessary to extract the sequence for both voltage and current [2]. To accomplish this, the dual current controller method is employed in this study, utilizing the dual second-order generalized integrator (DSOGI) technique for sequence extraction of voltage and current [2]. Controlling three-phase systems in a stationary reference frame poses challenges, thus reducing the number of phases by transforming them first into the $\alpha\beta$ reference frame and then into the dq-reference frame enables improved control [4]. This method reduces the THD and provides improved control of the sequence components.

2.2 Related Theory

2.2.1 Solar PV

A solar PV (photovoltaic) cell is a semiconductor device that directly converts sunlight into electrical energy using the photovoltaic effect. It consists of a thin layer of silicon or another semiconductor material sandwiched between two electrodes. When sunlight interacts with the cell, photons with sufficient energy generate electron-hole pairs within the semiconductor. This process creates an electric field that guides and propels the light-triggered electrons, resulting in a current flow when the solar cell is connected to an external load. PV cells can be represented by a current source in parallel with a diode. In the absence of light, the PV cell behaves like a diode. To generate more electricity, solar PV cells can be combined to form larger modules or arrays. They are increasingly employed as a renewable energy source in a wide range of applications, from small portable devices to large-scale power plants. In a PV module, the dominant resistance is the series resistance (R_s), while the shunt resistance (R_{sh}) is typically assumed to be infinite and has a negligible impact on performance, as depicted in Figure 2.1 [19].

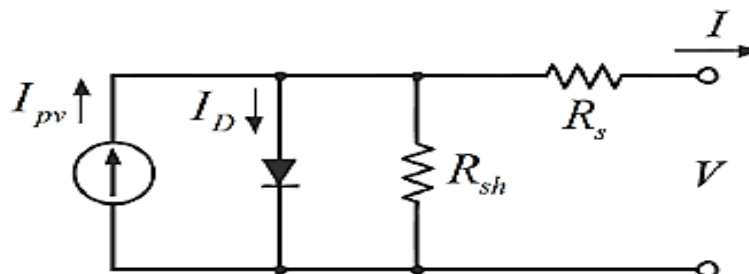


Figure 2.1: The equivalent circuit of a PV cell [19]

Figure 2.1 shows the equivalent circuit of a PV cell. A photovoltaic array is constructed by connecting multiple solar cells in a combination of series and parallel configurations. [19]. The I-V characteristics of PV cell are non-linear and the power production at different solar irradiation and ambient temperature varies. So, we use MPPT algorithm to gain maximum possible output.

2.2.2 DC-DC Buck-Boost Converter

A DC-DC Buck-Boost Converter is a type of converter that can modify the input voltage to produce a regulated output voltage, allowing for voltage step-up or step-down operations as required. Unlike other converters that rely on transformers, the Buck-Boost Converter utilizes a single inductor, making it more streamlined and compact. This converter is highly versatile and finds extensive use due to its ability to generate a wide range of output voltages, making it suitable for diverse applications. A buck boost converter is used commonly used in battery-powered devices, renewable energy systems, and automotive applications to regulate voltage and improve efficiency.

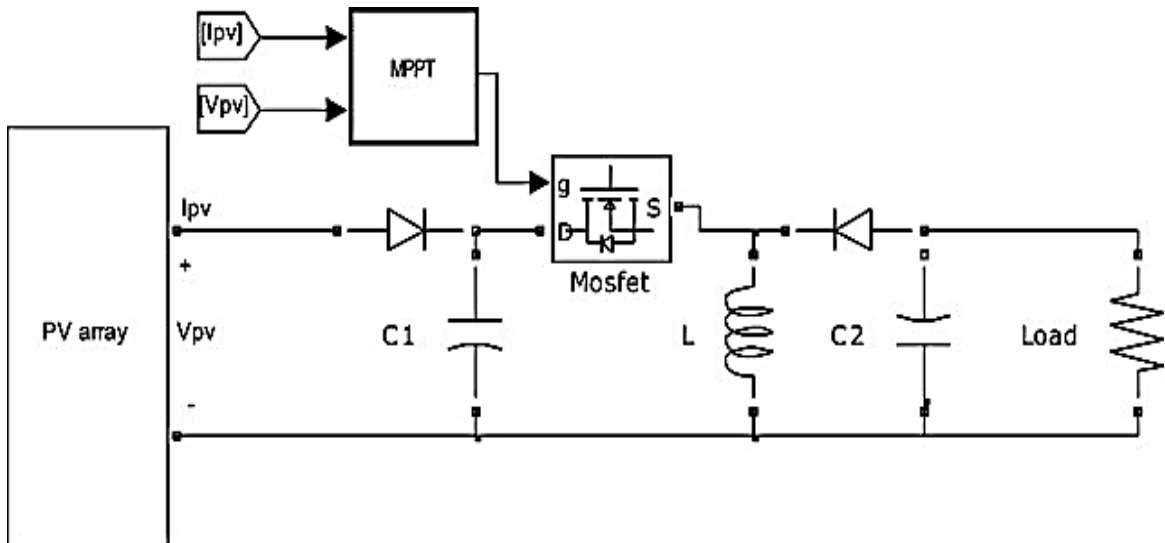


Figure 2.2: buck boost converter in PV system with MPPT [20]

Figure 2.2 shows the circuit diagram of buck boost converter consisting combination of inductor, capacitor, diode and Mosfet. The duty cycle of the converter is determined through the utilization of MPPT algorithm and PI controller thus controlling the output voltage. Efficiency plays a crucial role in mitigating the impact of intermittent solar and wind power generation, as their supply fluctuates [7]. Buck-boost converter controlled by MPPT

algorithm makes the system more efficient and regulates power output of PV array. Buck boost converter is more economical than other converters and has better cost performance ratio. A DC link capacitor is used at output of this converter to provide constant voltage to inverter and limits voltage fluctuations. Typical converter consists of single control loop to control either voltage or power flow of PV array. The PWM signal for the operation of buck-boost converter is generated by MPPT algorithm.

2.2.3 Reference Frame Generation

To effectively manage both active and reactive power in a system, it becomes necessary to control both voltage and current. However, in a three-phase system, controlling all three alternating phases simultaneously can be quite challenging. To simplify the control process, it is advantageous to transform the system into a reference frame that is easier to manage. This transformation reduces the number of phases that require control. There are two primary techniques for reference frame transformations: the $\alpha\beta$ transformation in a stationary reference frame and the dq transformation in a rotating reference frame [7]. The process of converting three-phase quantities into a rotating reference frame involves an initial step of transforming these quantities into an orthogonal component system (α - β). This transformation is achieved by projecting the three-phase quantities onto orthogonal axes, as illustrated in Figure 2.3. In the stationary reference frame, the total voltage vector is inclined at an angle θ to the orthogonal reference frame and rotates at a frequency of ω . By mapping the elements of the stationary reference frame onto the rotating reference frame, the system can be transformed into a simplified form resembling DC [21].

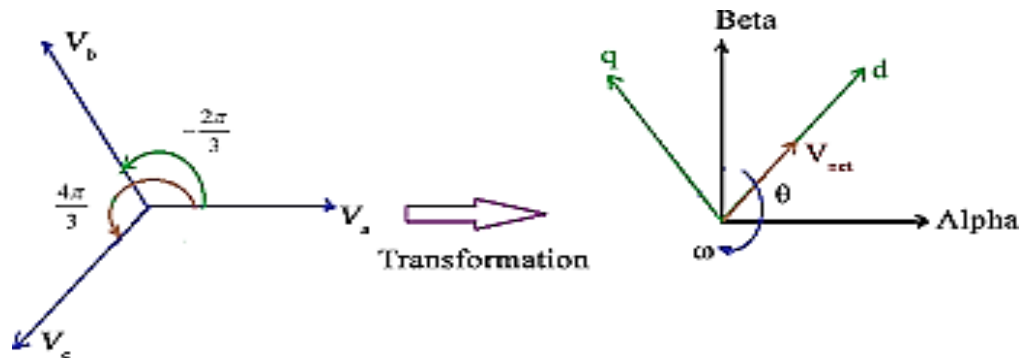


Figure 2.3: abc to $\alpha\beta$ and dq transformation [21]

Figure 2.3 shows the phasor representation of 3 phase components and transformation to dq and α - β -0 component, a-b-c to α - β transformation changes 3 components to 2 components

but both have stationary reference frame whereas d-q component has rotating reference frame. The transformation matrix associated is as follows:

$$\begin{pmatrix} V\alpha \\ V\beta \end{pmatrix} = \sqrt{2/3} \begin{pmatrix} 1/\sqrt{2} & 1/\sqrt{2} & 1/\sqrt{2} \\ 1 & -1/2 & -1/2 \\ 0 & \sqrt{3}/2 & -\sqrt{3}/2 \end{pmatrix} \begin{pmatrix} Va \\ Vb \\ Vc \end{pmatrix} \dots\dots\dots (2.1)$$

$$\begin{pmatrix} Vd \\ Vq \end{pmatrix} = \begin{pmatrix} \sin \theta & \cos \theta \\ \cos \theta & -\sin \theta \end{pmatrix} \begin{pmatrix} V\alpha \\ V\beta \end{pmatrix} \dots\dots\dots (2.2)$$

In α - β transformation, we assume that the voltage is balanced and to get the theta (θ) we are using a PLL. Therefore, its performance in unbalanced voltage conditions will not be good as d-q method. In d-q method we don't care about whether the voltage is balanced or not. The theta is calculated by transformation itself and we don't need a PLL. The three-phase current component a-b-c are converted into α - β -0 components in stationary frames. These components are then rotated by an angle θ in the synchronous reference frame using the Park transformation [22].

2.2.4 MPPT (Maximum Power Point Tracking)

Maximum Power Point Tracking (MPPT) is a method employed to enhance the power output of a solar PV module by continuously monitoring and adjusting the operating point to achieve the maximum power point (MPP). MPPT endeavors to ensure optimal efficiency for PV modules, which is impacted by factors such as sunlight conditions, shading effects, solar panel temperature, and the electrical properties of the connected load. Since these conditions fluctuate, the load impedance that results in the highest power transfer also changes. The MPPT system optimizes the operation of the solar array to achieve maximum efficiency in response to varying load characteristics [23]. It is possible to design circuits that offer ideal loads to photovoltaic cells, and subsequently convert the voltage, current, or frequency to match the requirements of other devices or systems. The MPPT controller controls the PV module output voltage using buck/boost converter to produce maximum power in different environmental conditions. P&O method in addition called ‘‘Hill-Climbing’’ is commonly used method for MPPT because of its simplicity in high efficiency [24]. In this particular work, P&O method is utilized as MPPT technique.

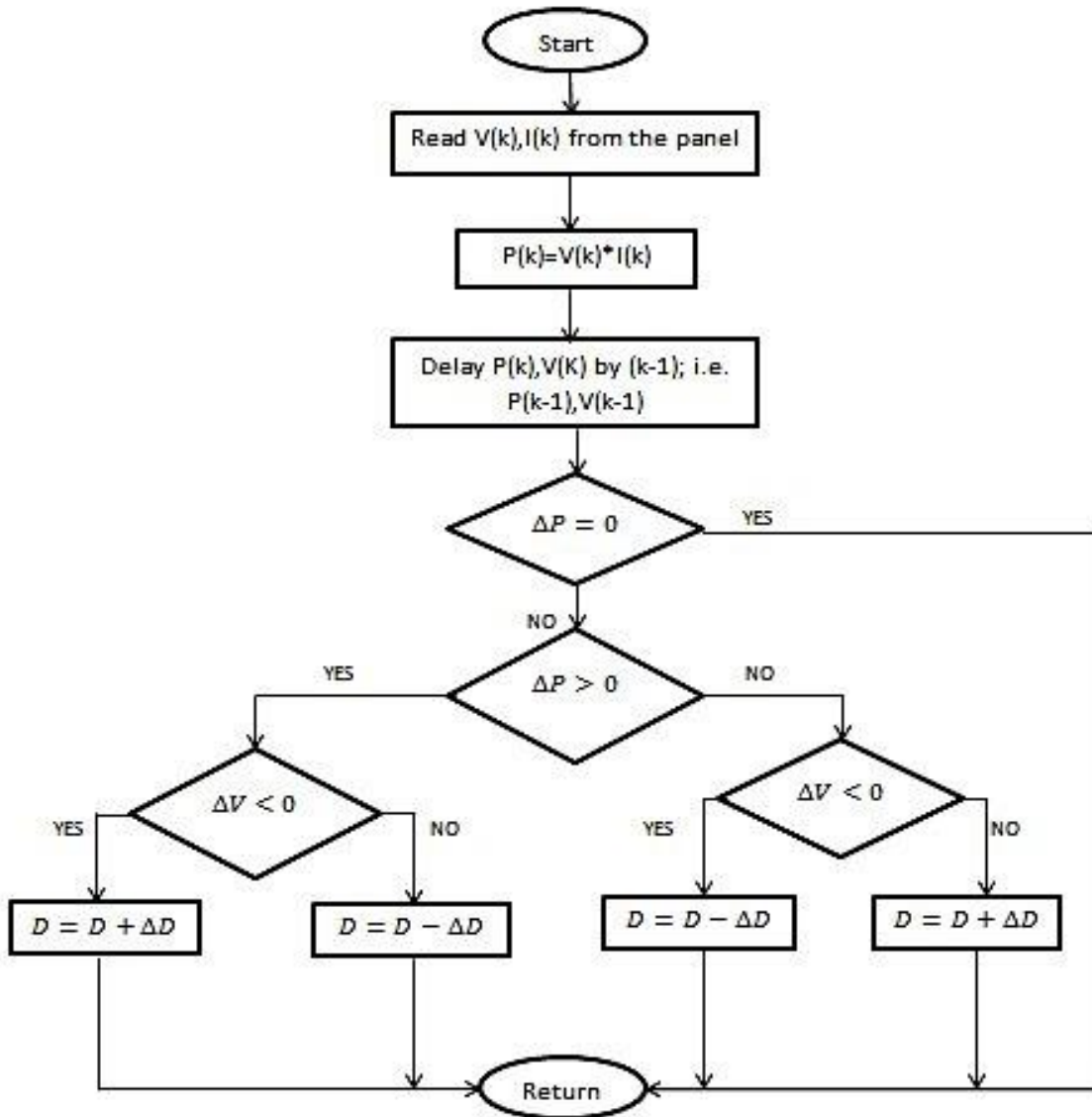


Figure 2.4: Flowchart for identifying MPPT [25]

Figure 2.4 shows the algorithm for MPPT system. Here voltage and current from PV output terminal is measured and power output is calculated. Reference voltage D is varied for which power is calculated and then increased or decreased to get to MPP. The loop of the system continues till the maximum power point is tracked and continuously works to keep power output at maximum point.

2.2.5 Three Phase Voltage Source Inverter (VSI)

A three-phase voltage source inverter (VSI) is a power electronic device employed for transforming DC voltage into AC voltage with adjustable frequency and magnitude. The switching action in inverters is carried out by utilizing a collection of semiconductor switches, such as IGBTs or MOSFETs.

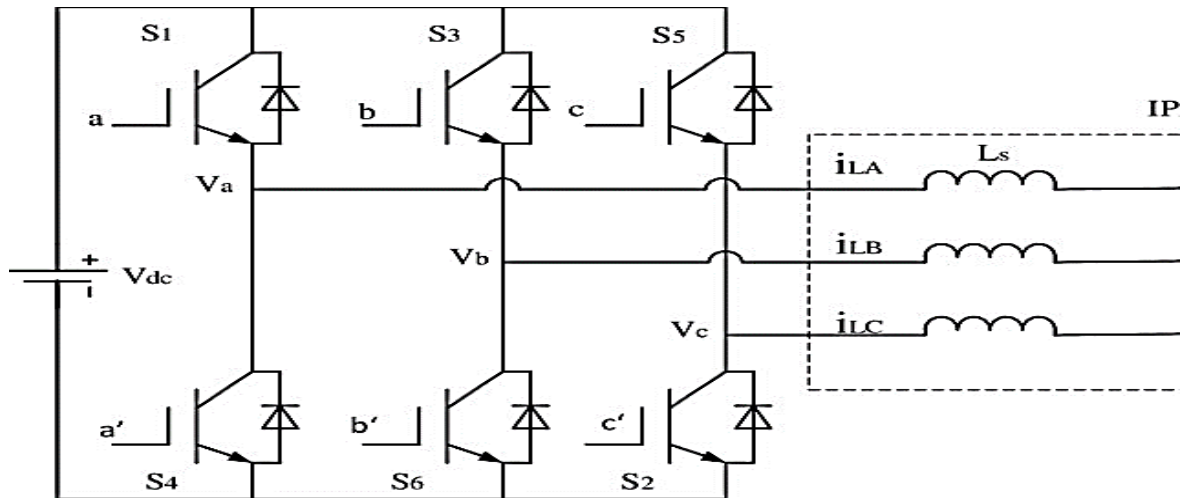


Figure 2.5: Three Phase VSI with L-filter

Figure 2.5 shows the circuit diagram of three phase voltage source inverter which involves the conversion of DC input voltage into a set of three-phase AC voltages followed by L filter. The output waveform of the VSI is a pulse-width modulated (PWM) waveform that can be regulated by adjusting the switching frequency and duty cycle of the semiconductor switches. The three-phase output voltage of the VSI can be either sinusoidal or non-sinusoidal depending on the type of modulation technique used. A three-phase VSI allows for the conversion of DC voltage generated by the PV array into AC voltage that can be fed into the grid. The VSI provides better control over the output waveform, allowing the system to operate at optimal levels and minimizing the impact of grid disturbances. The VSI is highly efficient and can handle high power levels, making it suitable for large-scale PV systems.

2.2.6 Hysteresis band control

Hysteresis band control is a technique utilized in the control of inverters within Renewable Energy Based Power Systems. It functions by comparing the instantaneous load current with a sine wave reference and ensuring that the difference remains within predetermined upper

and lower limits. It offers various advantages, including simplicity, resistance to variations in load parameters, rapid dynamic response, and inherent maximum current limitation. Due to its robust nature, it finds extensive use in renewable energy-based power plants, such as PV converter systems, Wind Energy conversion systems, and control systems for Wind Energy Applications. These controllers are simple and cost-effective to implement but do not provide precise control, as the output oscillates around the reference value within the hysteresis band.

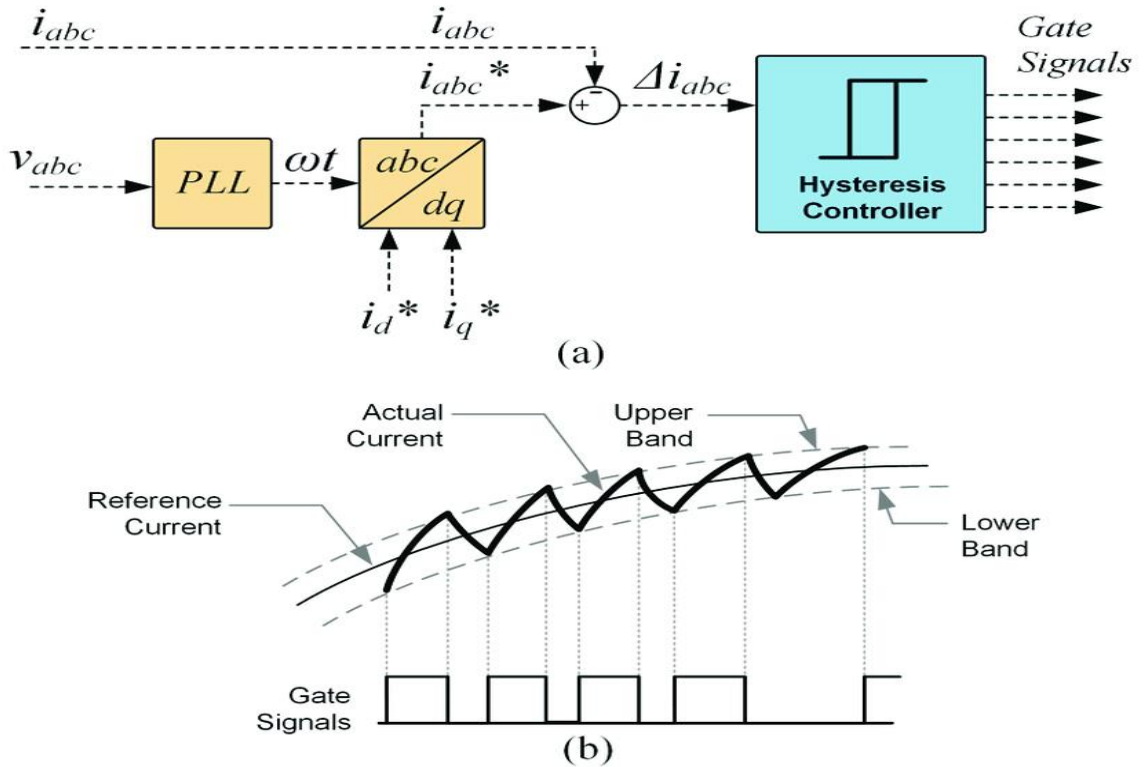


Figure 2.6: Schematic diagram and gate signals for hysteresis current controller [26]

Figure 2.6 consists of on/off control, dead band control, PID control, and its variations. On/off control, although simple and efficient, may not be responsive enough to rapid fluctuations in the process variable (PV). Dead band, or hysteresis control, is another form of on/off control where the action is delayed until a predetermined limit set point is reached, whether ascending or descending. For feedback control, mostly PID control is used. The fundamental concept behind hysteresis current control (HCC) is to ensure that the inverter's output current closely tracks a designated current reference, denoted as i^* . This is achieved by employing an online PWM control mechanism that rapidly stabilizes the

inverter's output voltage. The controller continuously compares the instantaneous current in the load with the reference signal and adjusts the duty cycle of the PWM signal to minimize the error signal (δ) [27]. The use of a hysteresis current controller in the control of a grid-tied VSI provides several advantages. Firstly, the hysteresis current controller ensures that the output current of the VSI follows the reference current closely, minimizing the impact of grid disturbances and ensuring the stability of the grid. Secondly, the hysteresis current controller provides fast response times, allowing the system to respond quickly to changes in the output current. Finally, the hysteresis current controller is a simple and robust method of control, requiring minimal computational resources and offering high reliability [18].

2.2.7 Sequence components extraction

The initial step of dual current control method involves extracting of positive and negative sequence components. For this work, DSOGI method has been applied, which integrates the QSG along with calculations for +ve and -ve sequence component. DSOGI method has advantages in terms of accuracy, speed, and adaptability to varying frequencies improving the overall controller performance. Moreover, it acts as a bandpass filter (BPF) by effectively rejecting higher-order switching frequencies [2]. The block diagram for extraction is illustrated below:

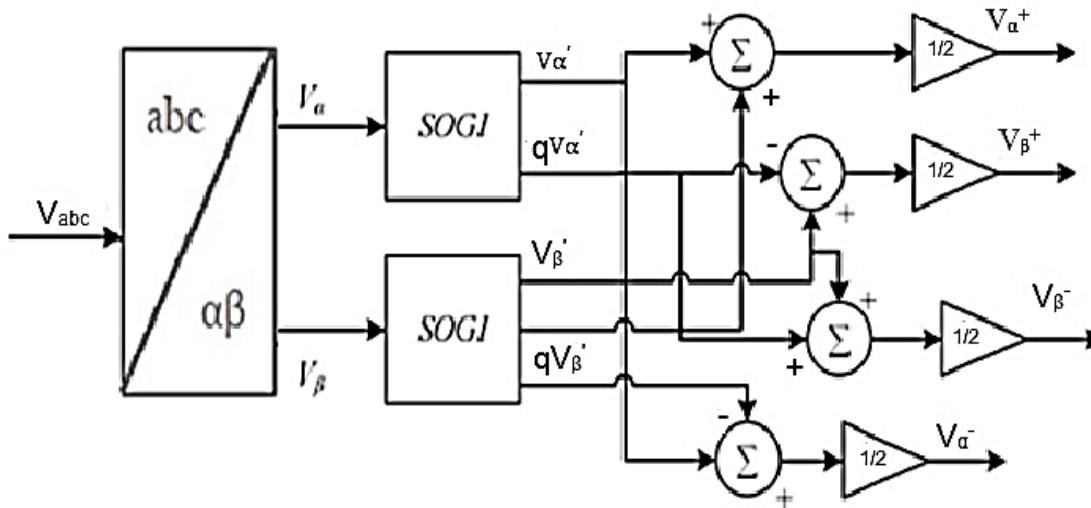


Figure 2.7: Block diagram of extraction of positive and negative sequence

The stationary voltages are transformed into two components that are orthogonal to each other, differing by 90 degrees [2]. The transfer function of the SOGI-QSG scheme is:

$$D(s) = \frac{V'}{V} (S) = \frac{K w' s}{s^2 + k w' s + w'^2} \dots\dots\dots (2.3)$$

$$Q(s) = \frac{qV'}{V} (S) = \frac{K w'^2}{s^2 + k w' s + w'^2} \dots\dots\dots (2.4)$$

As depicted in Figure 2.7, the voltage is converted into sequence components in $\alpha\beta$ voltages through an arithmetic calculation, commonly referred to as the sequence calculator, as demonstrated below.:

$$V_{\alpha}^+ = \frac{V\alpha' + qV\beta'}{2} \dots\dots\dots (2.5)$$

$$V_{\alpha}^- = \frac{V\alpha' - qV\beta'}{2} \dots\dots\dots (2.6)$$

$$V_{\beta}^+ = \frac{V\beta' - qV\alpha'}{2} \dots\dots\dots (2.7)$$

$$V_{\beta}^- = \frac{qV\alpha + V\beta'}{2} \dots\dots\dots (2.8)$$

2.2.8 SPWM (Sinusoidal Pulse Width Modulation)

SPWM is a modulation technique used in voltage source inverters to convert DC input to sinusoidal waveform. The method uses a high-frequency carrier signal modulated by a low-frequency sinusoidal signal to generate the output voltage. The modulation index and frequency of the sinusoidal signal determine the quality of the output waveform. The technique has benefits over other methods, such as lower harmonic distortion, lower switching losses, and simple implementation. It reduces electromagnetic interference and improves the efficiency of the inverter. As a result, SPWM is widely used in various applications [28].

In this approach, the reference frequency signal is compared with a triangular carrier to generate a switching signal for Pulse Width Modulation (PWM). This signal is used to control the upper and lower switches of the inverter in a complementary manner, as well as the switches of both legs [29]. The terminal voltages of the inverter, V_{AN} and V_{BN} , are obtained, and the output voltage of the inverter, V_{AB} , is calculated as follows:

$$V_{AB} = V_{AN} - V_{BN} \dots\dots\dots (2.9)$$

The waveform of V_{AB} alternates between +ve and -ve DC voltages, earning this scheme the name bipolar PWM, as illustrated in figure 2.8.

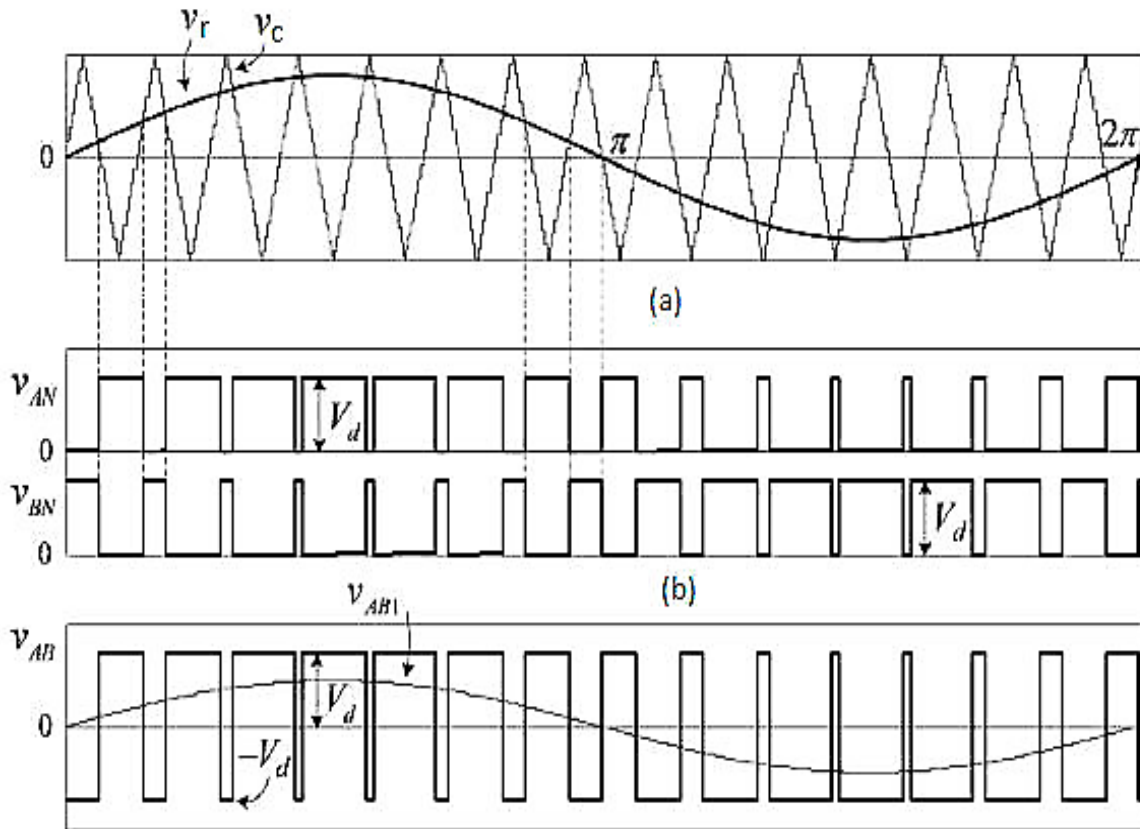


Figure 2.8: waveforms of working of SPWM technique [29]

In figure 2.8, the magnitude of carrier signal i.e., triangular is compared with the reference sinusoidal signal to get the pulse thus controlling switching of the IGBT's and obtaining the respective voltage at the output of the inverter.

CHAPTER THREE

METHODOLOGY

3.1 Overview

For the use of grid VSI in solar power plants to connect to the grid, it is preferable to directly control magnitude and voltage of the system to get better quality AC power. The methodology of proposed system is:

Step1: Study of basic theories and literature related to project.

Step 2: Development of MATLAB simulation model of 50 KW grid connected PV system using hysteresis band control

Step 3: Successfully injected the maximum power from PV to the grid.

Step 4: The sequence components of current and voltage were successfully extracted.

Step 5: Observed the effects of unbalanced load and unbalanced fault condition in grid tied inverter.

Step 6: Modified the hysteresis current controller to improve the performance of the inverter.

Step 7: A new inverter dual current control mechanism was developed replacing the hysteresis current controller to limit the current flowing through the inverter.

3.2 Simulation Tool

For modeling of our PV system and simulation is done in MATLAB/SIMULINK (2018a). MATLAB is a proprietary programming language and numeric computing environment that supports multiple paradigms. It facilitates matrix manipulation, visualization of functions and data, implementation of computational procedures, creation of user interfaces, and seamless integration with programs written in different programming languages.

3.3Description

3.3.1 Selection of PV panel

Table 3.1 : PV specifications

Components used	1 Soltech 1STH – 215 – P
Maximum Power	213.5 W
Open Circuit Voltage (V _{oc})	36.3 V
Short Circuit Current (I _{sc})	7.35 A
Parallel strings	11
Series-connected modules per string	22
Total open circuit voltage	$36.3 * 22 = 798.6 \text{ V}$
Total maximum Power	$22*11*213.5 = 51.667 \text{ KW}$

3.3.2 Structure of PV system

In the PV system there are mainly following components; PV array, Buck-Boost converter with MPPT control. In a photovoltaic system the buck-boost converter system is used to transmit the output voltage to higher voltage by changing the correct voltage to input of converter that consist of diode, inductor, capacitor elements and MOSFETS/IGBT as switch. To determine the MPP of a PV cell, it is necessary to operate the cell across a wide range of voltages (V) and currents (I). The MPP of an irradiated cell can be determined by incrementally raising its voltage from zero (short circuit) to its maximum value (open circuit). In this model, the P&O algorithm is employed to track the maximum power output of the solar panel. The P&O algorithm is aptly named as it observes the output power of the array and perturbs (increments or decrements) the power based on corresponding adjustments in the array voltage or current.

3.3.3 Block Diagram of grid connected PV system

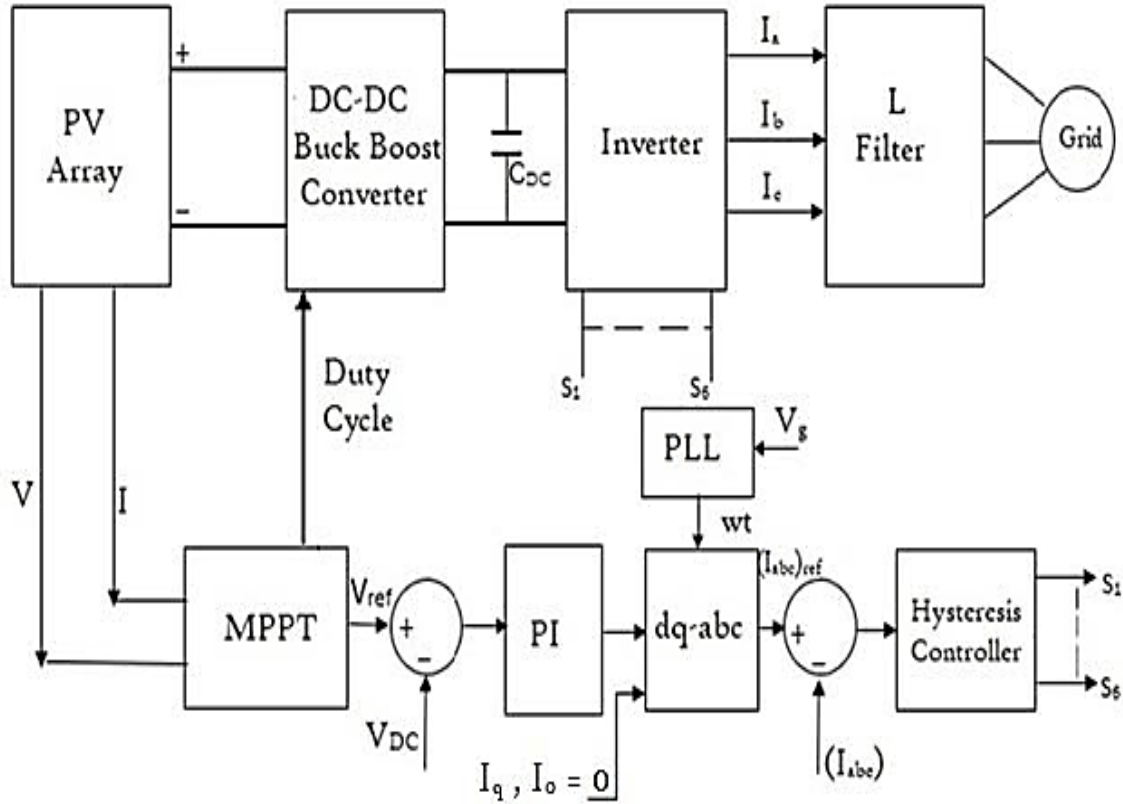


Figure 3.1: Block Diagram of Grid Connected PV System

Figure 3.1 shows the block diagram of Grid Connected PV System. The PV Array is connected to the inverter through buck boost converter to maintain the maximum power. To ensure maximum power tracking, it is crucial for the PV system to operate at the voltage that corresponds to the maximum power point. While a boost converter can be an option, it becomes ineffective when the PV voltage exceeds the maximum power voltage, requiring voltage reduction. However, this case is equivalent to open circuit condition which is rare during operating condition. So, for the efficient operation, a buck boost converter is used. The voltage across the PV and current flowing through the PV are sent to the MPPT which uses the P & O algorithm to generate a duty cycle that controls the operation of buck boost converter such that the PV works at the voltage corresponding to the maximum power. The voltage generated by the MPPT block is compared with the dc link capacitor voltage then uses PI controller to generate the reference d component of current. And then keeping the q component zero as there is no consideration of reactive power, the 3- ϕ current reference is

generated using dq - abc conversion. PLL block is used to generate the frequency of grid which is required for dq - abc conversion. The reference current is compared with the actual current flowing through the inverter to get the PWM signal to control switching operation of the IGBT's used in the inverter.

3.3.4 Simulation model of PV MPPT

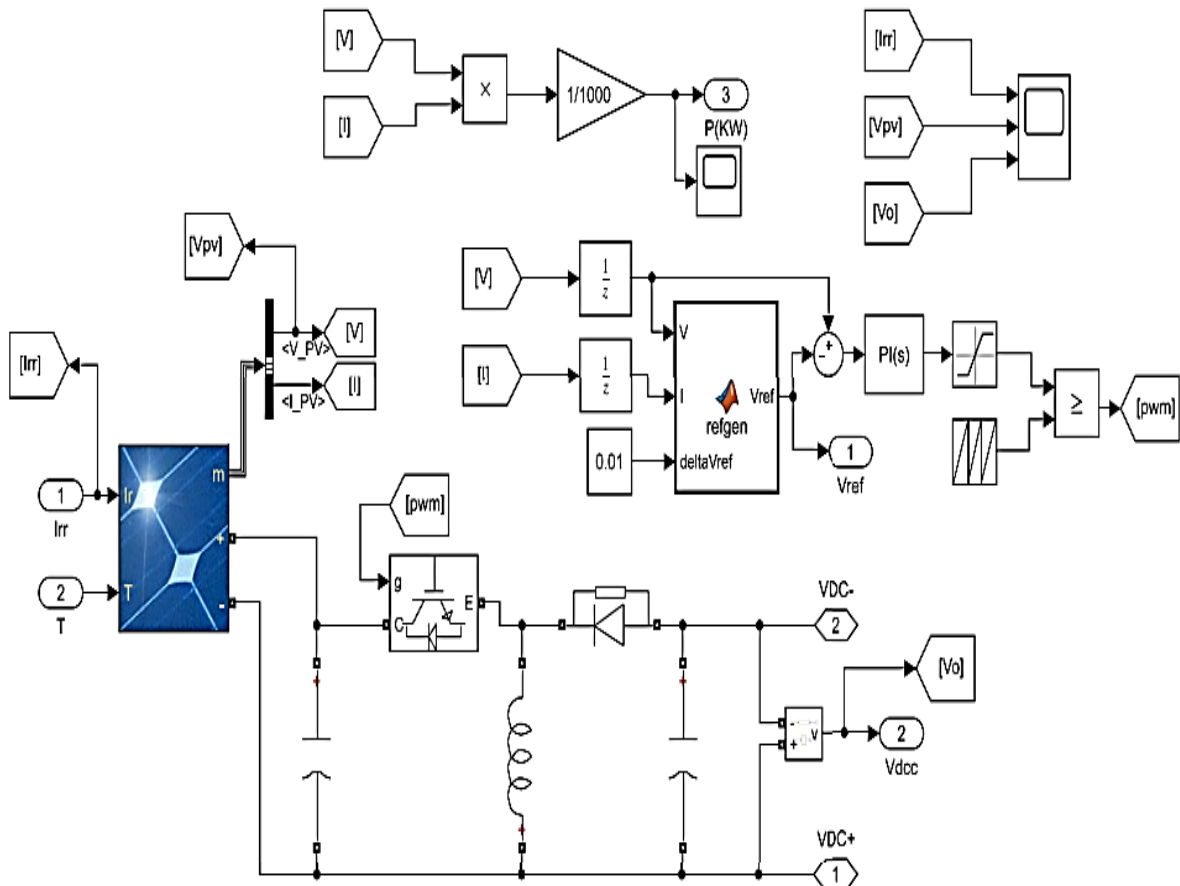


Figure 3.2: Simulation model of PV MPPT

Figure 3.2 shows the simulation model of solar panel connected with the dc-dc buck- boost converter followed by MPPT system. The voltage across of terminal and the current flowing through it is measured and sent as an input to MPPT block that uses P&O algorithm to generate the reference voltage corresponding to the maximum power. The reference voltage is passed through a PI controller and compared with carrier signal to generate the pwm signal. The pwm signal is used to control the switching IGBT of buck-boost converter thus tracking the voltage corresponding to the maximum power.

3.3.5 Simulation model of hysteresis band controller

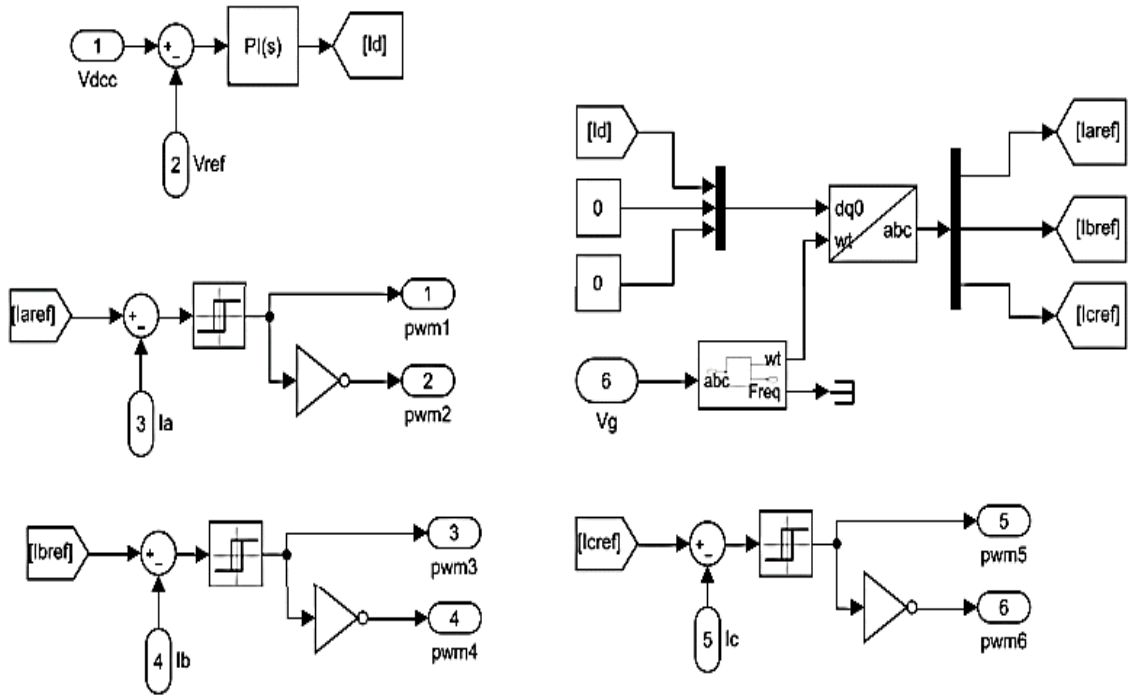


Figure 3.3: Simulation model of hysteresis band controller

Figure 3.3 illustrates the simulation model of hysteresis band controller. The voltage across dc link capacitor is compared to reference voltage generated by the MPPT and a PI controller is used to generate a control signal. The change in voltage across dc link capacitor is equivalent to the active power transfer through the inverter. The high voltage across capacitor i.e., overcharged condition means the power transfer through the inverter is less and vice versa. Thus, the control signal so generated can be used as a reference current for d- component of current i.e., I_d equivalent to the active power transfer. And then keeping the q component zero as there is no consideration of reactive power, the three-phase current reference is generated using dq - abc conversion. We have used PLL block to generate the frequency of grid which is required for dq - abc conversion. The three-phase reference current is compared to actual current flowing through the inverter and passed to a hysteresis band controller to generate the pwm signal. There is certain band limit of 5% for 1000 W/m^2 irradiance in the hysteresis control so as to minimize the switching loss. The pwm signal controls the switching operation of all the IGBT's.

3.3.6 Simulation model of grid connected PV system

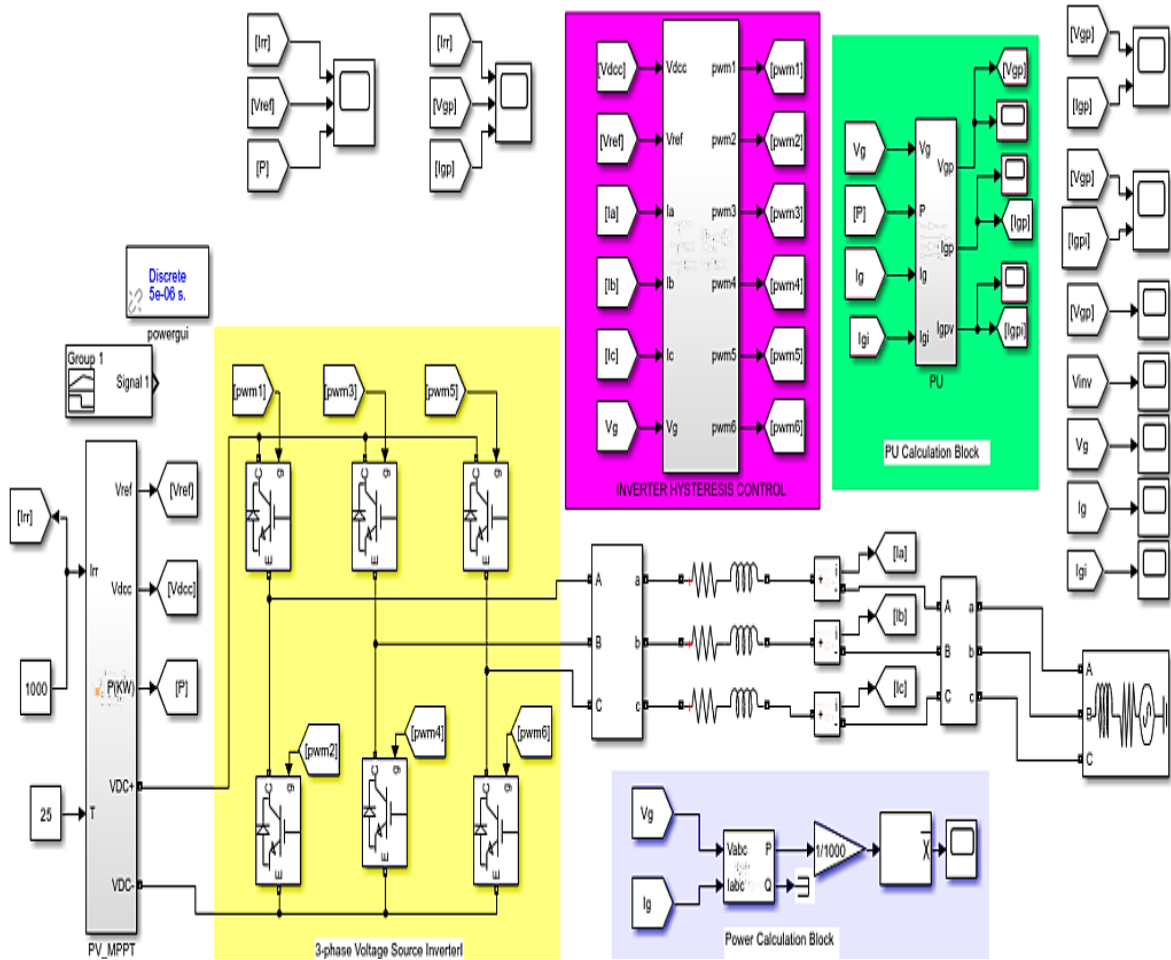


Figure 3.4: Simulation model of PV System

Figure 3.4 shows the simulation model of grid connected PV system using Hysteresis band control. The working mechanism is same as explained in figure 3.1. Here, we have designed a PV panel to connect it to the 400V grid system through the three- phase voltage source inverter and buck boost converter. The irradiances and temperature are the input to the PV panel. The signal builder block is used to provide varying irradiances as a input to the PV panel. We have used P&O algorithm for maximum power tracking in PV system by controlling the switching of the MOSFET used in the buck boost converter. And using the hysteresis band control, the actual current flows the reference current obtained by comparing the PV voltage corresponding to the maximum power and the voltage across the dc link capacitor. The pwm signal generated by hysteresis control is then used to control the

switching operation of the IGBT's used in the inverter. The PU calculation block is used to get the all voltages and current in pu which makes the visualization easier for the varying irradiances. And various scope blocks are used for observing the various parameters.

3.3.7 Inverter dual current control

The figure below depicts the control design of the inverter used in this study. In order to regulate specific system states, a conventional PI controller is employed, utilizing proportional gain and integrator components. The PI controller receives the error from tracking the positive and negative reference current. Next, the feed-forward voltage is merged with the corresponding voltage calculation, resulting in the generation of commanded voltages for the d-axis and q-axis according to the given equation:

$$U_d = (K_p + \frac{K_i}{s})(i_d^* - i_d) - \omega L i_q + V_d \dots\dots\dots (3.1)$$

$$U_q = (K_p + \frac{K_i}{s})(i_q^* - i_q) - \omega L i_d + V_q \dots\dots\dots (3.2)$$

The voltages u_d and u_q are initially expressed in the terms of d-q components, and it is necessary to convert them into stationary reference frame i.e abc voltages using the conversion process from dq to $\alpha\beta$ accomplished using equation shown below [2].

$$\begin{pmatrix} V_\alpha \\ V_\beta \end{pmatrix} = \begin{pmatrix} \sin \theta & \cos \theta \\ \cos \theta & -\sin \theta \end{pmatrix} \begin{pmatrix} V_d \\ V_q \end{pmatrix} \dots\dots\dots (3.3)$$

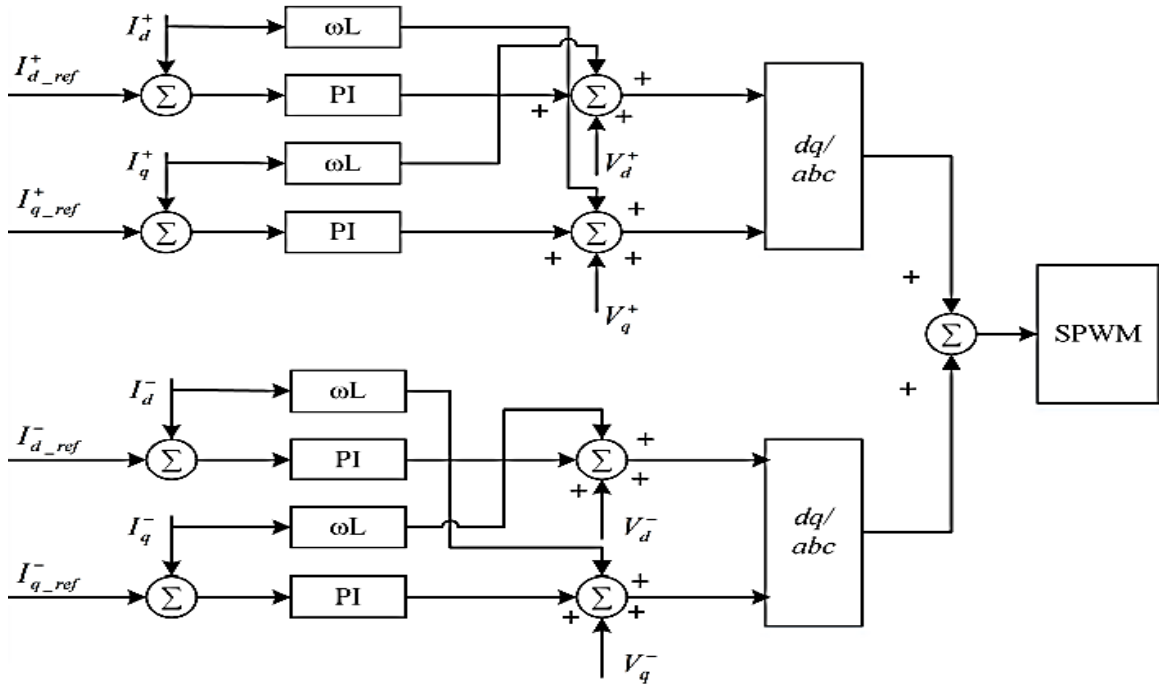


Figure 3.5: Inverter dual current control

Once the $\alpha\beta$ components are obtained, the calculation of the abc components is performed using:

$$V_a = V_\alpha \dots\dots\dots (3.4)$$

$$V_b = \frac{-V_\alpha}{2} - \frac{\sqrt{3}}{2}V_\beta \dots\dots\dots (3.5)$$

$$V_c = \frac{\sqrt{3}}{2}V_\beta - \frac{V_\alpha}{2} \dots\dots\dots (3.6)$$

Moreover, the PWM signal for three phases of the inverter is acquired through:

$$m_{a,b,c} = \frac{2V_{a,b,c}}{V_{dc}} \dots\dots\dots (3.7)$$

The modulating signal is utilized to control the SPWM (Sinusoidal Pulse Width Modulation) of the inverter, resulting in the generation of the desired voltage at the corresponding pole of the inverter. [2].

CHAPTER FOUR

RESULTS AND DISCUSSION

4.1 PV panel characteristics

242 PV panels of specifications shown in table 3.1 have been placed in combination such that it provides 51.667 KW power. The power supply varies according to irradiance and temperature. For maximum power delivery to the grid at given irradiance voltage has to be maintained at level where maximum power transfer is possible.

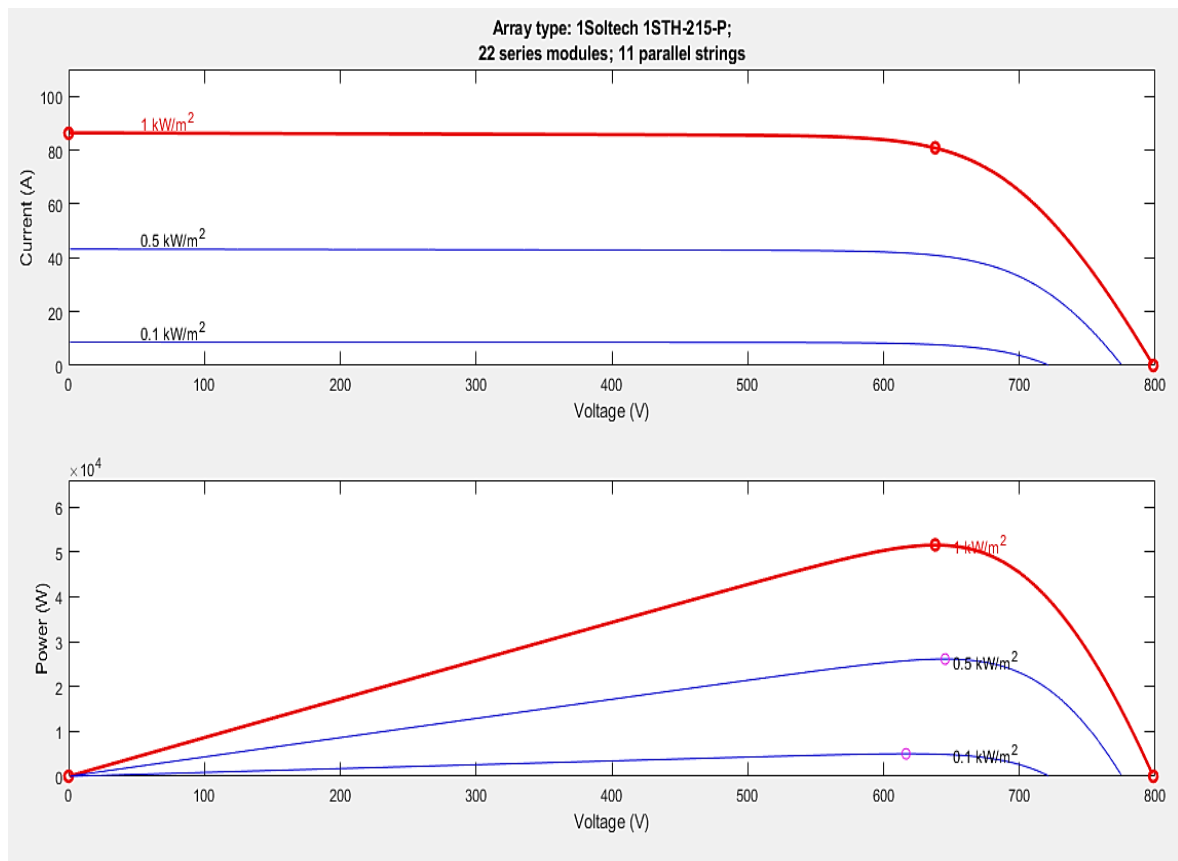


Figure 4.1: I-V and P-V characteristics of PV system at different irradiance level

From fig 4.1 shows the I-V and P-V characteristics of the selected PV array. From the figure the current and power variation with respect to voltage level can be observed at different irradiance level. The maximum power point for different irradiance level can also be observed along with the corresponding voltage level. The voltage level for maximum power and the maximum power varies according to irradiance level.

Observing the maximum power delivered by the PV array to the grid at different irradiance level we get the voltage corresponding to maximum power delivery for given irradiance.

At 1 KW/m² irradiances, max power = 51.58 KW at 638 V

At 0.5 1 KW/m² irradiances, max power = 26.13 KW at 645.3 V

At 0.1 KW/m² irradiances, max power = 5.005 KW at 616.5 V

4.2 MPPT verification in VSI using hysteresis band controller

The working of MPPT to deliver maximum power to the grid is better demonstrated by following graphs:

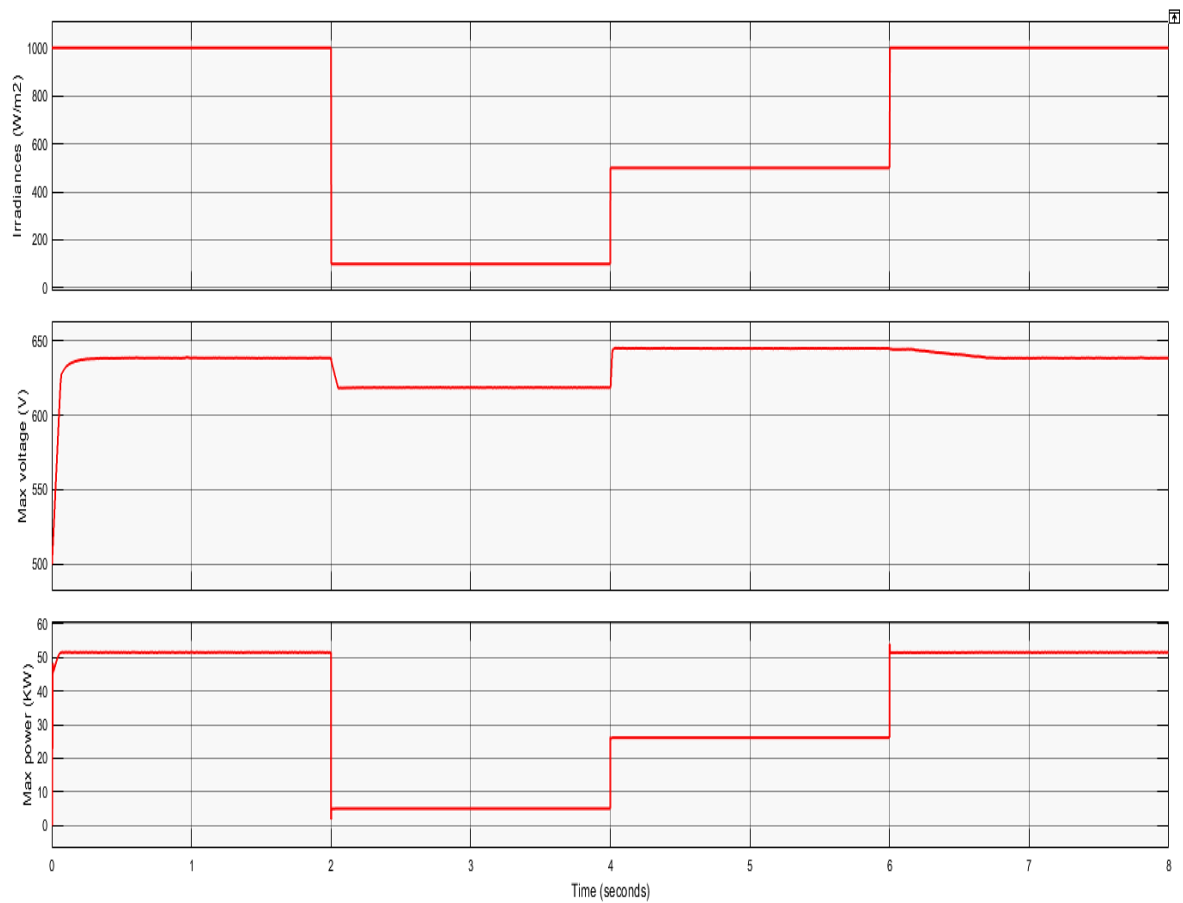


Figure 4.2: MPPT demonstration

The waveforms in figure 4.2 demonstrate the MPPT system at work as the PV system power delivery and corresponding voltage level for maximum power point is tracked by the MPPT. We can see that at 1000 w/m² irradiance the power delivered is maximum i.e., around 51KW and respective voltage is around 638 V. Similarly, the voltage level corresponding to maximum power is tracked at the output of PV terminal despite of the change in irradiance thus delivering maximum power at all varying irradiance.

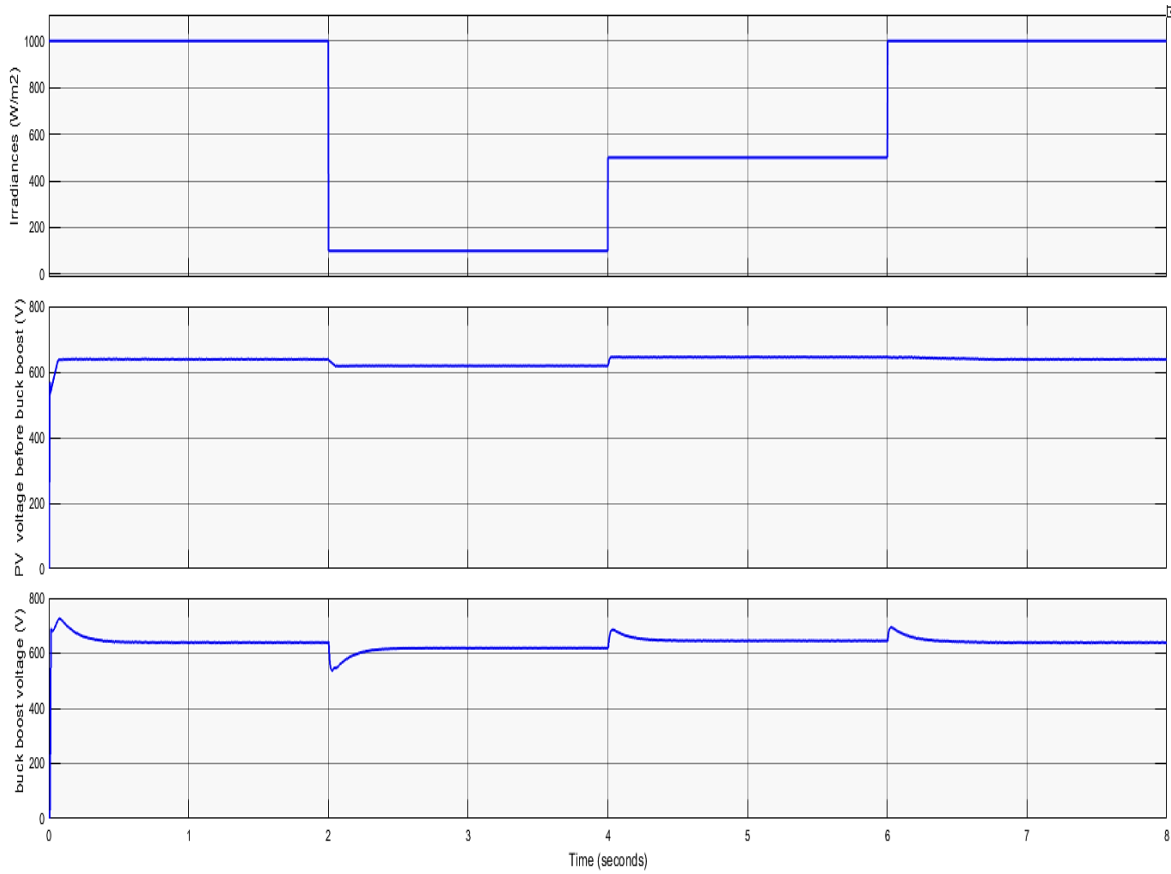


Figure 4.3: Voltage before and voltage after buck-boost converter

Figure 4.3 shows the voltage waveform before and after the buck-boost converter i.e., voltage across the PV terminal and dc link capacitor respectively for varying irradiances. We can see that the PV terminal voltage is maintained equivalent to the voltage corresponding maximum power and that voltage is tracked at the output of buck-boost converter thus maintaining the dc link capacitor voltage and delivering the power to the inverter.

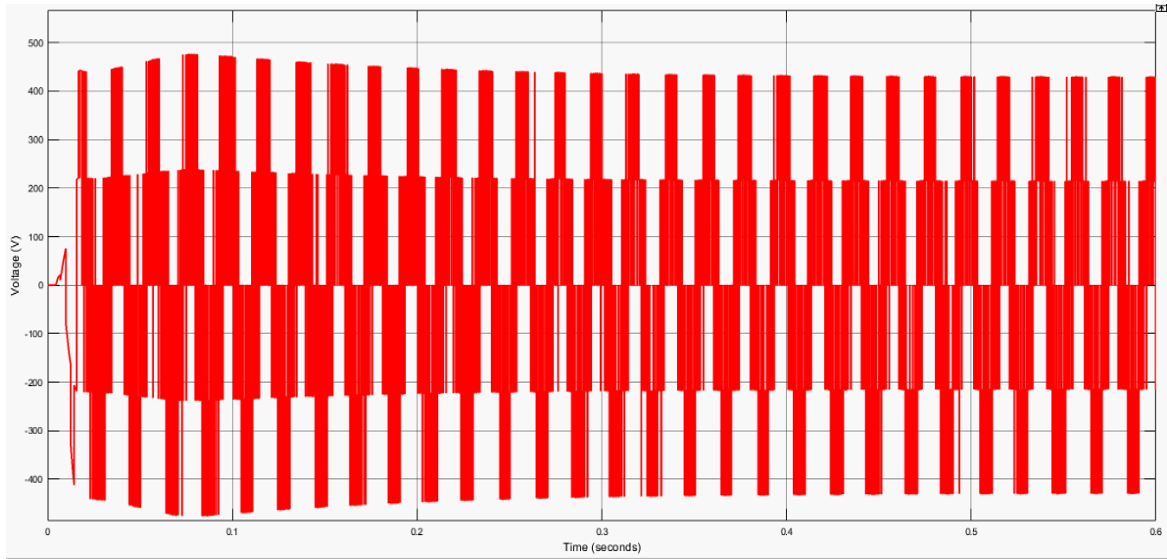


Figure 4.4: Inverter output line voltage before filter

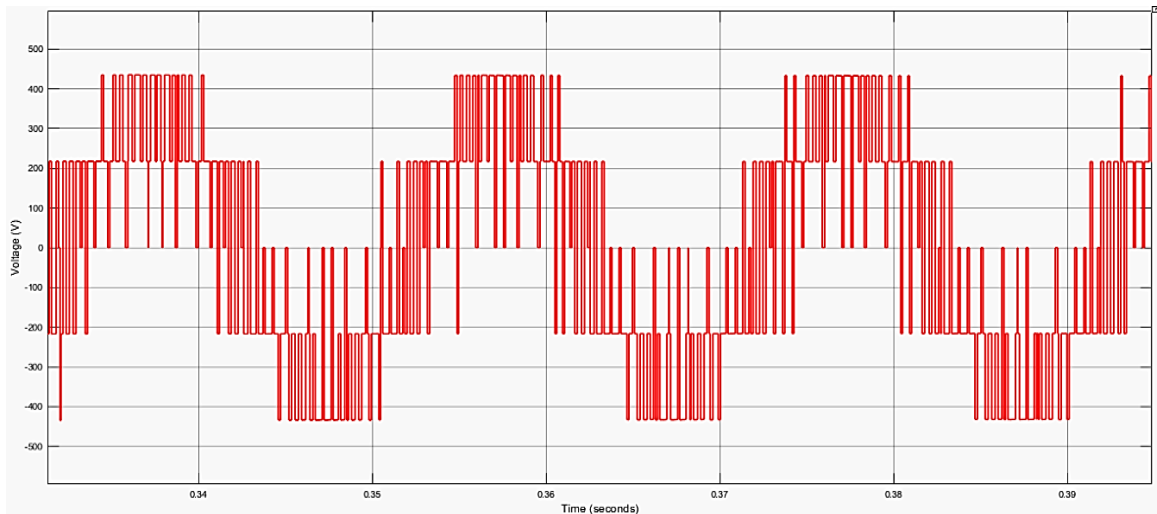


Figure 4.5 Magnified view of inverter output line voltage before filter

Figure 4.4 shows the line voltage waveform at the output of inverter i.e., before filter and figure 4.5 is its magnified view. We can observe that the voltage waveform is changing as per the switching of IGBT's forming the quasi - square type waveform and its peak value is about two-third of the input dc voltage.

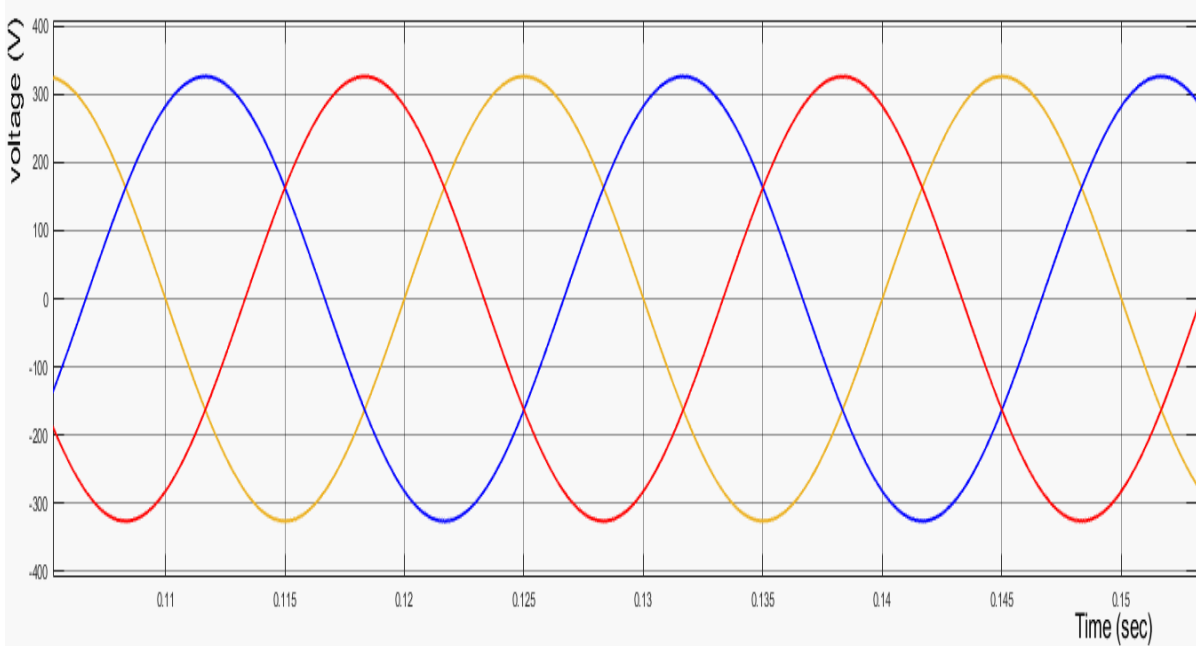


Figure 4.6: Magnified view of grid phase voltage

Figure 4.6 shows the magnified waveform of grid phase voltage. The grid voltage is of 400V(phase-phase) thus obtaining the peak phase voltage of around 326V and is pure sinusoidal.

Theoretical current value

- For 1 KW/m² irradiances, P= 51.58 kw

$$\begin{aligned} \text{Then, max per phase peak current} &= \frac{51.58 \times 1000}{3 \times \frac{400}{\sqrt{3}}} \times \sqrt{2} \\ &= 105.28 \text{ A} \end{aligned}$$

- For 500 W/m² irradiances, P= 26.13 kw

$$\begin{aligned} \text{Then, max per phase peak current} &= \frac{26.13 \times 1000}{3 \times \frac{400}{\sqrt{3}}} \times \sqrt{2} \\ &= 53.33 \text{ A} \end{aligned}$$

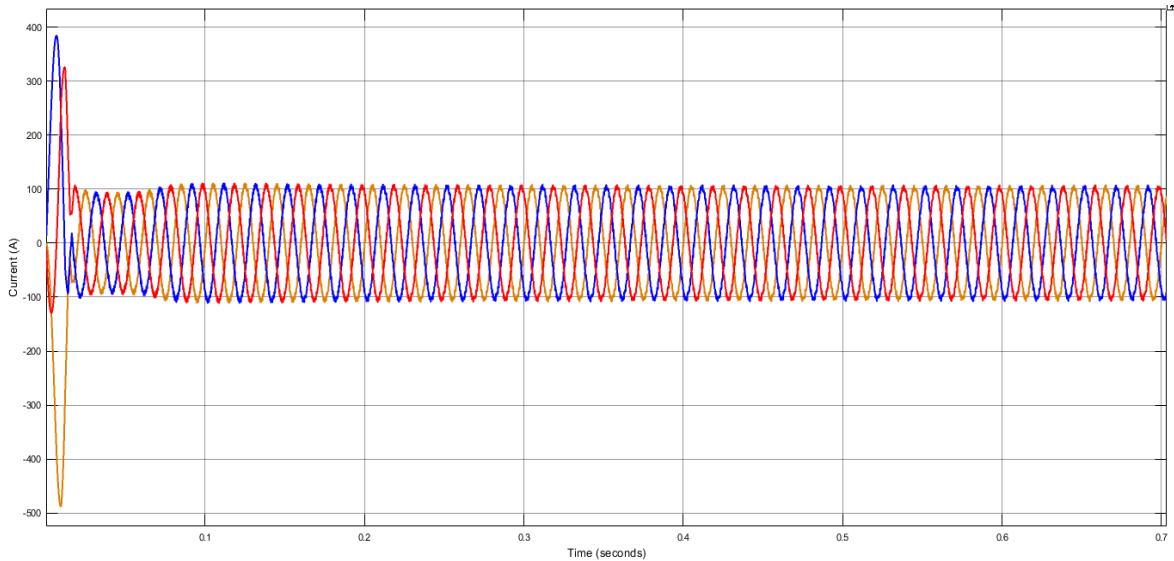


Figure 4.7 Phase current delivered to grid for irradiances of 1000W/m²

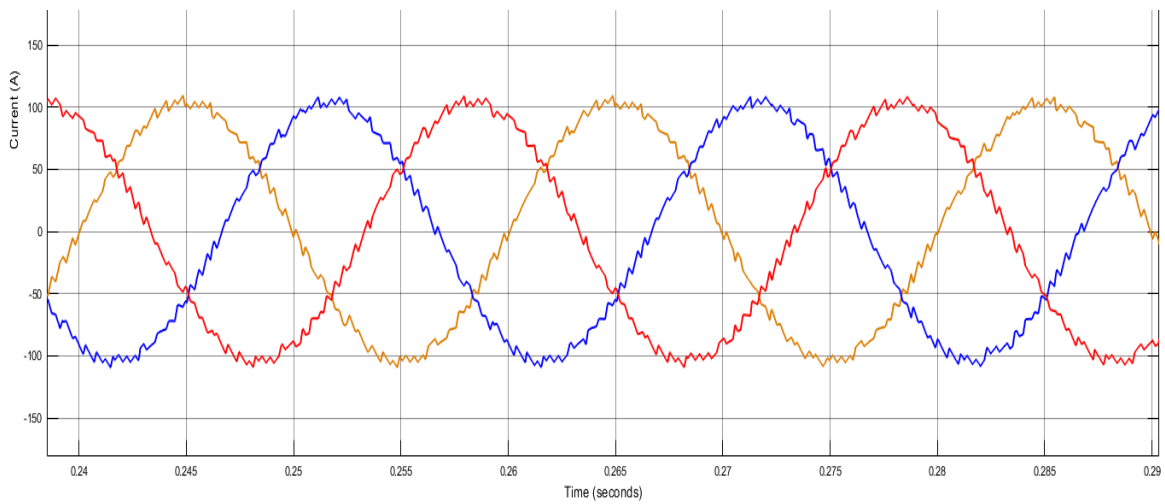


Figure 4.8: Magnified view of phase current delivered to grid for irradiances of 1000 W/m²

Figure 4.7 shows the phase current delivered by the inverter to the grid for irradiances of 1000W/m² and figure 4.8 is its magnified view whose peak value is around 105 A which is the actual theoretical value that should be flowing to the grid. As seen in the curve, the phase current delivered to the grid regulated by hysteresis band controller is not smooth. It is because we allow certain band limit in the hysteresis band controller. This is done so that the switching losses can be minimized which are quite high for low permissible error/deviation as switching is more frequent. The harmonics can be filtered out of the phase current smoothen it before supplying it to the grid.

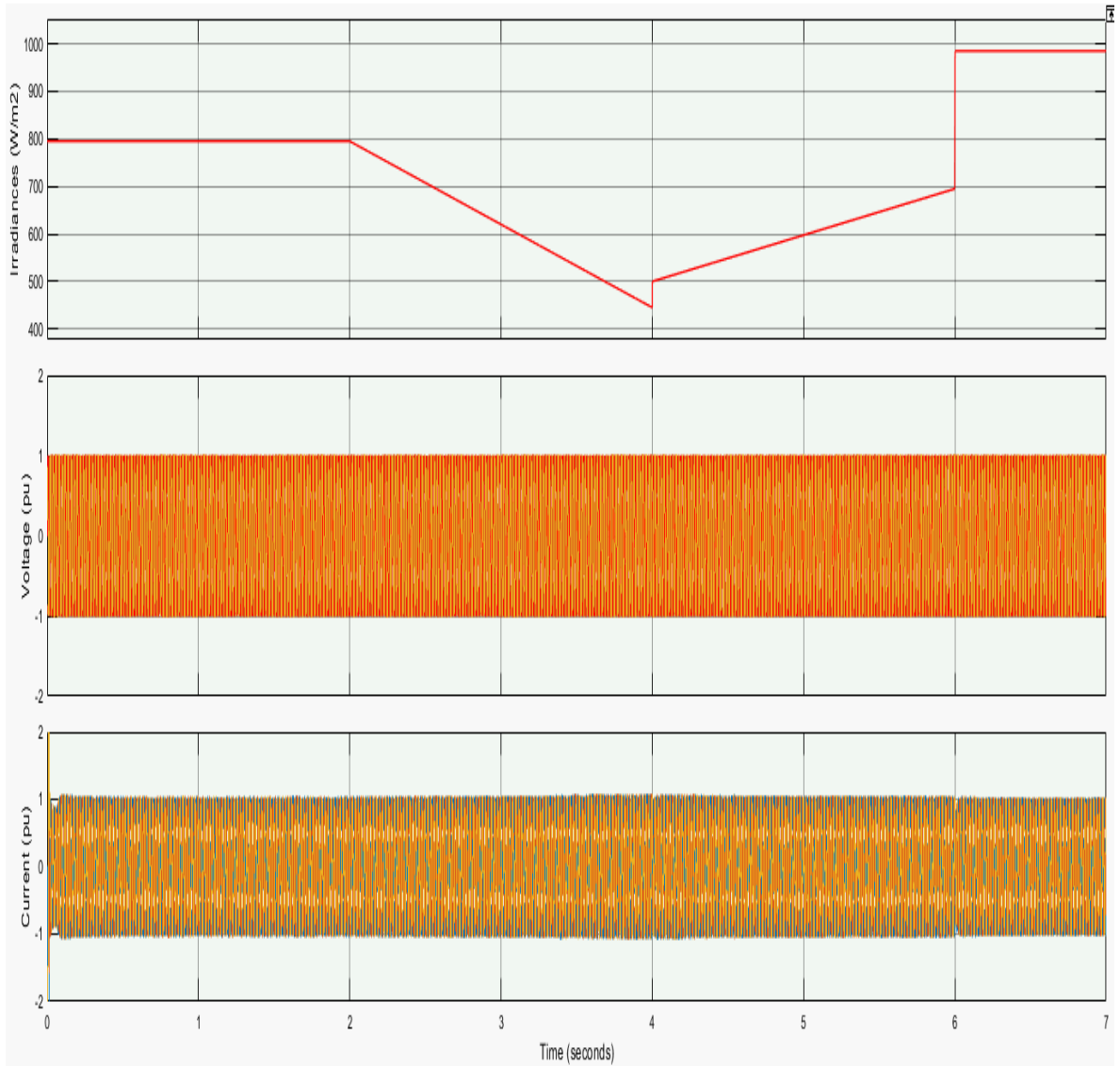


Figure 4.9 Per phase grid voltage and current under varying irradiances

Figure 4.9 shows the per phase grid voltage and current flowing through grid under varying irradiances. The 1 pu of voltage is equivalent to the peak value of rated grid voltage whereas 1 pu of current is equivalent to the peak value of phase current corresponding to the maximum power transfer. Here, we can observe that the peak value of voltage and current is always 1 pu despite of the random change in the irradiance thus delivering maximum current to the grid at rated voltage under varying irradiances.

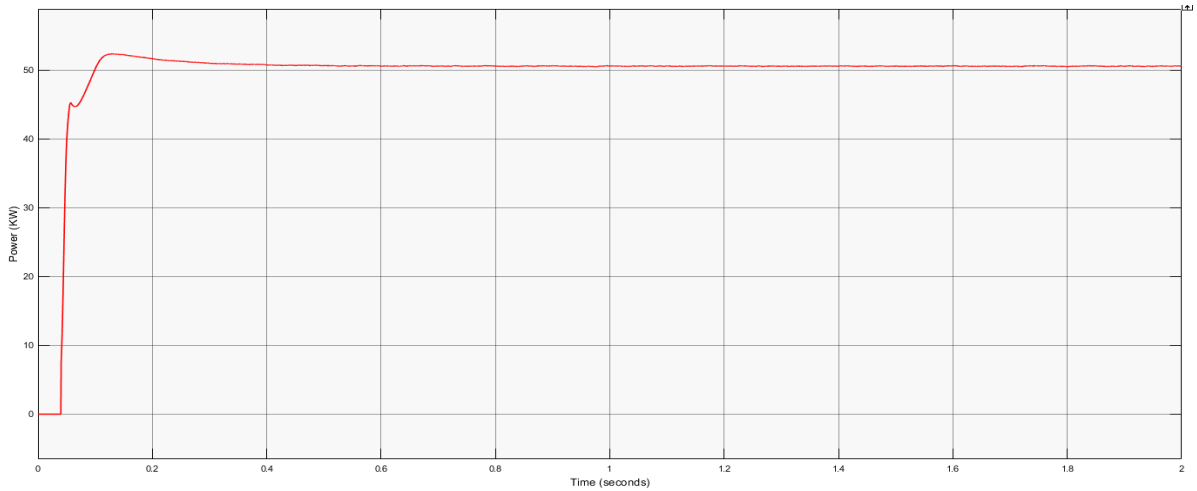


Figure 4.10 Power delivered to grid for irradiances of 1000W/m²

Figure 4.10 shows the active power delivered to the grid for irradiances of 1000W/m². At steady state, the power delivered is around 51 KW which is equal to the value observed from PV curve in figure 4.1.

4.3 Effects of unbalanced load condition in grid tied inverter

After developing simulation model of PV system with MPPT and hysteresis band-controlled inverter connected to the grid, the unbalanced load conditions were simulated in the simulation model to observe and understand its effects on the system as shown in figureA2.

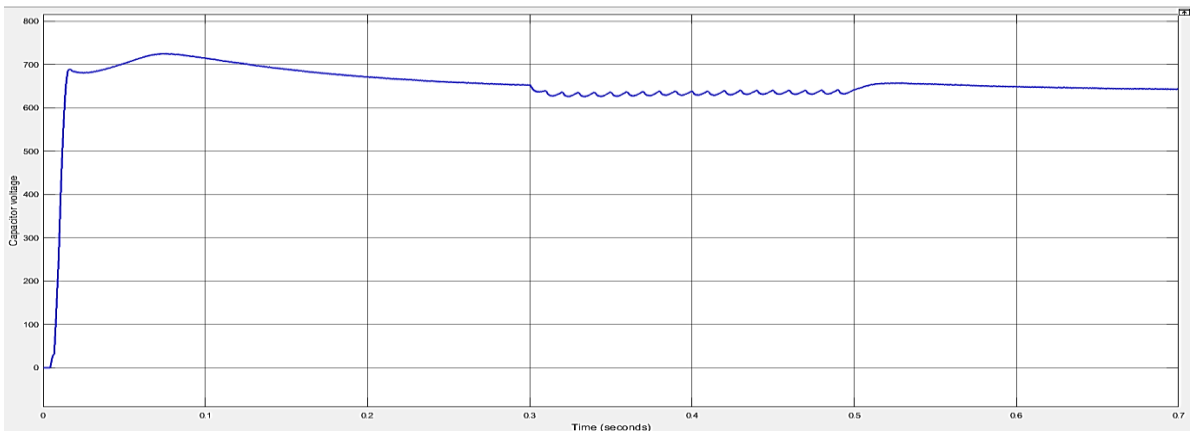


Figure 4.11: Voltage across the capacitor for unbalanced load at the inverter side between 0.3-0.4 sec

Figure 4.11 shows the voltage of DC link capacitor during unbalanced load condition. The unbalance period is from 0.3s to 0.4s. As we can see from the graph the capacitor voltage fluctuates within the time frame when load is unbalanced and smoothens once the system load is balanced.

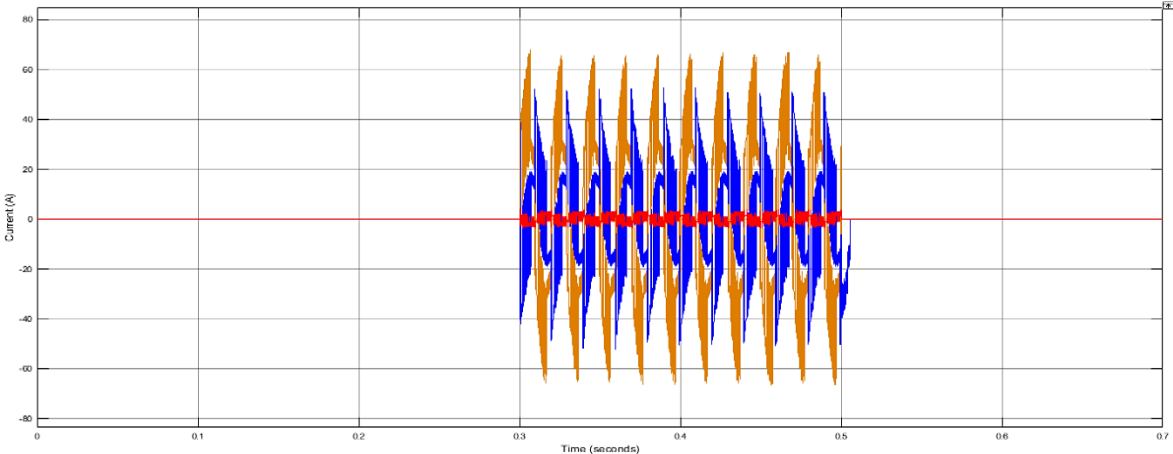


Figure 4.12: Phase current flowing through the grid for unbalanced load at the inverter side between 0.3-0.5 sec

Figure 4.12 shows the current flowing through the isolated unbalanced load at the inverter side between 0.3-0.4 sec. The small number of current flows through the lightly loaded phase i.e., R phase and a current of around 80A flows through the heavily loaded phase i.e., Y phase.

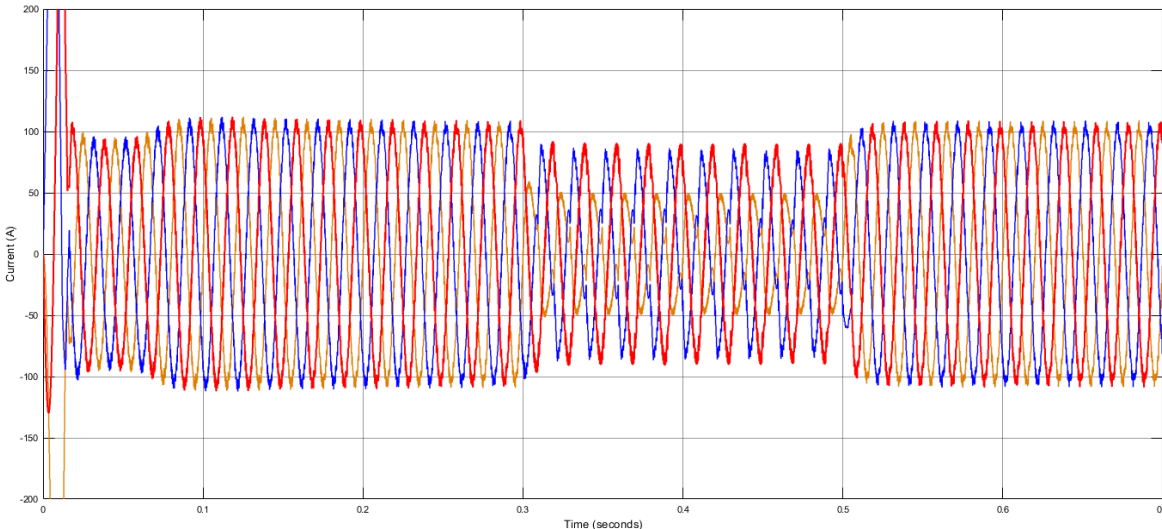


Figure 4.13: Phase current flowing through the grid for unbalanced load at the inverter side between 0.3-0.5 sec

Figure 4.13 shows the phase current flowing through the grid for unbalanced load at inverter side between 0.3-0.5 sec. We can see that the inverter supplies the rated amount of current at normal condition whereas there is decreasing of each phase current supplied to grid. This decrement is due to portion of current supplied by the inverter goes to unbalanced load.

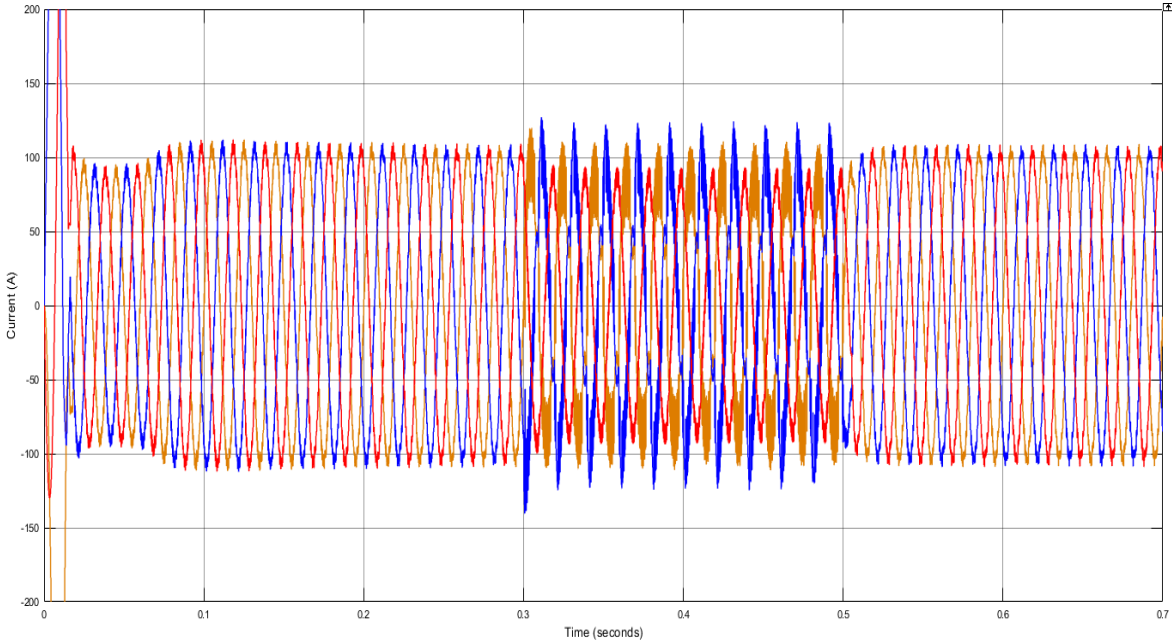


Figure 4.14: Phase current flowing through the inverter for unbalanced load at the inverter side between 0.3-0.5 sec

Figure 4.14 depicts the phase current flowing through the inverter for the unbalanced load at the inverter side between 0.3-0.5 second. We can see that the current supplied by the inverter remains doesn't fluctuate much as portion of current goes to grid as well as unbalance load during unbalanced loading condition.

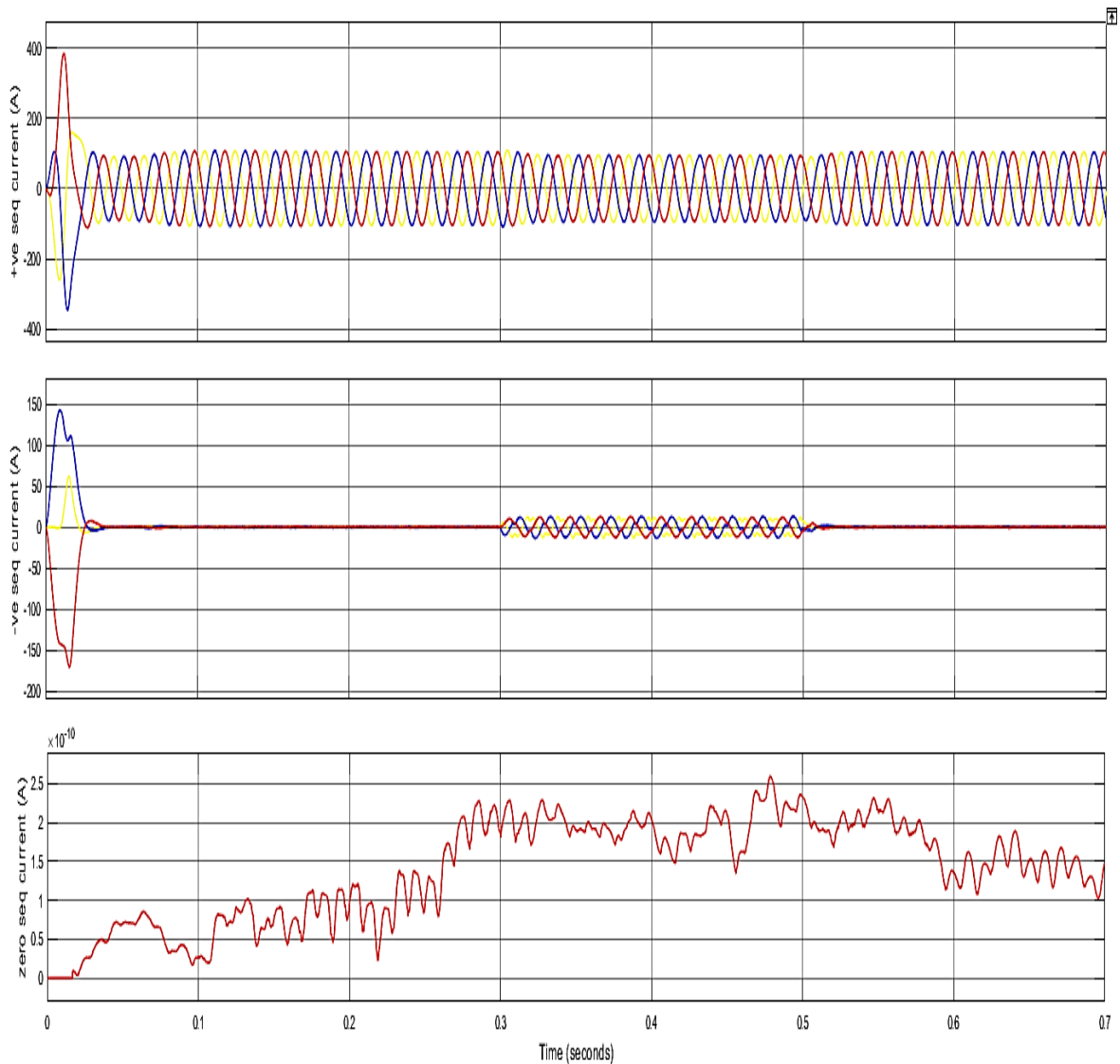


Figure 4.15: +ve, -ve and zero sequence components of current flowing through the inverter for unbalanced load at the inverter side between 0.3-0.5 sec

Figure 4.15 shows the current flowing through the inverter in term of its sequence components for unbalanced load at the inverter side between 0.3-0.5 sec. We can see that during unbalance load at the inverter side, the positive sequence current is almost unchanged, slightly variation in negative sequence current and the zero-sequence current is almost zero. From this we can conclude that inverter operation is not much affected by unbalance fault on inverter side.

Conclusion obtained from unbalanced load at inverter side

- Voltage across dc link capacitor doesn't change much.
- Inverter supplies the rated unbalanced load at the inverter side and rest is supplied to the grid.
- Small presence of -ve sequence current and zero sequence current is zero.
- Inverter operation isn't affected by the unbalanced load and is safe.

4.4 Effects of unbalanced fault condition at the grid side in grid tied inverter

Similarly, the LG fault was given on grid side using three phase fault block in the simulation model of PV system with MPPT and hysteresis band-controlled inverter as shown in figure A.3.

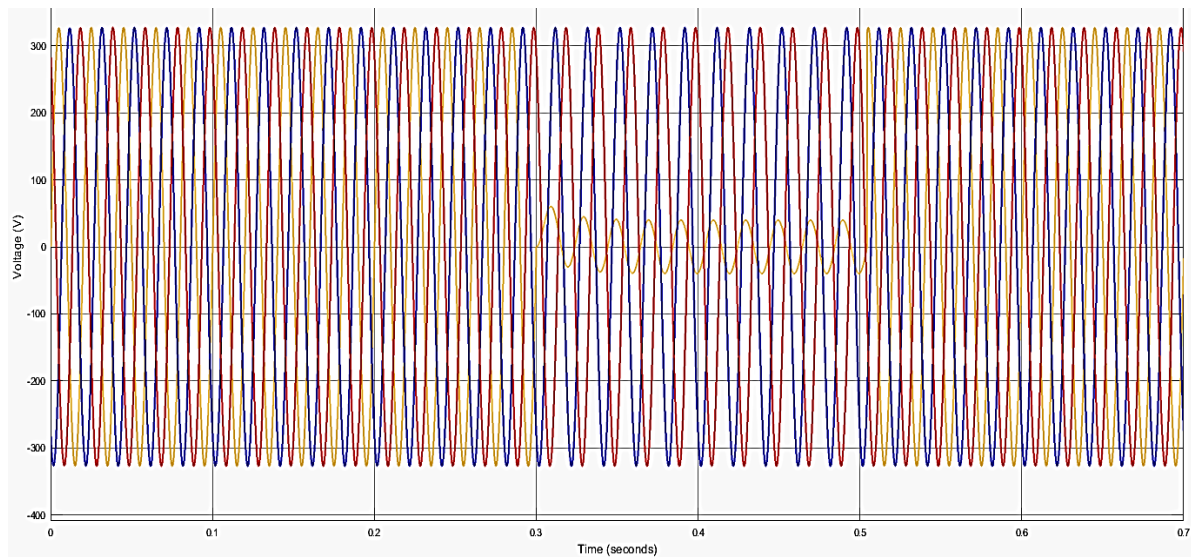


Figure 4.16: Grid phase voltage for unbalanced fault at the grid side between 0.3-0.5 sec

Figure 4.16 shows the grid phase voltage for the unbalanced LG fault in the Y phase and fault time is between 0.3-0.5 sec. We can see that when fault occurs, the faulty phase voltage undergoes nearly zero while others remain same.

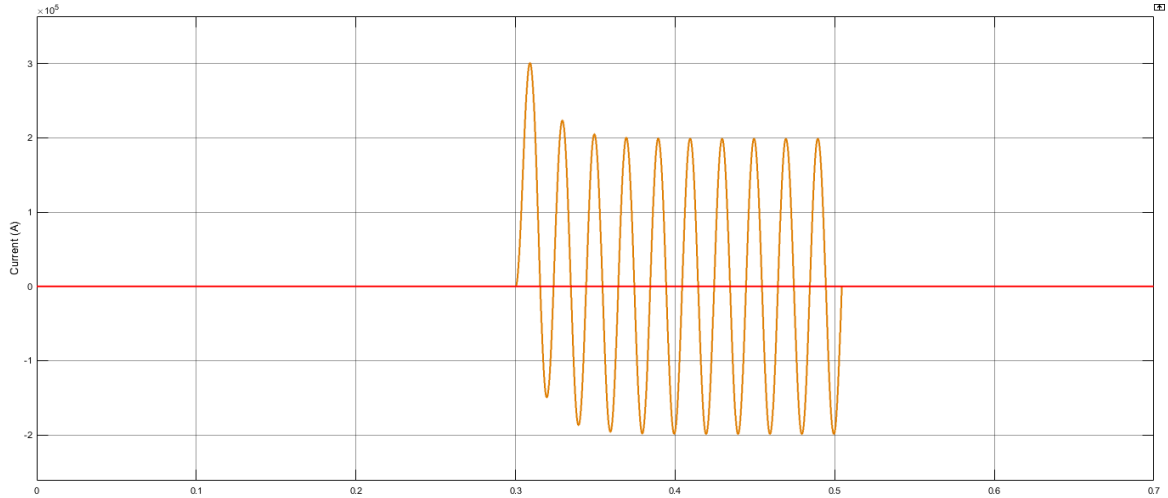


Figure 4.17: Total Fault current flowing through the faulted line for unbalanced fault at the grid

Figure 4.17 shows the fault current flowing through the faulty section. Here, the large amount of the current flows through the Y phase for the fault period 0.3-0.5 sec while the zero current flows through the healthy section.

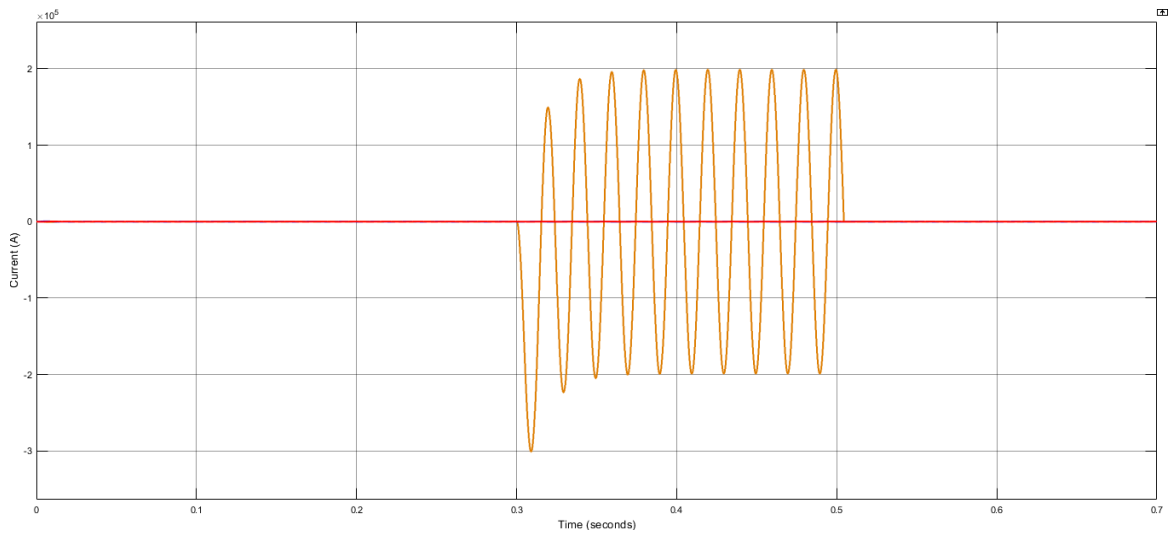


Figure 4.18: Phase current flowing through the grid for unbalanced fault at the grid side between 0.3-0.5 sec

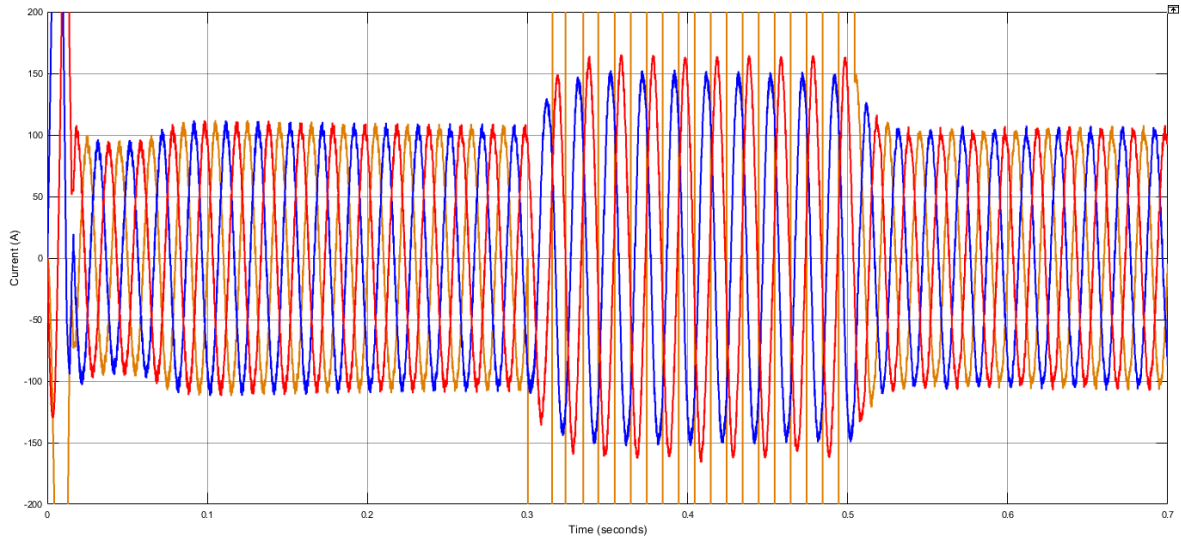


Figure 4.19: Magnified view phase current flowing through the grid for unbalanced fault at the grid side between 0.3-0.5 sec

Figure 4.18 shows the phase current flowing through the grid and figure 4.19 is the magnified view. It is observed that at normal condition, the inverter supplies the rated value of current to the grid while during unbalanced fault period of 0.3-0.5 sec, the grid supplies back the majority of fault current.

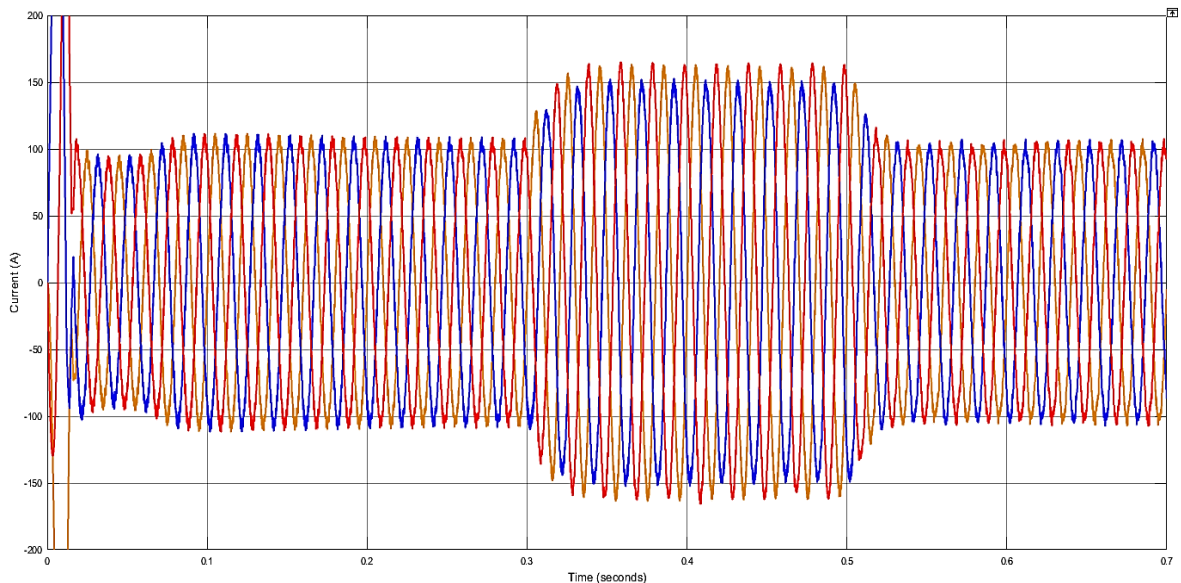


Figure 4.20: Phase current flowing through the inverter for unbalanced fault at the grid side between 0.3-0.5 sec

Figure 4.20 shows the phase current flowing through the inverter for unbalance fault at grid side between 0.3-0.5 sec. The inverter supplies the rated value of current to the grid during normal condition while the current increases by around 50 A during fault condition. The rise in current isn't much though the fault current flowing through the faulty section is too high. It is because of the fact that majority of fault current is supplied by the load.

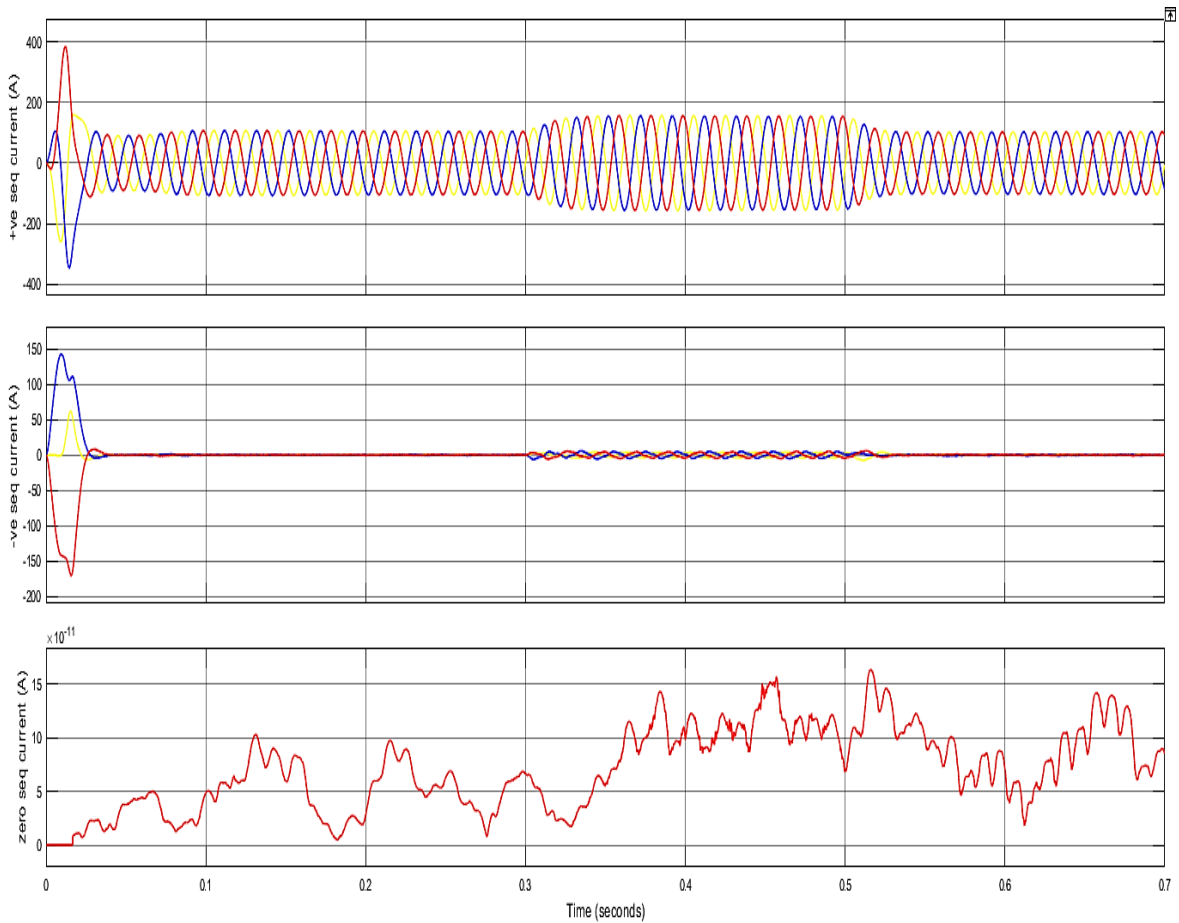


Figure 4.21: +ve ,-ve and zero sequence components of current flowing through the inverter for unbalanced fault at the grid side between 0.3-0.5 sec

Figure 4.21 depicts the current flowing through the inverter in terms of its sequence components. It is observed that at normal condition there is presence of only positive sequence component of current equivalent to the rated value of current that should be supplied by the inverter to the grid. During unbalanced fault period the positive sequence remains almost constant and zero sequence current is almost zero while there is the slight presence of -ve sequence component of current.

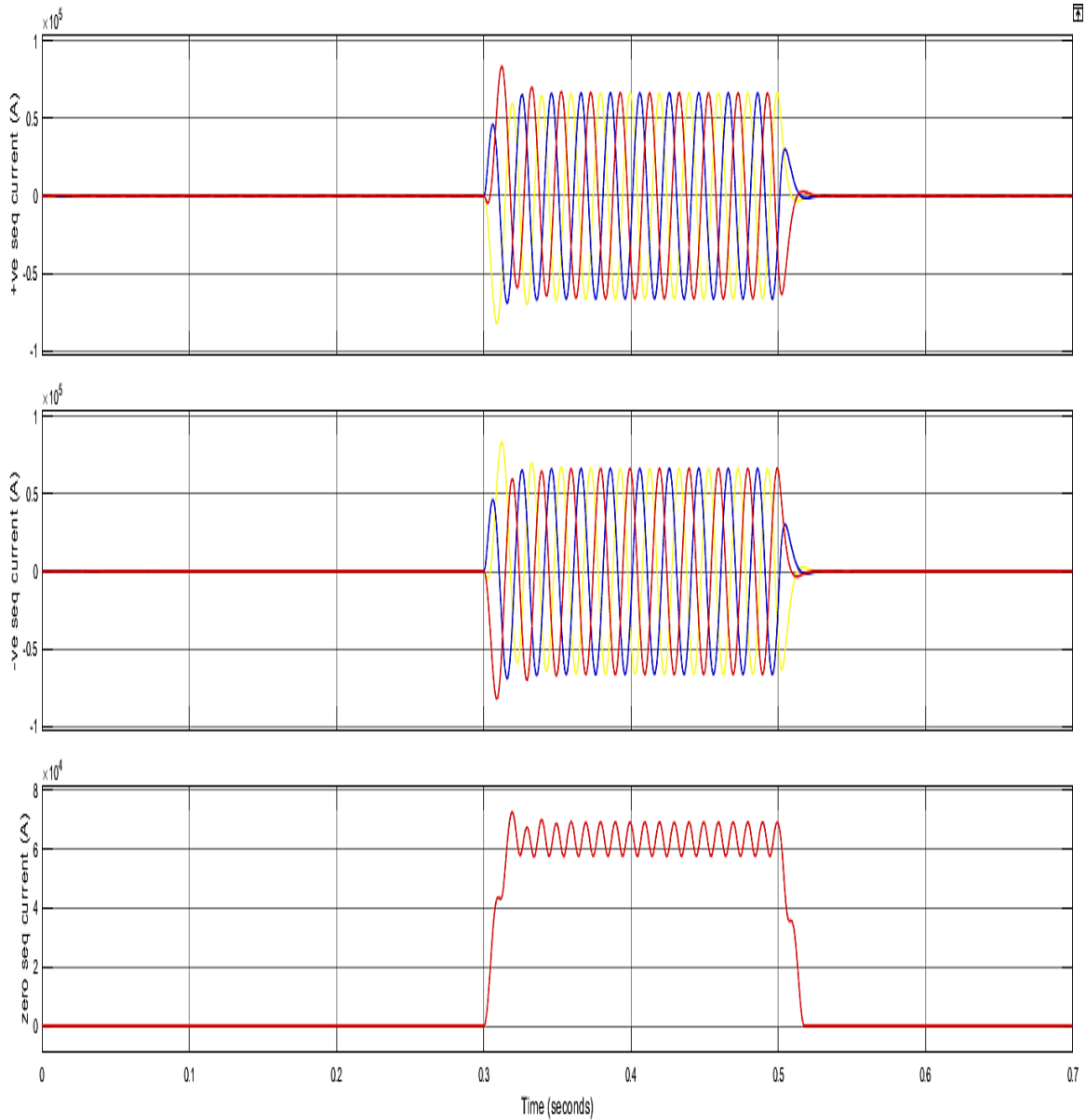


Figure 4.22: +ve, -ve and zero sequence components of current flowing through the grid for unbalanced fault at the grid side between 0.3-0.5 sec

Figure 4.22 depicts the sequence components of current flowing through the grid. At normal condition, the zero and -ve sequence component of current is zero whereas the positive sequence component of current is equivalent to the current supplied by the grid. But during unbalanced fault condition there is drastic increase in all the sequence components of current. It means all the zero-sequence component of current required for the unbalanced load caused by the LG fault is supplied by the grid.

Conclusion obtained from unbalanced fault at grid side

- Majority of the fault current is delivered by the grid and slight increase in the current flowing through the inverter if fault occurs at the grid side.
- No presence of –ve and zero sequence components in the current flowing through the inverter.
- Both –ve and zero sequence components of current is supplied by the grid.
- Voltage across the dc link capacitor changes within the permissible limit.

4.5 Effects of unbalanced fault condition at the inverter side in grid tied inverter

Fig A.4 shows the simulation model of grid connected PV system using hysteresis band control along with three phase faults on inverter side i.e., before filter. Now let us see different current graphs under unbalanced fault conditions.

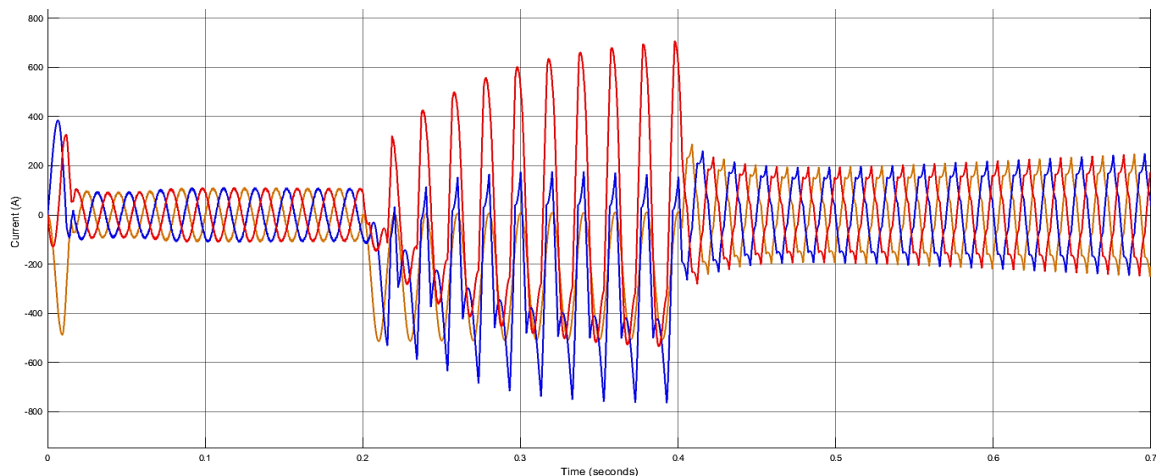


Figure 4.23: Phase current flowing through the grid for unbalanced fault at the inverter side between 0.2-0.4 sec

Figure 4.23 shows the phase current flowing through the grid when LG fault occurs at the inverter side for a duration of 0.2 sec. It is observed that before the fault occurs, the current flowing through the grid is equivalent to the rated value of current supplied by the inverter. During fault conditions, the current is unbalanced and the peak value is around 700 A. After the fault has been cleared, the current decreases suddenly and it starts growing up which indicates the instability of the system.

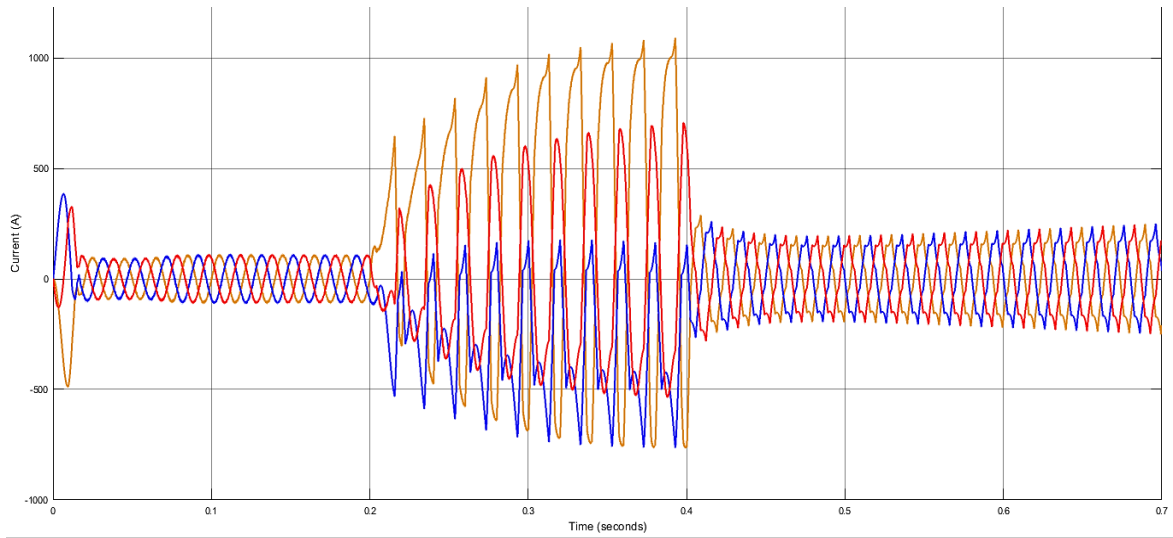


Figure 4.24: Phase current flowing through the inverter for unbalanced fault at the inverter side between 0.2-0.4 sec

Figure 4.24 shows the phase current flowing through the inverter. Before fault occurs, the inverter supplies the rated value of current i.e., 105A. During fault conditions of duration 0.2 sec, the inverter current rises significantly to around 1000A. This high current flowing through the inverter may damage the inverter. The current decreases suddenly and again start rising slowly leading a instability issue even after the fault has been cleared.

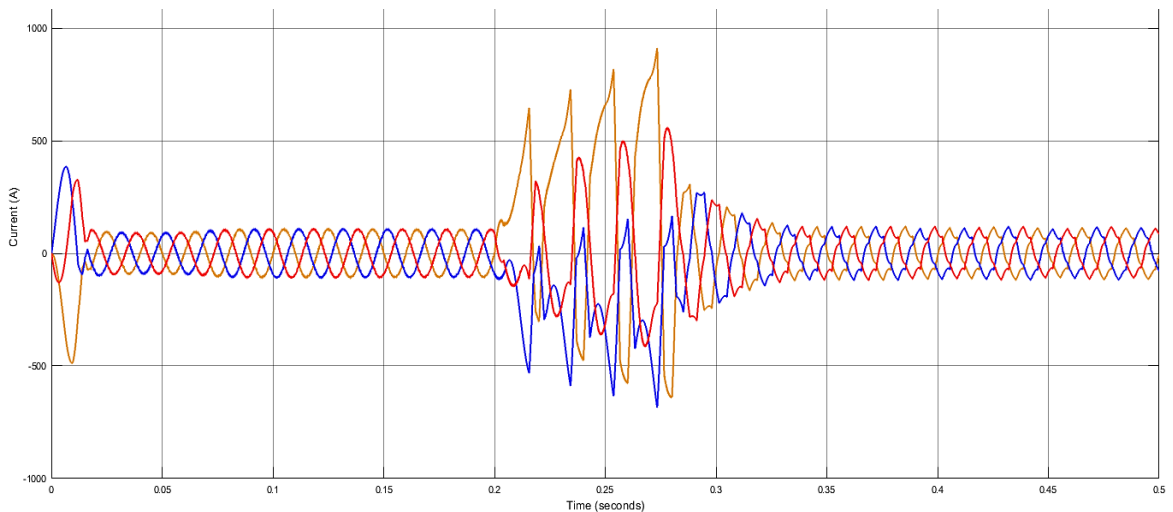


Figure 4.25: Phase current flowing through the inverter for unbalanced fault at the inverter side between 0.2-0.28 sec

Fig 4.25 depicts the phase current flowing through the inverter. Here, the fault period has been decreased to 0.08 sec. During fault conditions the current starts rising significantly up to 800A and then the fault has been cleared. After that the current decreases and slowly settle down to the previous rated value of current. It means that there occurs the stability issue only when the fault period exceeds 0.08 sec i.e., when the fault current exceeds around 800A.

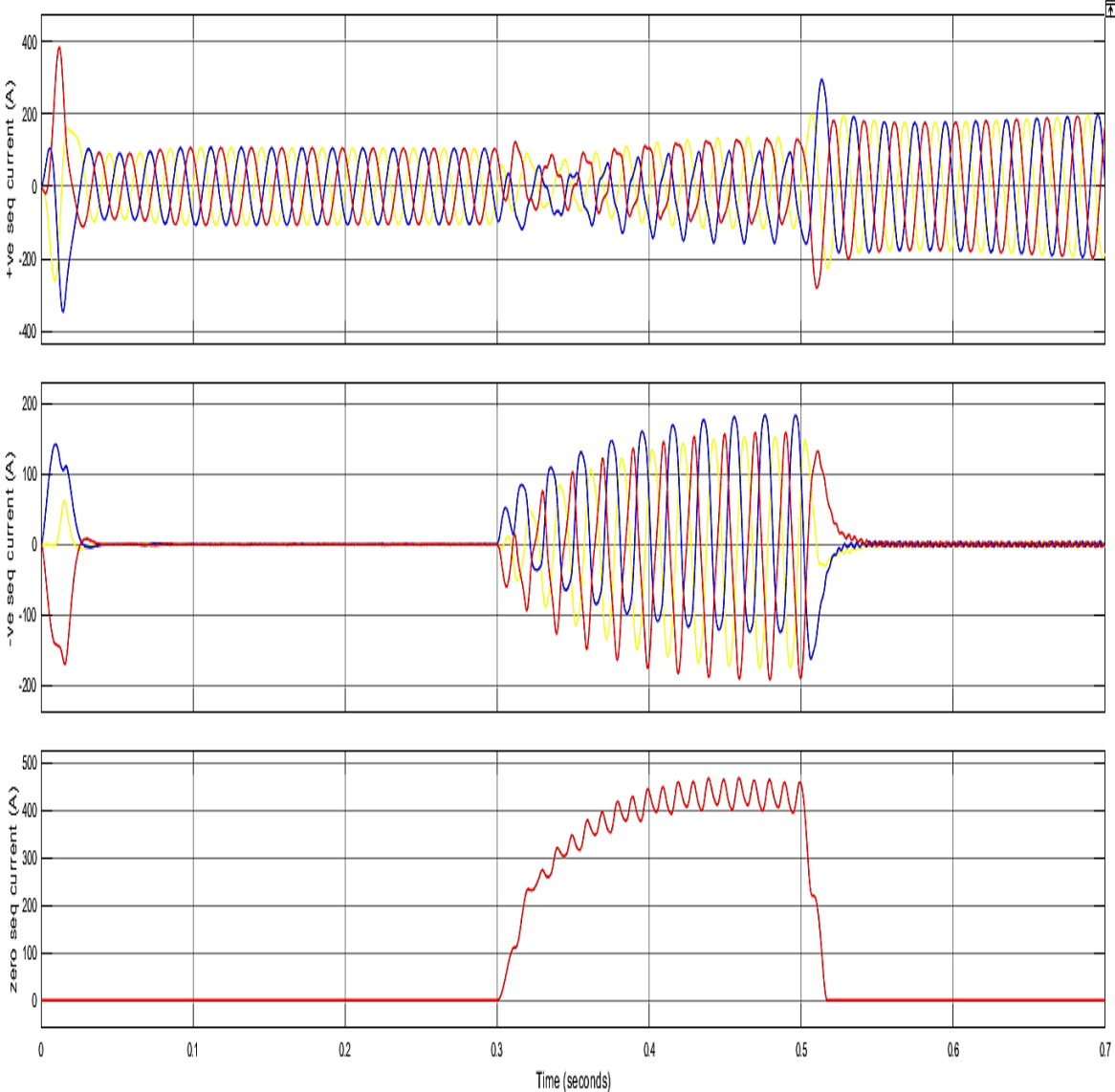


Figure 4.26: +ve, -ve and zero sequence components of current flowing through the grid for unbalanced fault at the inverter side between 0.3-0.5 sec

Figure 4.26 depicts the phase current flowing through the grid in terms of sequence components of current. At normal condition, there is the existence of positive sequence component of current equivalent to the rated value of current that should be delivered by the inverter to the grid while negative and zero sequence current are zero. After the LG fault occurs at the inverter side for a duration of 0.2 sec, there is fluctuation in the positive sequence of current as the inverter has to supply the current to the faulted line and there is also a mutual sharing to the load both by the inverter and the grid. And there is also increase in the both negative and zero sequence component of current. After the fault has been cleared, the negative and zero sequence current becomes zero but the positive sequence current increases to a high value and it goes on increases due to stability issue.

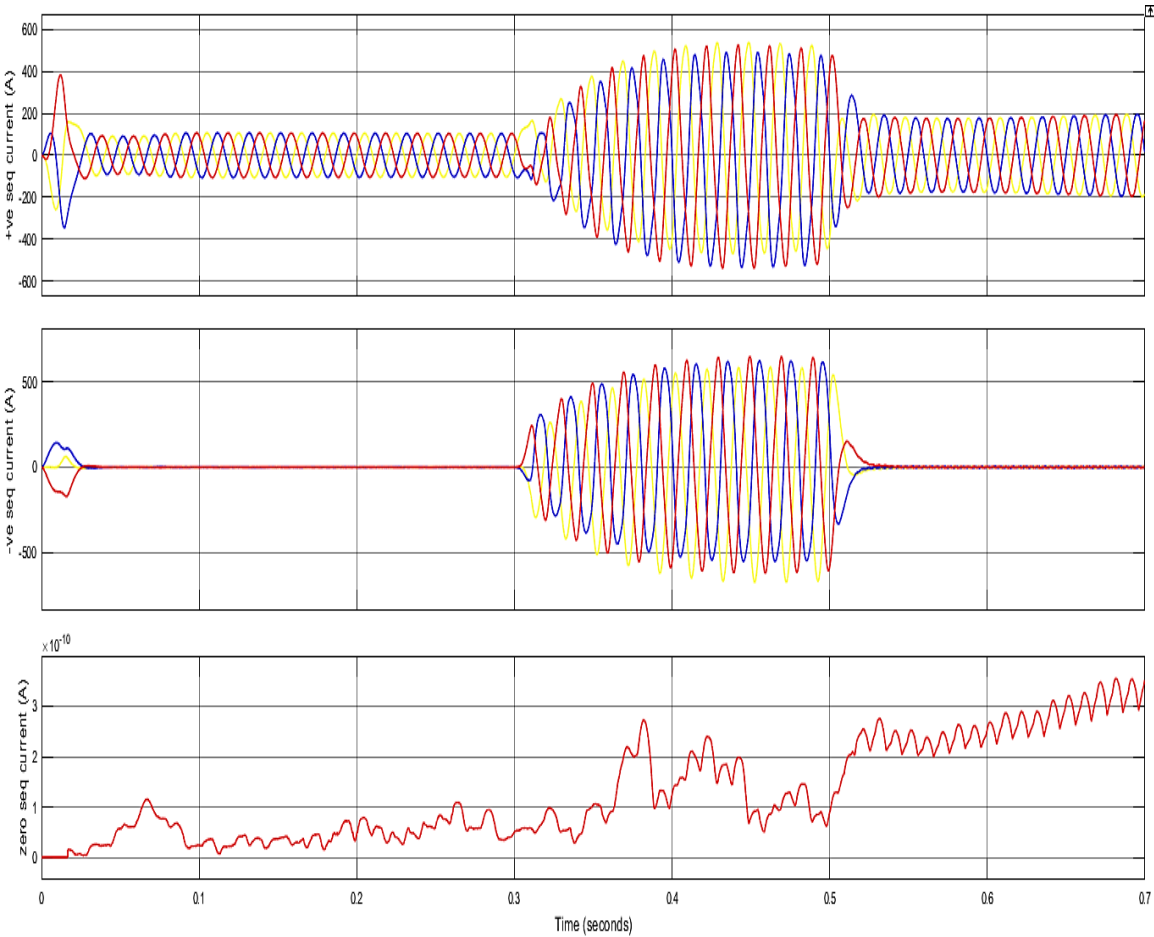


Figure 4.27: +ve, -ve and zero sequence components of current flowing through the inverter for unbalanced fault at the inverter side between 0.3-0.5 sec

Figure 4.27 depicts the sequence components of current flowing through the inverter. At normal conditions, as the system is balanced there isn't the existence of zero and negative sequence component of currents while the positive sequence current is equivalent value of rated current that should be supplied by the inverter to the grid. During fault conditions, the current becomes unbalanced and it is observed that the positive sequence current increases to around 550 A from 105 A and negative sequence current increases up to 600 A. This high current may damage the inverter. Also, the zero-sequence component of current remains almost zero even in the fault condition as all the zero-sequence current required for the faulted line is supplied by the grid. After the fault has been cleared, the negative and zero sequence current doesn't exist means the inverter supplies the balanced current to the grid. However, the positive sequence current doesn't settle down to the rated value of current leading to stability issue.

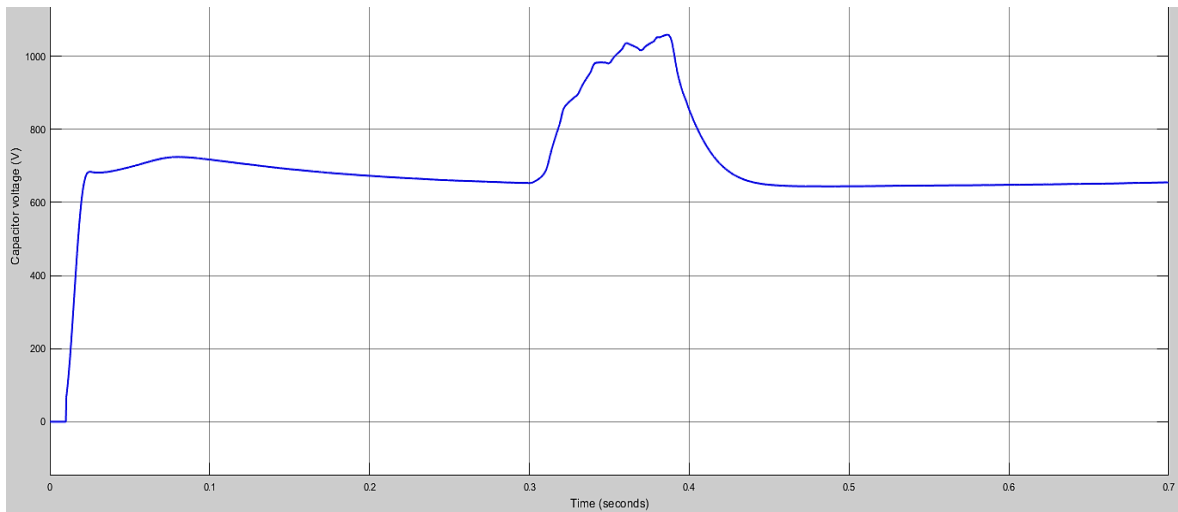


Figure 4.28: voltage across the capacitor for unbalanced fault at the inverter side between 0.4-0.48 sec

Figure 4.28 shows the voltage of the dc link capacitor. At normal condition, the voltage is settled down to around 640 V which is equivalent to the voltage corresponding to the maximum power of the PV system. The fault period is 0.08 sec. During fault condition, the voltage rises to around 1050 V and it settle down the previous rated value after the fault has been cleared.

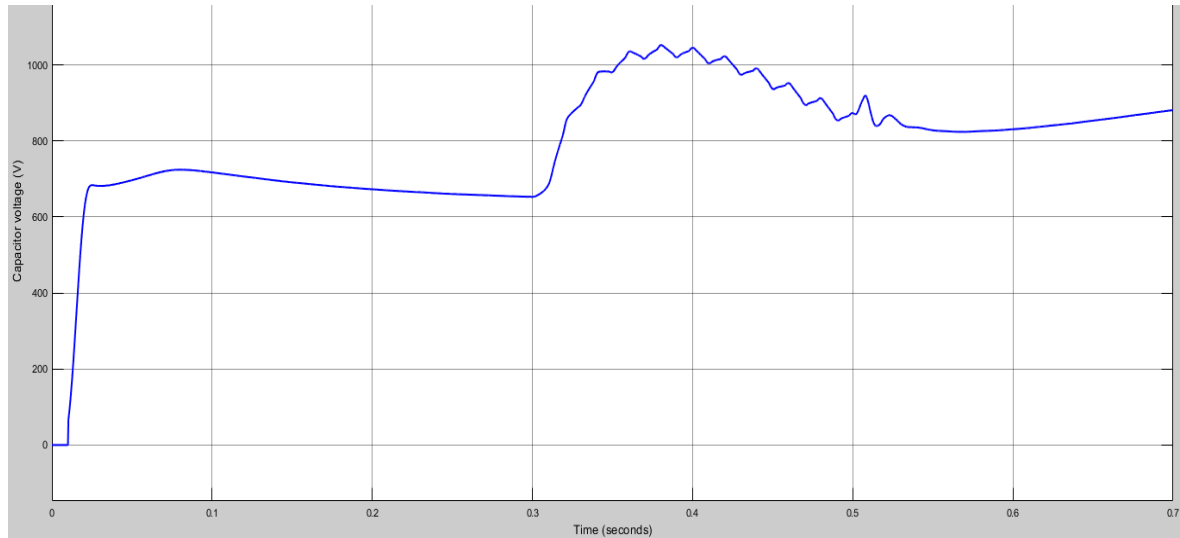


Figure 4.29: voltage across the capacitor for unbalanced fault at the inverter side between 0.3-0.5 sec

Figure 4.29 depicts the voltage across the dc link capacitor. Here, the fault period is increased to 0.2 sec. It is observed that the capacitor voltage rises to a round 1050 V from around 640 V. This high voltage may damage the capacitor and often requires a high rating of capacitor. And the capacitor voltage doesn't settle down to its rated value even after the fault has been cleared, it goes on increasing.

Conclusion obtained from unbalanced fault at inverter side

- Voltage across the dc link capacitor increases during LG fault.
- Majority of the fault current is delivered by the inverter and partially by the grid when fault occurs at the inverter side which may damage the inverter.
- There occurs a stability problem when fault period exceeds 0.08 sec (where current passes above 800A).
- -ve sequence component exists in both the current flowing through the inverter and the grid.
- All the zero-sequence current is supplied by the grid.

4.6 Summary of the problem

Table 4.1 : Current flowing through the inverter and capacitor voltage at different fault conditions

Disturbance Type	Current flowing through the inverter (A)				Capacitor Voltage (V)
	Total	+ve sequence	-ve sequence	Zero sequence	
Normal condition	105	105	0	0	640
Unbalanced load at inverter side	120	95	13	0	630
LG fault at grid side	160	155	5	0	655
LG fault at inverter side	950	550	600	0	1050

4.7 Observations of modified hysteresis band control

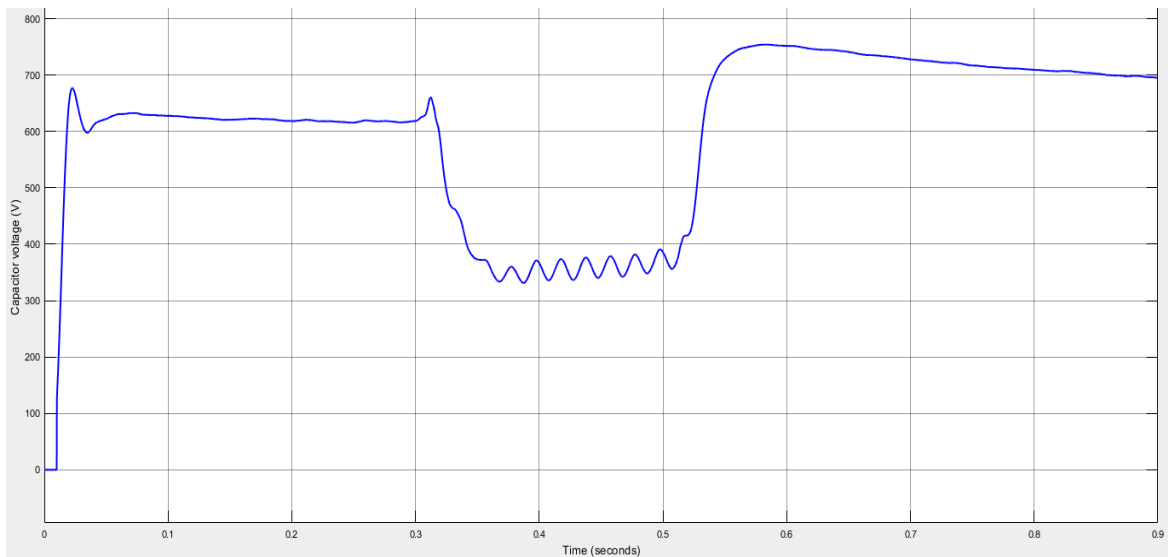


Figure 4.30: voltage across the capacitor for unbalanced fault at the inverter side between 0.3-0.5 sec after hysteresis controller modification

Figure 4.30 shows the voltage across dc link capacitor after the modification of the hysteresis band controller. It is observed that the voltage decreases during the fault condition instead of increasing. After the fault has been cleared, the voltage slowly settles down to its rated value even though the fault period is increased beyond 0.08 sec thus solving stability issue.

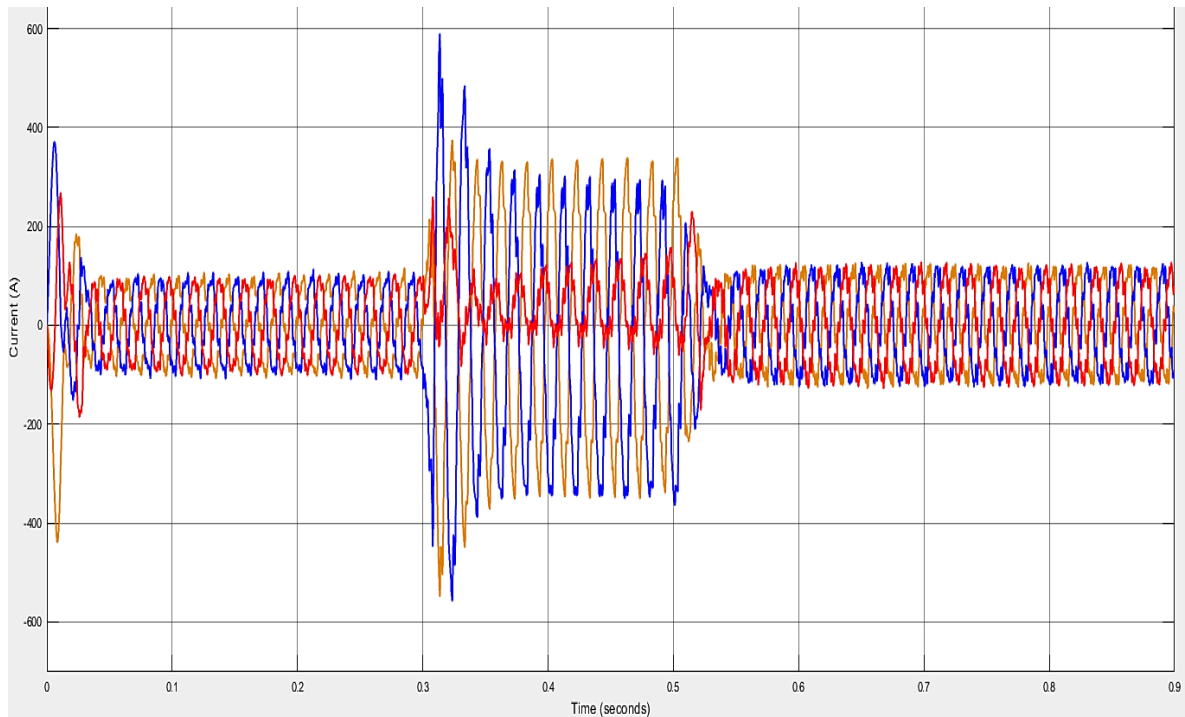


Figure 4.31: Phase current flowing through inverter for unbalanced fault at the inverter side between 0.3-0.5 sec after controller modification

Figure 4.31 depicts the phase current flowing through the inverter for the unbalanced LG fault at the inverter side after the modification of hysteresis band controller. The fault duration is 0.2 sec. During fault condition, the inverter current is now limited to around 330 A from around 1000A. And the current also settle down to its rated value of 105A slowly after the fault has been cleared. The modification in hysteresis band controller able to solve the stability issue and decrease the fault current but not in the acceptable range.

4.8 Observations of Inverter dual current control

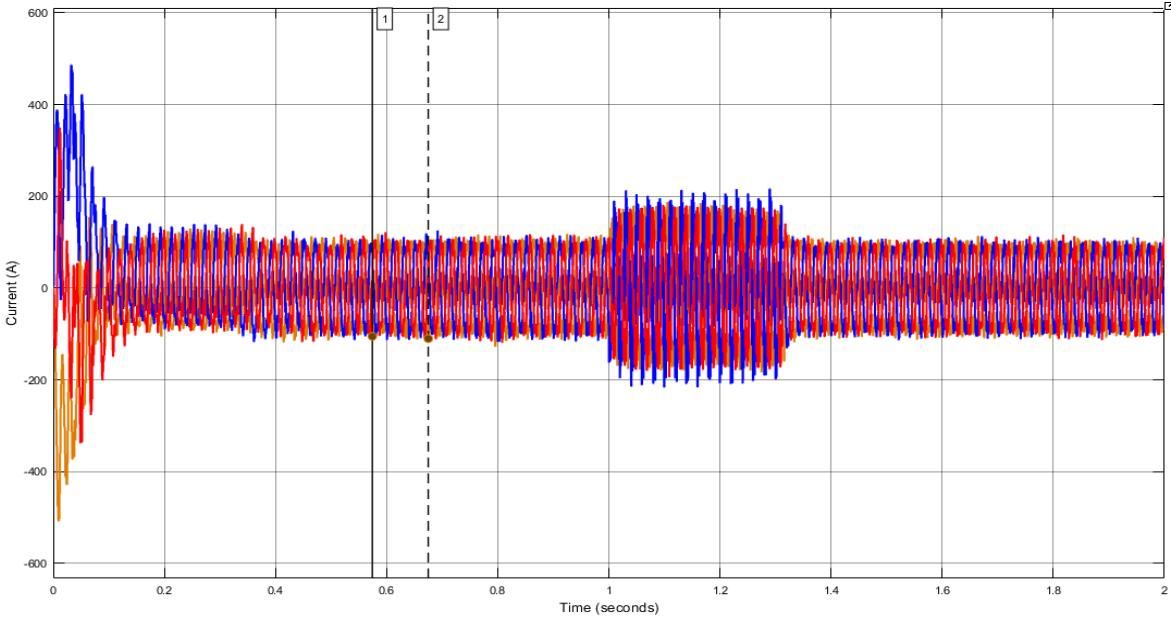


Figure4.32: Phase current flowing through inverter for unbalanced fault at the inverter side between 1-1.3 sec after inverter dual current control

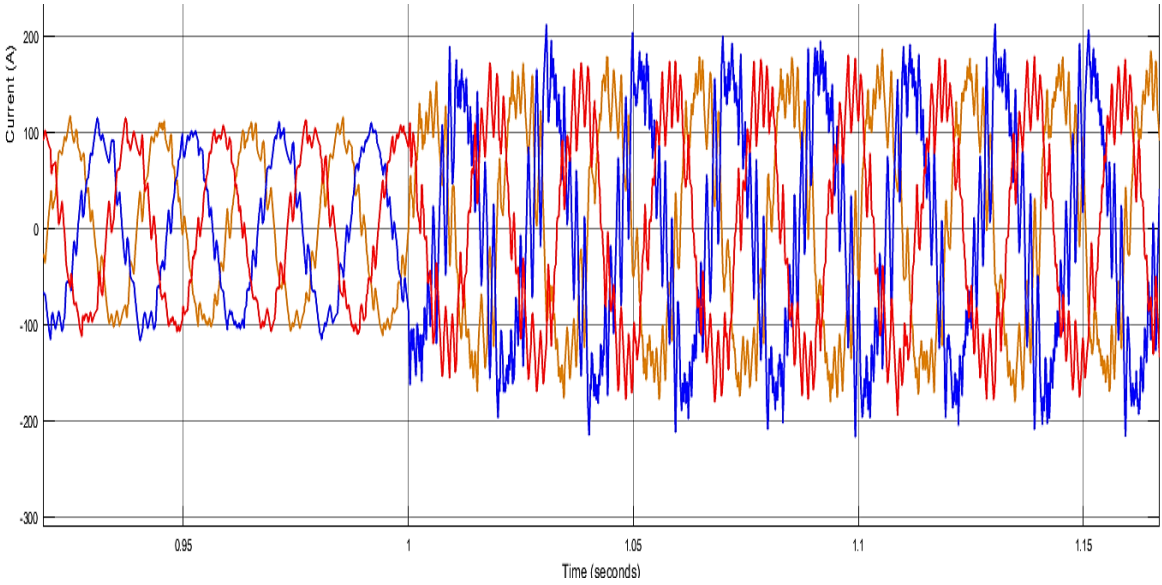


Figure4.33: Magnified view of Phase current flowing through inverter for unbalanced fault at the inverter side between 1-1.3 sec after inverter dual current control

Figure 4.32 shows the phase current flowing through the inverter after the replacement of hysteresis controller by the inverter dual current control and figure 4.33 is its magnified view. After the replacement of the controller, the current takes slightly larger time to settle down to its rated value in comparison to the hysteresis controller. But during fault condition, the inverter current reduces to around 200 A which is acceptable and prevent the inverter from damages. Also, the inverter current has been settled down to its rated value quickly after the fault has been cleared thereby solving stability issue.

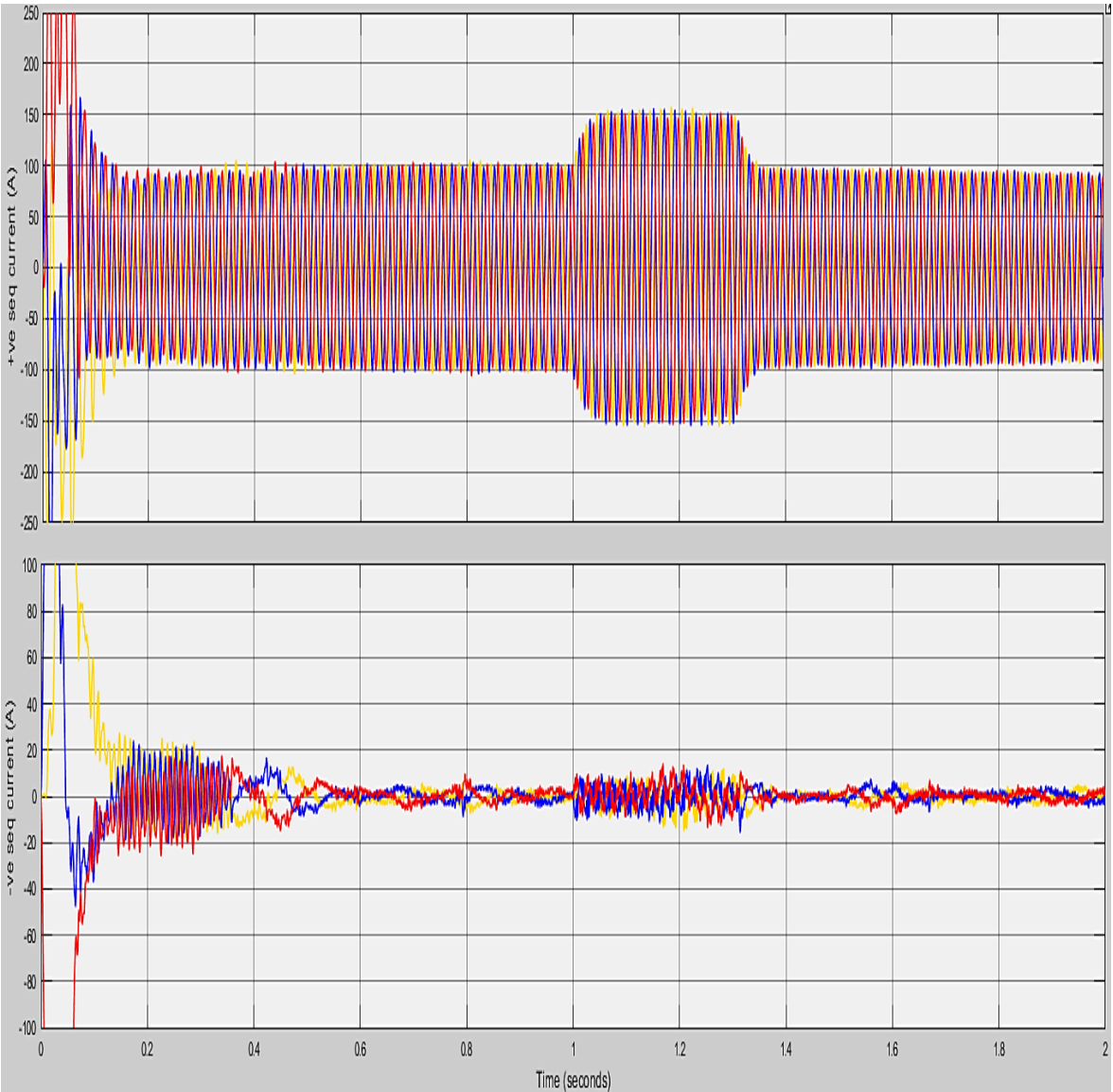


Figure 4.34: +ve and -ve sequence components of current flowing through the inverter for unbalanced fault at the inverter side between 1-1.3 sec after inverter dualcurrentcontrol

Figure 4.34 depicts the phase current flowing through the inverter in terms of its sequence components after the addition of new inverter dual current controller. It is observed that the positive sequence component of inverter current is now reduced to around 150 A from 550 A and the negative sequence current is reduced to almost zero from around 600A during unbalanced fault condition. Thus, the addition inverter dual current controller able to reduce the positive sequence current to an acceptable value and to mitigate the negative sequence zero.

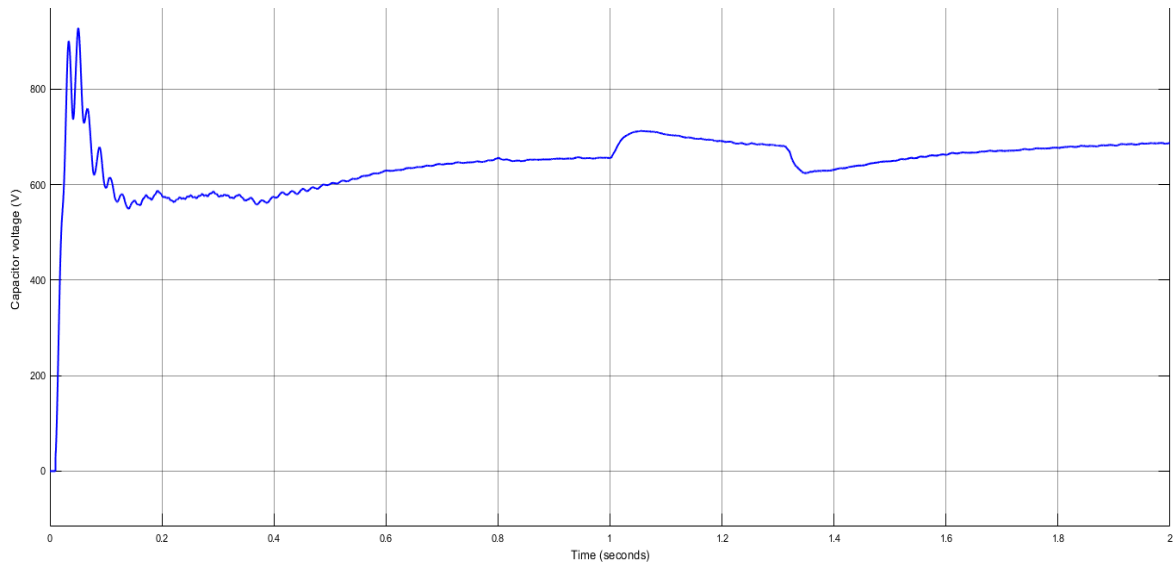


Figure 4.35: voltage across the dc link capacitor for unbalanced fault at the inverter side between 1-1.3 sec after inverter dual current control

Figure 4.35 shows the dc link capacitor voltage waveform after the addition of new inverter dual current controller replacing the hysteresis band controller. The capacitor voltage now limits to around 700V from 1050V during the fault condition. And the voltage settles down to its rated value of around 640V after the fault has been cleared thus solving the stability issue and preventing the capacitor from damages.

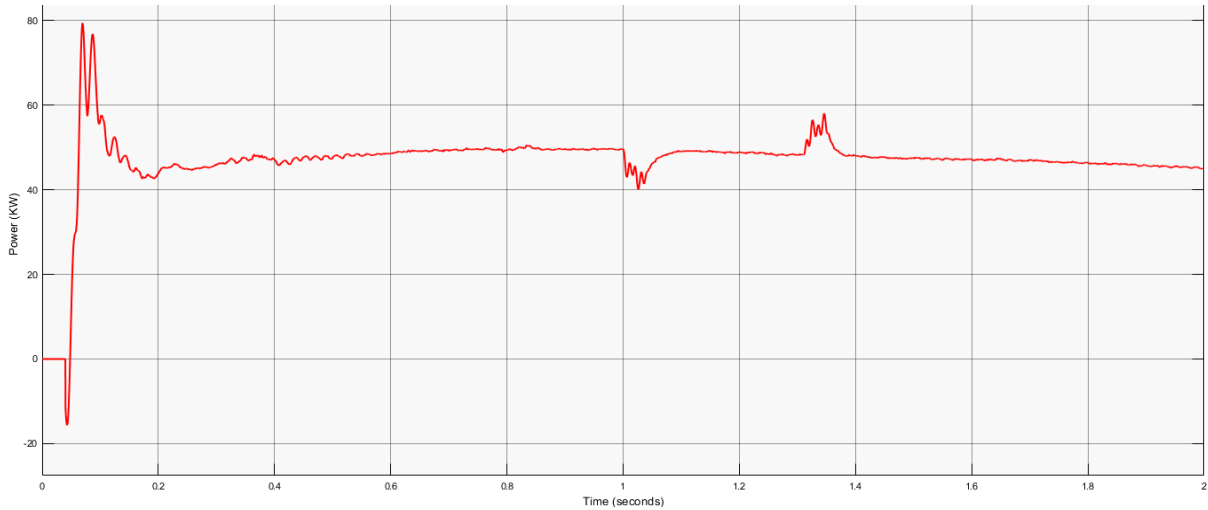


Figure 4.36: Active power flowing through the inverter for unbalanced fault at the inverter side between 1-1.3 sec after inverter dual current control

Figure 4.36 shows the active power flowing through the inverter after addition of inverter dual current controller. During faulty period i.e., from 1s to 1.3s the power flowing through the inverter is equal to power flowing through the inverter in normal operating condition. Thus, our designed inverter module is able to supply constant power even during unbalance load and fault condition.

4.9 Comparison of the results before and after compensation

Table 4.2 : Comparison of result before and after compensation

	Type of controller	Current flowing through the inverter (A)				Capacitor Voltage (V)
		Total	+ve sequence	-ve sequence	Zero sequence	
Before compensation	Hysteresis Controller	950	550	600	0	1050
After Compensation	Modified Hysteresis Controller	330	250	170	0	350
	Inverter Dual Current Controller	200	150	10	0	700

CHAPTER FIVE

CONCLUSION AND RECOMMENDATION

5.1 CONCLUSION

The problems caused by the unbalanced load and unbalanced fault condition is studied in grid tied PV connected inverter using hysteresis band control in MATLAB Simulink. The unbalanced fault at the inverter side is found to be more severe causing high value of current flowing through the inverter and increase in voltage of dc link capacitor affecting the stability of system. A modified hysteresis controller is studied to compensate the problems, it limits the current flowing through the inverter from around 950A to 330A during LG fault at the inverter side which can still damages the inverter and it also solves the issue of stability. Then, an inverter dual current control is introduced into the system replacing hysteresis band controller such that the current flowing through the inverter is limited from 950A to 200A and voltage across the dc link capacitor is limited to 700V from 1050V during LG fault at the inverter side. So, both current and voltage are limited to a tolerable value and it also addresses the stability issue ensuring safe and reliable operation of the inverter.

5.2 RECOMMENDATION

The grid tied inverter module so developed can now be operated even in voltage dip condition. However, the +ve sequence component of current is limited to 150A during LG fault at the inverter side. Further work can be performed on reducing the +ve sequence component of current to a rated value and also improving its performance operating in the islanded mode.

References

- [1] M. M. M. A.M Lede, "Microgrid architectures for distributed generation: A brief review," Vols. 2017-Janua, pp. 1-6, 2017.
- [2] P. V. PATEL, "MODELING AND CONTROL OF THREE-PHASE GRID-CONNECTED PV," pp. 29-31, 2018.
- [3] A. T. ., . M. ., F. B. P.Rodriguez, "Flexible Active Power Control of Distributed Power Generation Systems During Grid Faults," vol. 54, pp. 2583-2592, 2007.
- [4] K. H.S. Song, "Dual current control scheme for PWM converter under unbalanced input voltage conditions," *IEEE Transactions on Industrial Electronics*, pp. 953-959, 1999.
- [5] Y. Luo, C. Liu and F. Yu, "Design and Evaluation of an Efficient Three-Phase Four-Leg Voltage Source Inverter with Reduced IGBTs," 2017.
- [6] Z. C. a. S. K. F.Blaabjerg, "Power electronics as efficient interface in dispersed power generation systems," vol. 19, pp. 1184-1194, 2004.
- [7] R. T. ., M. ., A. T. F.Blaabjerg, "Overview of control and grid synchronization for distributed power generation systems," 2006.
- [8] N. K. ., T. A.K Devarakonda and P. B. R. S. S. varai, "A Comparative Analysis of Maximum Power Point Techniques for Solar Photovoltaic Systems," *Energies*, 2022.
- [9] M. A. B. h. G. Abdullah, "Comparison between neural network and P&O method in optimizing MPPT control for photovoltaic cell," 2020.
- [10] A. A. M. Sarvi, "A comprehensive review and classified comparison of MPPT algorithms in PV systems," *Energy Syst*, pp. 281-320, 2021.
- [11] P. M. ., N. G. P.K. Atri, "Comparison of Different MPPR Control Strategies for Solar Charge Controller," pp. 65-69, 2020.
- [12] P. I.Chtouki, "Comparison of Several Neural Network Perturb and Observe MPPT Methods for Photovoltaic Applications," pp. 909-914, 2018.
- [13] S. H. ., D. K. J. R. M. Khosravi, "A Novel Hybrid Model -Based MPPT Algorithm Based on Artificial Neural Networks for Photovoltaic Applications," pp. 1-6, 2017.
- [14] A. A. H. ., B. W. N.E. Zakzouk, "PV Single Phase Phase Grid Connected Converter: DC-Link Voltage Sensorless Prospective," vol. 5, pp. 526-546, 2017.

- [15] A. M. W. T. ., K. H. ., Y. S.Fahad, "Particle Swarm Optimization Based DC-Link Voltage Control for Two Stage Grid Connected PV Inverter," pp. 2233-2241, 2018.
- [16] D. H. ., B. M. R. Kabiri, "Control of active and reactive power ripple to mitigate unbalanced grid voltages," vol. 52, pp. 1660-1668, 2015.
- [17] Y. Y.-S. H. ., T. T.-L. J. C.T.P. Ching-Tsai Pan, "A constant hysteresis-band current controller with fixed switching frequency," vol. 3, pp. 1021-1024, 2002.
- [18] M. B. H. Ahmed, "Adaptive observer based grid synchronization and sequence extraction techniques for renewable energy systems," 2021.
- [19] M. J. Hasan, "Modeling and simulation of 1kw single phase grid tied inverter for solar photovoltaic system," *IOP Science*, vol. 881, 2020.
- [20] P. V. V. Soares, "An Instantaneous Active and Reactive Current Component Method for Active Filters," *IEEE Transactions on Power Electronics*, vol. 15, 2000.
- [21] H. M. ., M. E. A. K.Boudaraia, "Modeling and control of three phases grid connected photovoltaic system," *International renewable and sustainable energy conference*, pp. 812-816, 2016.
- [22] A. Y. A. A. Y. A. Ahmed M Atallah, "Implementation of perturb and observe MPPT of PV system with direct control method using buck and buck boost converters," pp. 31-44, 2014.
- [23] X. Y. ., Z. C. W. Huifeng Mao, "A Hysteresis Current Controllers For Single Phase Three Level Voltage Source Inverters," *IEEE Transactions on Power Electronics*, vol. 27, p. 7, 2012.
- [24] J. Bialasiewicz, "Comparison of carrier-based PWM strategies for three phase five level voltage source inverter," *IEEE Transactions on Power Electronics*, vol. 19, 2004.
- [25] M. Taghizadeh, M. Mardaneh and M. S. Sadeghi, "A new method of voltage and frequency control in isolated microgrids using enhanced droop controller optimized by frog algorithm," *Journal of Renewable and Sustainable Energy*, 2014.
- [26] C. Jeong, J. Cho, Y. Kang and G. Rim, "A 100 kVA power conditioner for three-phase four-wire emergency generators," 1998.
- [27] J. R. Rodriguez, "Hysteresis current control algorithms for grid-tied photovoltaic inverters unbalance and fault conditions," pp. 55-65, 2017.

APPENDIX

Appendix: A (Simulink model)

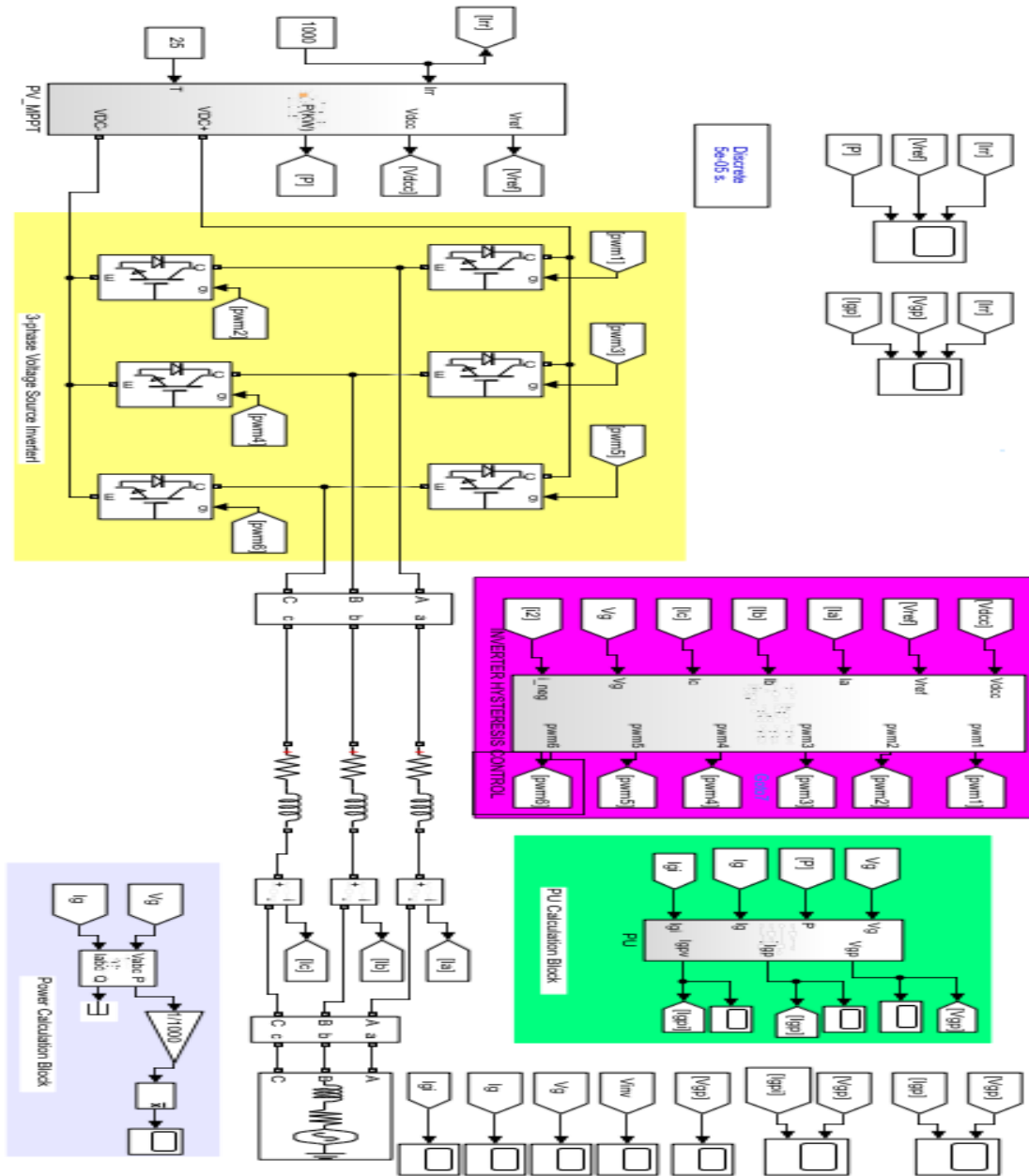
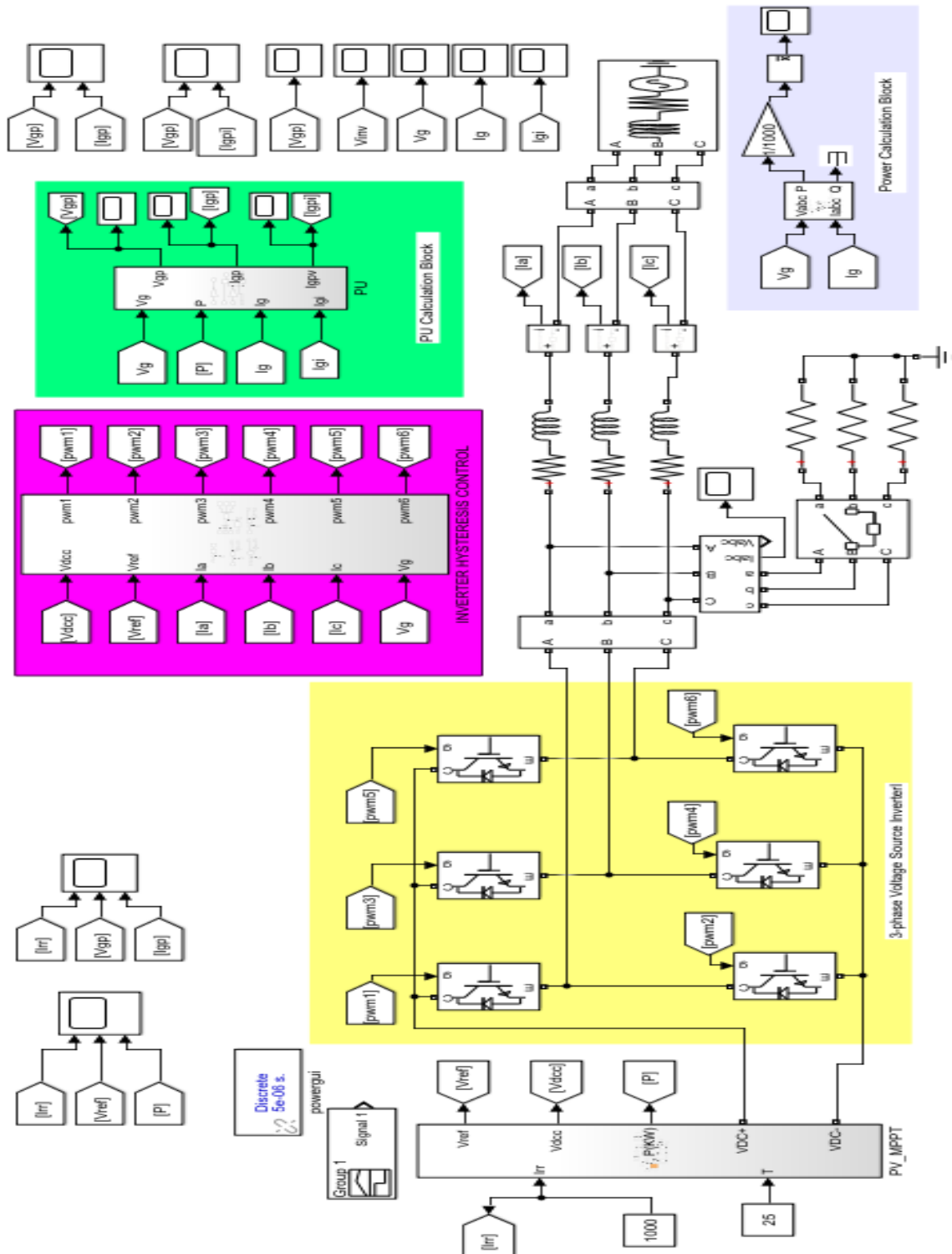


Figure A.1: Simulation model of PV system



FigureA.2 : Simulink model of grid connected PV along with unbalanced load of 25kw, 15kw and 1kw in respective phases at the inverter side

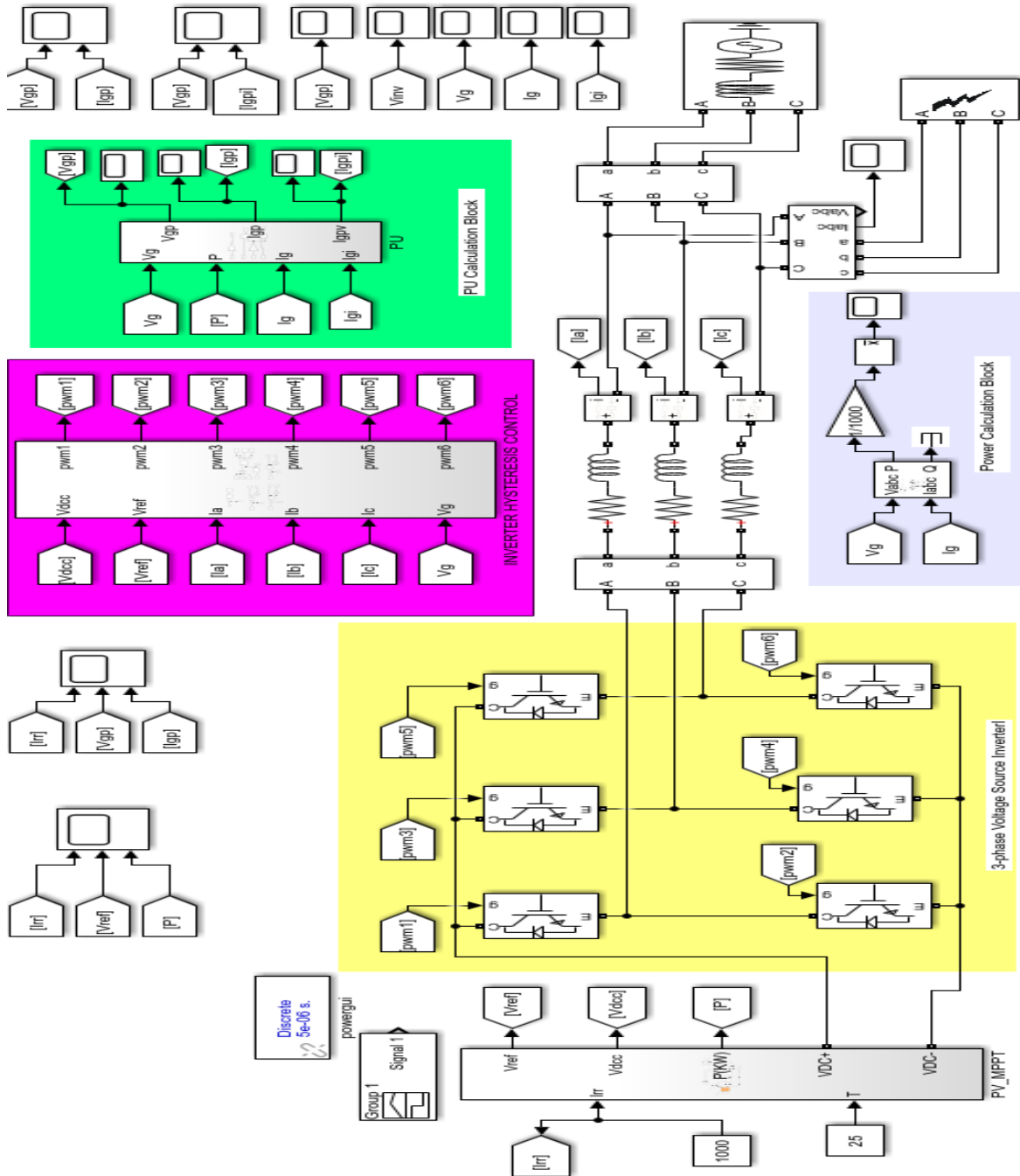


Figure A.3: Simulink model of grid connected PV using hysteresis band control and 3 phase fault block

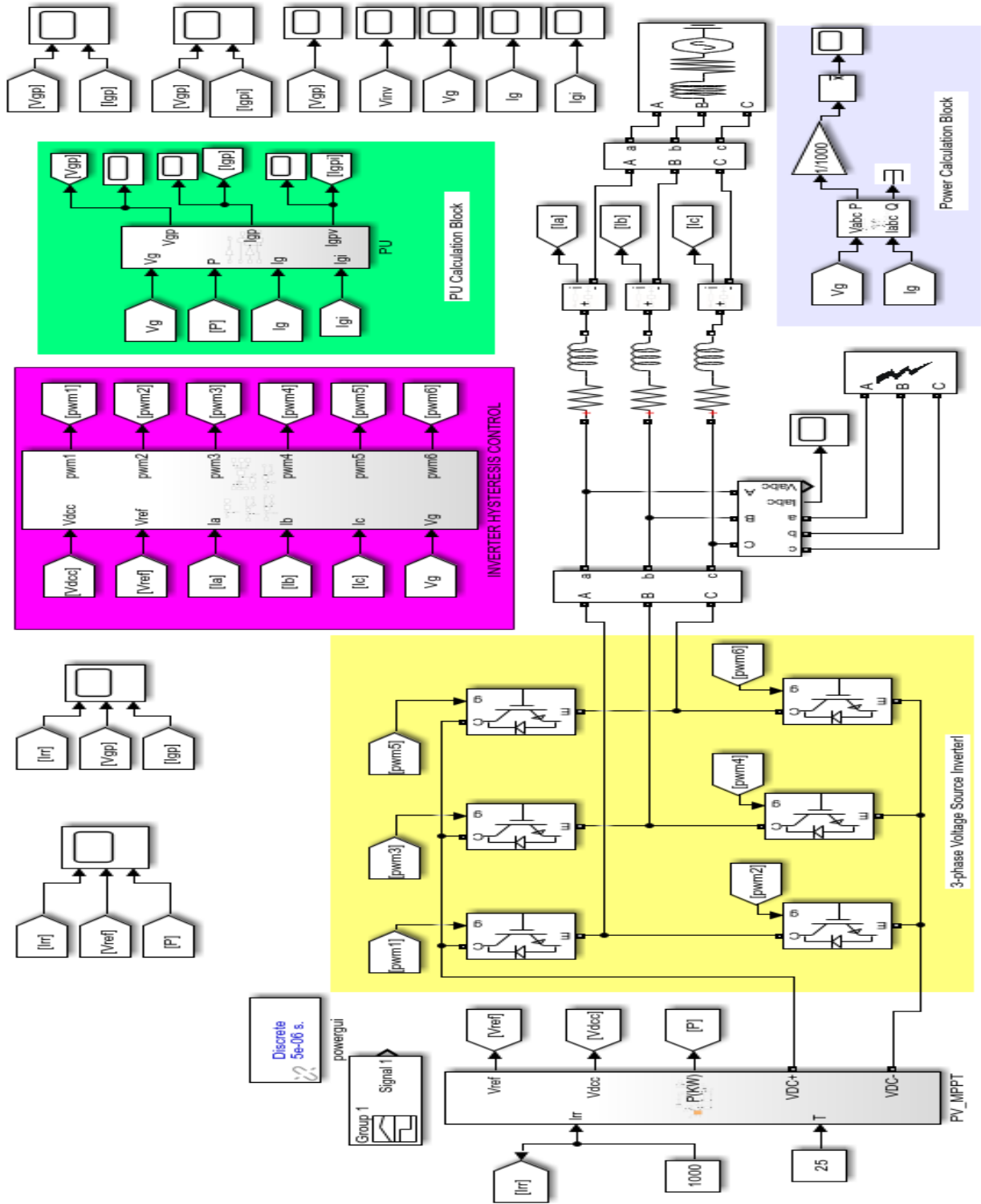


Figure A.4: Simulink model of grid connected PV using hysteresis band control and 3 phase fault block at inverter side

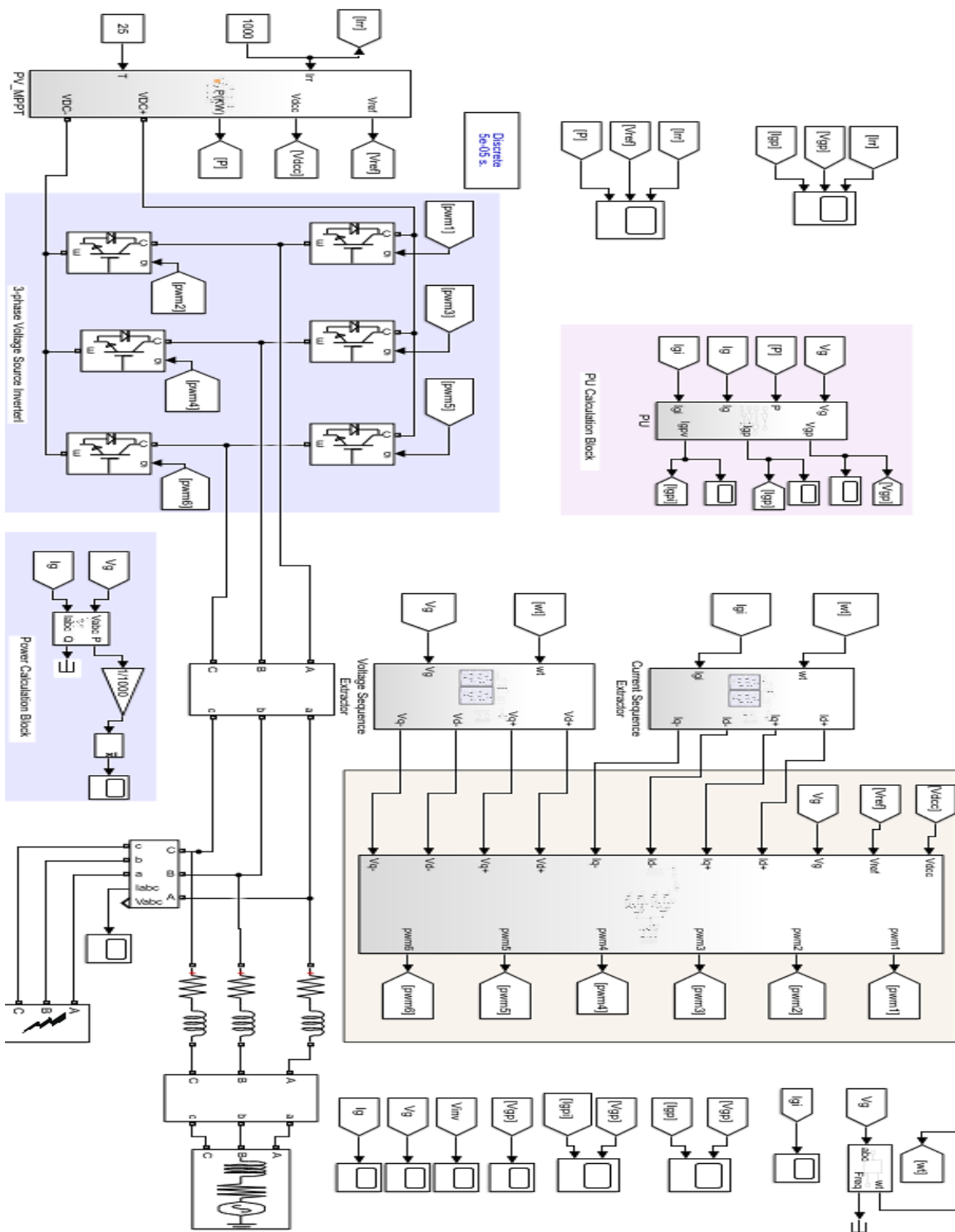


Figure A.6: Overall simulation diagram for Inverter Dual current control

Appendix: B (Script)

MATLAB function code for MPPT

Function Vref = refgen(V,I,deltaVref)

Vrefmax = 800;

Vrefmin = 0;

Vrefinit = 500;

Persistent VoldVrefoldPold;

if isempty (Vold)

Vold = 0;

Pold = 0;

Vrefold = Vrefinit;

End

P = V*I;

dV = V - Vold;

dP = P - Pold;

if dP ~= 0

if dP < 0

if dV < 0

Vref = Vrefold + deltaVref;

else

Vref = Vrefold - deltaVref;

end

else

```
if dV < 0
Vref = Vrefold - deltaVref;
else
Vref = Vrefold + deltaVref;
end
end
else
Vref = Vrefold;
end
if Vref >= Vrefmax || Vref < Vrefmin
Vref = Vrefold;
end
Vrefold = Vref;
Vold = V;
Pold = P;
end
```

18%

SIMILARITY INDEX

PRIMARY SOURCES

1	scholarsmine.mst.edu Internet	206 words — 2%
2	Green Energy and Technology, 2015. Crossref	90 words — 1%
3	www.researchgate.net Internet	72 words — 1%
4	www.mdpi.com Internet	63 words — 1%
5	doi.org Internet	55 words — 1%
6	Zhikang Shuai. "Chapter 2 Transient Characteristics of Current Controlled IIDGs During Grid Fault", Springer Science and Business Media LLC, 2021 Crossref	48 words — < 1%
7	core.ac.uk Internet	47 words — < 1%
8	F. Blaabjerg. "Overview of Control and Grid Synchronization for Distributed Power Generation Systems", IEEE Transactions on Industrial Electronics, 10/2006	40 words — < 1%

-
- 9 www.scirp.org 39 words — < 1%
Internet
-
- 10 "Advances in Smart Grid and Renewable Energy", Springer Science and Business Media LLC, 2018 36 words — < 1%
Crossref
-
- 11 Jyoti Joshi, Anurag Kumar Swami, Vibhu Jatelly, Brian Azzopardi. "A Comprehensive Review of Control Strategies to Overcome Challenges during LVRT in PV Systems", IEEE Access, 2021 34 words — < 1%
Crossref
-
- 12 P.K. Jain, J.R. Espinoza, N.A. Ismail. "A single-stage zero-voltage zero-current-switched full-bridge DC power supply with extended load power range", IEEE Transactions on Industrial Electronics, 1999 31 words — < 1%
Crossref
-
- 13 www.degruyter.com 30 words — < 1%
Internet
-
- 14 "Digital Technologies and Applications", Springer Science and Business Media LLC, 2023 27 words — < 1%
Crossref
-
- 15 Ashwin Kumar Devarakonda, Natarajan Karuppiah, Tamilselvi Selvaraj, Praveen Kumar Balachandran et al. "A Comparative Analysis of Maximum Power Point Techniques for Solar Photovoltaic Systems", Energies, 2022 26 words — < 1%
Crossref
-
- 16 A. M. Shiddiq Yunus, Sri Swasti, Purwito. "Overview of Hysteresis Current Controller 25 words — < 1%

17 Alsharif, Bandar S.. "The Influence of Loading and Voltage Supply Conditions LV Feeder on Harmonic Emission", King Fahd University of Petroleum and Minerals (Saudi Arabia), 2023 25 words — < 1%

ProQuest

18 vbn.aau.dk 25 words — < 1%

Internet

19 D. Laird. "Rule based decision support system for single-line fault detection in a delta-delta connected distribution system", Conference Proceedings Power Industry Computer Application Conference, 1993 24 words — < 1%

Crossref

20 Patel, Hetal V.. "Modified Sinusoidal Pulse Width Modulation Technique for Speed Control of Permanent Magnet Brushless DC Motor", Maharaja Sayajirao University of Baroda (India), 2023 23 words — < 1%

ProQuest

21 J. Sottile, J.L. Kohler. "An on-line method to detect incipient failure of turn insulation in random-wound motors", IEEE Transactions on Energy Conversion, 1993 22 words — < 1%

Crossref

22 livrepository.liverpool.ac.uk 22 words — < 1%

Internet

23 O.A. Ciniglio, D.P. Carroll. "Improved power transfer during single pole switching: a symmetrical sequence filtering approach (AC transmission lines)", IEEE Transactions on Power Delivery, 1993 21 words — < 1%

Crossref

24 K. R. Padiyar, Anil M. Kulkarni. "Dynamics and Control of Electric Transmission and Microgrids", Wiley, 2019
Crossref 20 words — < 1%

25 Abdellah Benabdelkader, Azeddine Draou, Abdulrahman AlKassem, Toufik Toumi et al. "Enhanced Power Quality in Single-Phase Grid-Connected Photovoltaic Systems: An Experimental Study", Energies, 2023
Crossref 19 words — < 1%

26 Irshad, Usama Bin. "Efficient Islanding Detection Method for Inverter-Based DG System", King Fahd University of Petroleum and Minerals (Saudi Arabia), 2023
ProQuest 19 words — < 1%

27 O. Jasim. "Operation of an induction motor with an open circuit fault by controlling the zero sequence voltage", 2009 IEEE International Electric Machines and Drives Conference, 05/2009
Crossref 19 words — < 1%

28 ijret.org
Internet 18 words — < 1%

29 Adel A. Elbaset, M. S. Hassan. "Design and Power Quality Improvement of Photovoltaic Power System", Springer Science and Business Media LLC, 2017
Crossref 17 words — < 1%

30 repository.najah.edu
Internet 17 words — < 1%

31 Shuilong He, Xuhong Shen, Zhansi Jiang. "Detection and Location of Stator Winding Interturn Fault at Different Slots of DFIG", IEEE Access, 2019
Crossref 16 words — < 1%

32	ijece.iaescore.com Internet	16 words — < 1%
33	realtide.eu Internet	16 words — < 1%
34	www.farzadrazavi.com Internet	16 words — < 1%
35	www.yumpu.com Internet	16 words — < 1%
36	Tse, . "Hysteresis-Modulation-Based Sliding Mode Controllers", Sliding Mode Control of Switching Power Converters Techniques and Implementation, 2011. Crossref	15 words — < 1%
37	lup.lub.lu.se Internet	15 words — < 1%
38	scholarworks.uaeu.ac.ae Internet	15 words — < 1%
39	F. Blaabjerg, Z. Chen, S.B. Kjaer. "Power Electronics as Efficient Interface in Dispersed Power Generation Systems", IEEE Transactions on Power Electronics, 2004 Crossref	14 words — < 1%
40	acikerisim.karabuk.edu.tr:8080 Internet	14 words — < 1%
41	vtechworks.lib.vt.edu Internet	14 words — < 1%
42	"Intelligent Data Analytics for Power and Energy Systems", Springer Science and Business Media	13 words — < 1%

43 M. Djarallah, B. O. Zeidane, B. Azoui. "Energy transfer mechanism for a grid-connected residential PV system within the Matlab/Simulink environment", 2007 42nd International Universities Power Engineering Conference, 2007

13 words — < 1%

Crossref

44 Shuvra Prokash Biswas, Md. Shamim Anower, Md. Rafiqul Islam Sheikh, Md. Rabiul Islam et al. "A Modified Reference Saturated Third Harmonic Injected Equal Loading PWM for VSC-Based Renewable Energy Systems", IEEE Transactions on Applied Superconductivity, 2021

13 words — < 1%

Crossref

45 www.electrooobs.com

Internet

13 words — < 1%

46 Ayedh H. ALQahtani, Muthanna S. Abuhamdeh, Yazan M. Alsmadi. "A simplified and comprehensive approach to characterize photovoltaic system performance", 2012 IEEE Energytech, 2012

12 words — < 1%

Crossref

47 Ikram Ullah, Muhammad Ashraf. "Comparison of Synchronization Techniques Under Distorted Grid Conditions", IEEE Access, 2019

12 words — < 1%

Crossref

48 i-rep.emu.edu.tr:8080

Internet

12 words — < 1%

49 mdpi-res.com

Internet

11 words — < 1%

50

Internet

10 words — < 1%

51

Deepak Verma, S. Nema, A. M. Shandilya. "A Different Approach to Design Non-Isolated DC-DC Converters for Maximum Power Point Tracking in Solar Photovoltaic Systems", Journal of Circuits, Systems and Computers, 2016

Crossref

10 words — < 1%

52

Mahdi Benaouadj, Zouhir Boumous, Samira Boumous. "Active Harmonic Filtering for Improving Power Quality of an Electrical Network", Journal Européen des Systèmes Automatisés, 2022

Crossref

10 words — < 1%

53

S. Dasgupta. "A FBD theory based grid frequency independent current reference generation method for a three phase inverter interfacing renewable energy sources to generalized micro-grid", IECON 2011 - 37th Annual Conference of the IEEE Industrial Electronics Society, 11/2011

Crossref

10 words — < 1%

54

Subramanian Vasantharaj, Vairavasundaram Indragandhi, Mohan Bharathidasan, Belqasem Aljafari. "Power Quality Analysis of a Hybrid Microgrid-Based SVM Inverter-Fed Induction Motor Drive with Modulation Index Diversification", Energies, 2022

Crossref

10 words — < 1%

55

Zhaoyong Zhou, Tiejai Li, T. Takahashi, E. Ho. "FPGA realization of a high-performance servo controller for PMSM", Nineteenth Annual IEEE Applied Power Electronics Conference and Exposition, 2004. APEC '04., 2004

Crossref

10 words — < 1%

-
- 56 www.nrel.gov Internet 10 words — < 1%
-
- 57 www.umanitoba.ca Internet 10 words — < 1%
-
- 58 Ali Keyhani. "Design of Smart Power Grid Renewable Energy Systems", Wiley, 2019 Crossref 9 words — < 1%
-
- 59 C NAYAR. "Power electronics for renewable energy sources", Power Electronics Handbook, 2007 Crossref 9 words — < 1%
-
- 60 Hongfei Yong, Shengmin Pan, Yiyun Huang, Hulin Feng, Baocan He. "Control method of DC component for NNBI accelerator power supply", Energy Reports, 2023 Crossref 9 words — < 1%
-
- 61 Ioana-Monica Pop-Calimanu, Septimiu Lica, Sorin Popescu, Dan Lascu, Ioan Lie, Radu Mirsu. "A New Hybrid Inductor-Based Boost DC-DC Converter Suitable for Applications in Photovoltaic Systems", Energies, 2019 Crossref 9 words — < 1%
-
- 62 Ishaque, Kashif, Zainal Salam, Muhammad Amjad, and Saad Mekhilef. "An Improved Particle Swarm Optimization (PSO)-Based MPPT for PV With Reduced Steady-State Oscillation", IEEE Transactions on Power Electronics, 2012. Crossref 9 words — < 1%
-
- 63 Javaid, Muhammad Sharjeel. "Electric Spring Control for Smart Grid Performance Improvement", King Fahd University of Petroleum and Minerals (Saudi Arabia), 2023 ProQuest 9 words — < 1%
-

64 Yuwei Xiong, Wei Chen. "Positive sequence current differential protection based on least square method for distribution network with distribution generation", 2021 IEEE 4th International Electrical and Energy Conference (CIEEC), 2021
Crossref 9 words — < 1%

65 digitalcommons.fiu.edu
Internet 9 words — < 1%

66 es.slideshare.net
Internet 9 words — < 1%

67 oaktrust.library.tamu.edu
Internet 9 words — < 1%

68 www.nature.com
Internet 9 words — < 1%

69 www.red.pe.org.pl
Internet 9 words — < 1%

70 "Intelligent Computing in Control and Communication", Springer Science and Business Media LLC, 2021
Crossref 8 words — < 1%

71 Dhivya, P., V. Chamundeeswari, and R. Seyezhai. "Design and Implementation of Perturb and Observe (P&O) MPPT Technique for Negative Output Super-Lift Luo Converter", Applied Mechanics and Materials, 2015.
Crossref 8 words — < 1%

72 Di Tommaso, Antonino, Fabio Genduso, and Rosario Miceli. "Analytical Investigation and Control System Set-up of Medium Scale PV Plants for Power Flow Management", Energies, 2012. 8 words — < 1%

73 Gishin Jacob George, R Rakesh, N. Arun. "PMBLDC motor drive with Power Factor correction controller", 2012 International Conference on Computing, Electronics and Electrical Technologies (ICCEET), 2012

Crossref

8 words — < 1%

74 Gupta, N, SP Singh, and SP Dubey. "DSP based adaptive hysteresis-band current controlled active filter for power quality conditioning under non-sinusoidal supply voltages", International Journal of Engineering Science and Technology, 2011.

Crossref

8 words — < 1%

75 J. Aristizabal, G. Gordillo. "Performance of the first grid-connected, BIPVS installation in Colombia over three years of continuous operation", 2008 33rd IEEE Photovoltaic Specialists Conference, 2008

Crossref

8 words — < 1%

76 K.P. Basu, S.K. Mukerji. "Experimental Investigation Into Operation Under Single-Phasing Condition of a Three-Phase Induction Motor Connected Across a Zigzag Transformer", IEEE Transactions on Education, 2004

Crossref

8 words — < 1%

77 Nahla E. Zakzouk, Ahmed K. Abdelsalam, Ahmed A. Helal, Barry W. Williams. "PV Single-Phase Grid-Connected Converter: DC-Link Voltage Sensorless Prospective", IEEE Journal of Emerging and Selected Topics in Power Electronics, 2017

Crossref

8 words — < 1%

78 Pablo Horrillo-Quintero, Pablo García-Triviño, Raúl Sarrias-Mena, Carlos A. García-Vázquez, Luis M. Fernández-Ramírez. "Model predictive control of a microgrid

with energy-stored quasi-Z-source cascaded H-bridge multilevel inverter and PV systems", Applied Energy, 2023

Crossref

79 Peter Kiss, Andras Dan. "Novel Method for Modelling and Calculating the Harmonic Effect and Psophometric Disturbance of High Power Electric Traction", 2007 7th International Symposium on Electromagnetic Compatibility and Electromagnetic Ecology, 2007 8 words — < 1%

Crossref

80 R. Kabiri, D. G. Holmes, B. P. McGrath. "Control of distributed generation systems under unbalanced voltage conditions", 2014 International Power Electronics Conference (IPEC-Hiroshima 2014 - ECCE ASIA), 2014 8 words — < 1%

Crossref

81 Thekkath, Preethi, and S.U. Prabha. "Adaptive hysteresis current controlled Shunt Active Power Filter for power quality enhancement", 2013 International Conference on Circuits Power and Computing Technologies (ICCPCT), 2013. 8 words — < 1%

Crossref

82 dlibrary.univ-boumerdes.dz:8080 8 words — < 1%

Internet

83 dspace.upt.ro 8 words — < 1%

Internet

84 fdocuments.net 8 words — < 1%

Internet

85 krishikosh.egranth.ac.in 8 words — < 1%

Internet

86 link.springer.com

Internet

		8 words — < 1%
87	pserc.wisc.edu Internet	8 words — < 1%
88	repositorio.uchile.cl Internet	8 words — < 1%
89	spectrum.library.concordia.ca Internet	8 words — < 1%
90	stax.strath.ac.uk Internet	8 words — < 1%
91	thesis.cust.edu.pk Internet	8 words — < 1%
92	www.essaysauce.com Internet	8 words — < 1%
93	www.scilit.net Internet	8 words — < 1%
94	www2.mdpi.com Internet	8 words — < 1%
95	A. Dell'Aquila. "Single-phase grid-connected photovoltaic systems with power quality conditioner functionality", 2007 European Conference on Power Electronics and Applications, 09/2007 Crossref	7 words — < 1%
96	Eman Hegazy, Mona Shokair, Waleed Saad. "Recursive bit assignment with neural reference adaptive step (RNA) MPPT algorithm for photovoltaic system", Scientific Reports, 2023	7 words — < 1%

97 Muhammad Ahmed Qureshi, Francesco Torelli, Salvatore Musumeci, Alberto Reatti, Andrea Mazza, Gianfranco Chicco. "A Novel Adaptive Control Approach for Maximum Power-Point Tracking in Photovoltaic Systems", *Energies*, 2023

Crossref

98 Rohit Agarwal, Rajesh Kumar, Gajendra Suthar, Hrushikesh Dalicha. "Design and Analysis of Hysteresis Feedback Controlled dc Power Supply for Solid State Power Amplifier", *IETE Journal of Research*, 2020

Crossref

99 hdl.handle.net

Internet

100 D. Mahalakshmi, V.S. Archana, J. Komathi. "Reactive power control in microgrid by using Photovoltaic Generators", 2016 International Conference on Computation of Power, Energy Information and Commuincation (ICCPEIC), 2016

Crossref

101 Deepak Kumar Chy, Md. Khaliluzzaman. "Experimental assessment of PV arrays connected to Buck-Boost converter using MPPT and Non-MPPT technique by implementing in real time hardware", 2015 International Conference on Advances in Electrical Engineering (ICAEE), 2015

Crossref

102 Ihssane Chtouki, Patrice Wira, Malika Zazi. "Comparison of several neural network perturb and observe MPPT methods for photovoltaic applications", 2018 IEEE International Conference on Industrial Technology (ICIT), 2018

Crossref

103 M. Vitelli. "Experimental characterization of the photovoltaic generator for a hybrid solar vehicle", 2007 IEEE International Symposium on Industrial Electronics, 06/2007 6 words — < 1%

Crossref

104 Natesan Saritha, Venkatesan Jamuna. "A SRF-PLL Control Scheme for DVR to Achieve Grid Synchronization and PQ Issues Mitigation in PV Fed Grid Connected System", Circuits and Systems, 2016 6 words — < 1%

Crossref

105 Shi, Xiaojie, Zhiqiang Wang, Leon M. Tolbert, and Fred Wang. "Analysis and control of DC voltage ripple for modular multilevel converters under single line to ground fault", 2013 IEEE Energy Conversion Congress and Exposition, 2013. 6 words — < 1%

Crossref

106 Tole Sutikno, Hendril Satrian Purnama, Rizky Ajie Aprilianto, Awang Jusoh, Nuryono Satya Widodo, Budi Santosa. "Modernisation of DC-DC converter topologies for solar energy harvesting applications: A review", Indonesian Journal of Electrical Engineering and Computer Science, 2022 6 words — < 1%

Crossref

EXCLUDE QUOTES ON

EXCLUDE SOURCES OFF

EXCLUDE BIBLIOGRAPHY ON

EXCLUDE MATCHES OFF